Post-Earthquake Fire Performance of Building Structures

Mohmmad Hany Yassin

A Thesis

In

The Department

of

Building, Civil and Environmental Engineering

Presented in Partial Fulfillment of the Requirements
for the degree of Master of Applied Science (Civil Engineering) at
Concordia University
Montreal, Quebec, Canada

August 2008

Your file Votre référence
ISBN: 978-0-494-45358-2
Our file Notre référence
ISBN: 978-0-494-45358-2

ABSTRACT

Post-Earthquake Fire Performance of Building Structures

Mohmmad Hany Yassin

The potential of fire event after a strong earthquake is quite high and the damage caused by this fire could be significantly higher as compared to normal fire not accompanied by an earthquake. Thus it is important to know the behavior of structures under such circumstances. Modern buildings are designed to have adequate resistance against an expected level earthquake, and sufficient fire safety, considering these events to occur separately. However, fire following a seismic excitation is not uncommon. After an earthquake the structure may sustain a considerable damage and the fire resistance of the system will be significantly impaired. In this case, the fire performance of the structure will be significantly reduced, and such condition may pose a serious threat to structural integrity, which is detrimental to the life safety of the occupants and rescue workers. Thus, it is necessary to consider such scenarios in the design of a building constructed in a seismic zone. In this study the performance of two types of structures has been studied. Load bearing wood stud walls and moment resistant steel frames under such condition has been modeled and analyzed. The performance analysis of the wood stud wall in fire has been verified with the results from the NRC fire tests. For the steel frames, the results are validated with different finite element systems such as SAFIR and ANSYS. The analysis includes heat transfer analysis and thermal stress analysis by using numerical model for wood wall and finite element solver for steel frame. Existing numerical model for stability analysis of wood frame walls cannot be applied to cases with fire and earthquake induced fire. Modifications are proposed to the existing methods in order to account for the time dependent changes in strength, stiffness and geometry due to

earthquake and fire in order to determine the fire resistance of the structures. Two analytical approaches have been proposed for modeling the damage in the steel structure after earthquake. Fire resistance rates are investigated for both normal and post earthquake fire scenarios. It is observed from the study that the fire followed by an earthquake reduces the fire resistance of a structure in both wood-frame and steel-frame structures. The study presented here forms a preliminary understanding of the PEF phenomenon and its effect on structures. Further studies are needed to enhance the understanding, quantify the parametric changes and formulate design guidelines to account for PEF hazard to structures in seismic zones.

Keywords: post-earthquake fire hazards, conflagration, performance-based design, structural strengthening, monitoring, simulation.

ACKNOWLEDGEMENTS

It is my pleasure to express my sincere gratitude to my thesis supervisor Dr. Ashutosh Bagchi, Assistant Professor, Department of Building, Civil and Environmental Engineering, Concordia University, for his guidance and encouragement in the research work. I would also like to thank Dr. Vankatesh K.R Kodur, Professor of Civil Engineering at Michigan State University, for his collaboration and technical help. I also appreciate the valuable discussion with Dr. M. Sultan and Dr. N. Benichou at the National Research Council of Canada, Ottawa, during my visit to NRC's fire testing laboratory.

I would like to thank all the faculty-members of Building, Civil and Environmental Engineering Department for their guidance and suggestion during my course work.

My grateful thanks are to my parents, my brothers and sisters for their support and encouragement to complete this work. I would specifically thank my mother and dad for all kind of support they provide up to the moment of finishing this work.

I also like to specially thank my wife for her help and great support through the research work; her continuous encouragement and patience helped me a lot in the tough days and enabled me to reach the coast safely.

Finally I would like to thank my colleagues, my friends and Dr. Bagchi's research group members for their encouragement and active help during the research period.

Table of Contents

List of Figures

List of Tables

Notation and Abbreviation

List of Symbols and Abbreviations

Symbol/Abbreviation	Definition/Explanation
P	Gravity loads on a building frame
S_a	Spectral acceleration corresponding to seismic hazard
T_0	Fundamental period of vibration of a structure
Δ	Lateral deformation in a building frame
t	Time
T	Temperature
Q	Heat Flux
PEF	Post-Earthquake Fire
FRP	Fibre Reinforced Polymer
HSC	High Strength Concrete
SHM	Structural Health Monitoring
DFAE	Damage in the frame after earthquake.
V	Lateral load.
W	Distributed load per length unit.

Chapter 1

Introduction

1.1 Introduction:

While the performance of structural systems under fire exposure received some attention earlier, it is only after the tragic incident of the World Trade Centre collapse on September 11, 2001 that more emphasis is given on developing robust fire safety guidelines for buildings (Chen *et al.* 2004). The Federal Emergency Management Agency (FEMA) and other organizations (e.g., National Institute of Standards and Technology – NIST) in the United States have initiated a number of projects including emergency response and structural safety of buildings against fire. Earthquakes represent an extreme event causing enormous damage to built infrastructure and loss of human lives. The occurrence of a fire following an earthquake, which is not very uncommon, can lead to catastrophe. Although, ground shaking is a major concern in most earthquakes, subsequent fire can pose a major risk to urban infrastructure. The Post-Earthquake Fire (PEF) can grow, intensify and spread out of control, in one or more neighborhoods which is often referred to as *conflagration.*

Historically fire following earthquakes in Japan and America has been a major factor for post-earthquake damage in the twentieth century. According to Scawthorn *et al.* (2005), fires following San Francisco (1906) and Tokyo (1923) earthquakes represent some of the largest peacetime urban fires in human history, (Figures 1.1 and 1.2). The 1994 Northridge earthquake caused relatively minor damage due to PEF events perhaps due to lower level of damage to the water distribution system and quick response of fire departments (Todd *et al.* 1994). There were about 30 to 50 major fires in the San Fernando Valley after the earthquake and a few low rise buildings were completely destroyed and some multi storey buildings suffered extensive damage. The Kobe earthquake in 1995 resulted in huge damage due to both ground shaking and corresponding PEF events (EQE 1995). The earthquake was followed by several major conflagrations totaling 142 fire events. The water supply was available only for 2 to 3 hours for fire fighting. On the other hand, the loss of life and injuries due to fire was comparatively lower in the Turkey earthquake in 1999 which had a magnitude of 7.4 and it took more than 17,000 lives. There were no major conflagrations in that event mainly due to the fact that the construction materials in the area were non-flammable, like reinforced concrete and masonry. However, the earthquake was followed by a major fire in an oil refinery that lasted for several days.

There are many factors that could lead to a fire to go out of control. Ground shaking due to a strong earthquake may cause severe damage to buildings and infrastructure such as, roads, bridges, and life-line systems. A hot dry and windy weather help in the spread of fire, while damaged communication and transportation systems can limit access of fire

fighting in the disaster area; and the damage of water supply system can limit the fire control measures. In that case, more effort and extinguisher material like water to control the fire. Therefore, it is essential to set up fire safety objectives for buildings and urban design. It is also necessary to ensure the structural integrity of the affected buildings for certain duration of a PEF event that the emergency resources can be availed. These factors should be considered for the design of new buildings, and the retrofit of existing structures.

This study investigates behavior of structures in similar scenarios and tries to devise appropriate methodologies for analyzing structures under post earthquake fires.

Figure 1-1 1906 San Francisco earthquake (Wikipedia, 2008)

Figure 1-2 1906 San Francisco earthquake, Subsequent fire (Wikipedia, 2008)

1.2 Objectives:

Since the structure provides the last line of defense against fire, structural integrity in post-earthquake fire (PEF) event is essential. The main objective of the present research is to simulate the PEF scenario on different types of structures by using analytical or finite element simulators and models to simulate the fire following earthquake. The combination of different methods or tools used for each stage of analysis is needed to ease the simulation and faster the analysis procedure. It is also intended to capture some of the basic behavior of structures under PEF events in order to gain an understanding of performance of structures in such events.

1.2.1 The scope of this thesis:

As mentioned above, the main aim of this study is to understand the physical concepts of a structure's performance in the event of fire following an earthquake. The structural analysis is performed in 2D (two-dimensions). In heat transfer analysis, a 2D transient analysis has been performed for the structural sections in case of steel structures and 1D transient heat transfer analysis for the wood members. The seismic ground acceleration has been applied in one horizontal direction. The models consider the nonlinear behavior of materials under high temperatures and/or large displacements.

1.3 Organization of the Thesis:

The thesis has been organized into nine chapters. Objective of the thesis with some introductory materials are presented in the current chapter i.e. Chapter 1. A review of previous work and the ongoing work on this topic is incorporated in the Chapter 2. Structural response in the earthquake event and methods of analyzing such response considered in the present research are presented in Chapter 3. Chapter 4 presents the heat transfer analysis procedures and mechanisms. Material Properties at elevated temperatures are described in Chapter 5. Structural performance in normal and Post-earthquake fire has been discussed in chapter 6. Description of the models and relevant results for the wood-frame and steel-frame are presented in Chapters 7 and 8, respectively. The summary of the thesis including the conclusions is presented in the Chapter 9. A list of references is put at the end of the thesis followed by an appendix.

Chapter 2

Literature Review

2.1 Introduction:

In addition to causing vibration in structures, earthquakes have several other undesired aspects associated with them, such as, landslide, and fire (Scawthorn *et al.*, 2005). Although, shaking is a major concern in most earthquake events, other features like fire, and weather conditions that can make a fire spread, can pose a major risk to urban infrastructure. The Post-Earthquake Fire (PEF) can grow, intensify and spread out of control, in one or more neighborhoods which is known as *conflagration.*

The history shows that the lack of adequate attention to PEF in both individual building design and urban design can result in a catastrophe. There are many factors that may lead to a fast growing fire to grow. A hot dry and windy weather can speed up the fire spread. Following an seismic event damaged roads can limit facilitation of fire fighting in the disaster area, and the damage of water supply system can limit the fire control measures. The "problem area" could grow fast which could require more effort and extinguisher material like water to control the fire. Earthquake motions could affects the water distribution system resulting in drainage of water and reduction in water supply capacity

in the network, which makes fire fighting more difficult. Communication is another important aspect that could be affected, which can disrupt the emergency services. Therefore, it is essential to set up fire safety objectives for buildings and urban design. It is also necessary to ensure the structural integrity of the affected buildings for certain duration of fire following earthquake such that the emergency resources can be mobilized and expended. These aims should cover all possible areas including retrofitting design of existing structures and design of new buildings. Strengthening of existing buildings is especially important because a great number of them for various reasons have come close to the end of their lifecycle and do not comply with current codes. On the other hand, replacing these buildings is impossible because the number of such structures is larg and replacing them will require huge financial recourses. For that reason fire strengthening design presents a very important alternative.

According to Bernhart (2004), fire safety objectives may include: (*a*) Life safety of occupants, emergency crews and others (b) Protection of properties including the building's structure and its contents (*c*) Down time reduction, and (*d*) Environmental side effects consisting of fire byproducts and fire extinguisher materials.

Performance requirements may consist of: (*a*) Sufficient way out time to safe areas (*b*) adequate access of fire crews to areas subjected to fire (*c*) safe and continuous operation of essential facilities, and (*d*) avoiding fire to spread across the building and to the adjacent buildings. Also, the followings should be taken into account in fire structural design phase: (*a*) damage to the structural elements should be limited (*b*) provisions in

preventing local collapse (*c*) limiting deformation of structural components so that it would not have a negative impact on, non structural elements (e.g., compartmentation walls and other fire protection systems), and (*d*) prevent progressive collapse of buildings.

In this chapter, a revision of the current state of the art on fire safety design, mitigation, and performance assessment of structures in regard to post-earthquake fire hazard is presented.

2.2 Research Significance:

Structural members are to be designed to satisfy the requirements of serviceability and safety limit states for various environmental conditions. Fire represents one of the most severe conditions and hence the provision of appropriate fire safety measures for structural members is a major safety requirement in building design. The basis for this requirement can be attributed to the fact that, when other measures for containing the fire fail, structural integrity is the last line of defence. Fire resistance is the duration in which a structural member or system exhibits resistance with respect to structural integrity, stability and temperature transmission. Typical fire resistance requirements for specific building members are specified in the building codes (e.g. NBCC 2005). Fire resistance can play a crucial role in the performance of buildings and built-infrastructure (and cause

significant damage and destruction) in the event of post-earthquake fires as illustrated in the previous section.

Generally, structural members are designed for required fire resistance ratings prescribed in the building codes. However, this criterion is mainly developed for fire exposure under normal conditions (without earthquake). These guidelines may not be fully applicable in the case of PFE since the structure under fire exposure may experience significant lateral loads due to seismic events and aftershocks from earthquake. Furthermore, recent studies clearly show that the structural members composed of some of the new materials may not exhibit the same level of fire performance of conventional materials.

The following sections review the main parameters and strategies that have to be considered to minimize the impact of PEF damage in buildings and built infrastructure. They also discuss various research needs to develop the much needed guidelines for fire safety design of structural systems under combined action of fire and earthquake.

2.3 Factors affecting Post-Earthquake Fire Hazard:

For mitigation of PEF hazards, it is important to understand the causes of such hazards. It is essential to know the behavior of structural and non-structural components of buildings under interactive combination of seismic loads and the fire following it. In addition, proper attention should be given to the interaction of the causes and building's status because of the fact that the change in either of them influences the magnitude and intensity of the other.

Fire is an uncontrolled process of combustion of inflammable materials producing heat and light and often smokes. Unlike the seismic activities, aftermath fire ignitions are not natural phenomena but are a function of man-made origin agents that could be affected by environmental factors like wind direction and speed. Man-made agents include construction materials, building usage, loss of water supplies for extinguishing fire, the response times of occupants and emergency crews, obstructed access and insufficient resources, and architectural configuration including improper building separation. Spread of fire can be significantly accelerated by the influence of wind pressure and stack effect, (particularly in tall buildings). Also, improper reliance on codes' allowance for reduction in passive fire protection systems, where active systems like sprinklers are provided, may increase the inadequacy of overall fire protection systems in the event of severe earthquakes. Codes may allow for increase in use of sophisticated active fire safety systems where design of building is performance based and risk of reduction in passive systems is properly taken into consideration. Although, the possibility of such fire incidence will be low in such cases, the consequences of failure of active fire protection

systems can be catastrophic, particularly in tall buildings. PEF, in a performance-based design process, should suitably be dealt with, since it is a design scenario; this is particularly important in regions where significant earthquakes can take place.

It is important to note that majority of the low-rise residential buildings in North America are made of wood frame, and that building envelopes in all forms of buildings utilize flammable materials such as insulating boards and plastic sheets. Also, the wood-frame joints in these houses are quite vulnerable to fire hazards Furthermore, in the North American context there are gas lines in most buildings and the probability of damage to these gas connections, which can induce significant fires, are quite high. .

Post-earthquake fire may also be viewed as a course of events consisting of the following (Scawthorn et al., 2005):

1. Earthquake occurrence that may result in damages and throw things down like candles down or over turning stoves.
2. Ignition that can take place in a variety of ways including breakage of utility lines such as gas line, electrical wiring shortcut, or highly combustible material leakage such as alcoholic based substances.
3. Finding out about the existence of the fire is the next thing that may be difficult because of panic following earthquake.
4. Report of fire to fire department is the next important step if the fire is not self-extinguished and/or put out by occupants.
5. Fire department response

2.4 Strategies for Mitigation of Post-Earthquake Fire Hazards:

Mitigation of PEF can be categorized into the following levels: (a) regional (area) and, (b) individual building. To accomplish the mitigation at the individual stage, the following four-fundamental-types of analyses need to be followed in order to provide a clearer, more scientific result and a reliable way of handling hazards and uncertainties (Chen et al., 2004):

a) analysis of the hazard that provides input data like duration of earthquake and its intensity, fire load and compartment temperatures,
b) analyses of the structural and non structural parts based on the prior estimation of hazards that include structural demand parameters like drift and acceleration experienced by the building, peak structural temperatures and deflections,
c) damage analysis of the buildings including condition evaluation and required modifications, and
d) Loss analysis consisting of casualties, injuries, direct and indirect financial losses.

2.5 PEF Hazard Mitigation Strategies at the Area Level:

At the area level, a Geographical Information System (GIS) based approach can be employed in the analysis process (Chen *et al.*, 2004). This will provide enough information on geographical distribution of human injuries and ignited fires, location of facilities for urgent situation such as fire station and hospitals, damage intensity of the facilities and transportation system and the localized area due to earthquake and the fire following it. Knowing this information will help the decision makers to prioritize and optimize their emergency services, for instance, assigning the emergency crews and vehicles.

Optimal emergency services can be provided and assigned if causes and difficulties in the area level are identified. Once the problems are well understood and the facilities are known, the problems and their solutions can be prioritized and best possible decision can be made. Using methods like GIS provides decision makers with data such as distribution of injured people, location and amount of facilities that they can rely on, the distance of emergency stations from the sites that they are needed, weather condition and so on. This makes an optimized emergency delivery possible (Chen *et al.*, 2004). A simulation study on PEF using GIS data has been presented in Zhao *et al.* (2006).

Moreover, there are several factors that need adequate attention and enhancement in the regional level. Some of which are as follows (Chung et al., 1995):

a) *Post-earthquake fire ignitions due to short circuit:* Such cases could be prevented if there is a regional earthquake-activated power shutoff mechanism in place that is capable of disconnecting the power of the area at the beginning of the earthquake.

b) *Fire ignition due to the breakage of gas distribution system:* Supplementary mechanism to control gas distribution systems to minimize the gas services breaks that have been common in the past events. Automatic shutoff valves, extra gas valves on the supply network and how to promptly and securely empty gas lines that have already been shut down are of such mechanisms.

c) *Fire spread between buildings:.* There exists a large likelihood for PEF happening in regions with particular building, landscape and terrain configuration and weather condition. Such regions should be recognized and dealt with to minimize the possibility of fire spread.

d) *Disruption of the water distribution network:* Water supply is another concern in fighting the fire and providing the necessary service to the public. Reliability on water supply should be improved in any possible way like planning of alternative sources of water such as tank trucks, swimming pools, or other strategies in place for fast repair of damaged water mains.

e) *Enhancing the water based fire protection systems:* In order to prevent the piping system from failing, it is necessary to make sure of the existence of adequate sprinkler bracing and standpipes, proper anchorage of suction tanks, and fire

pumps. Other adequate measures should also be taken at the points which have been found to be weak in the past events.

f) *Life-line systems design for earthquake and fire following the events:* Communication, water distribution, power transmission lines, and transportation network are examples of life-line systems which need to be carefully designed and constructed so that there would be less likelihood of their non-functionality at the aftermath of an earthquake and during a potential PEF. Moreover, there should be a safe and efficient repair in terms of effectiveness and well-timed recovery. A number of issues as mentioned above related to the PEF performance of Life Line systems have been identified in a Workshop organized by the National Institute of Standards and Technology, U.S.A. (NIST, 1995).

An effective approach to mitigate PEF in the area level should include the following actions: (*a*) identifying major pipelines in the network, (*b*) mapping up the hazards on them and then determining alternatives for them including replacement and upgrade, and (*c*) constructing above the ground ultra large diameter hose pipe bypass (Eidinger, 2004).

2.6 PEF Hazard Mitigation Strategies in the Individual Building Level:

2.6.1 Hazard Analysis:

The first step in hazard analysis is to evaluate the level of danger associated with an event, such that there is proper information about the hazardous conditions at which the structure would be subjected to. Probability of occurrence and the magnitude of earthquake as a natural event is a function of factors like return periods, nearby fault, building's distance from the fault, and the site status in which the building is located (Chen et al., 2004, Taylor, 2003).

To achieve a reliable PEF hazard mitigation approach in cases of tall buildings it is important to incorporate diversity, redundancy and independency into the fire safety systems, such that, where one mechanism fails to function at its presumed level there will another system to fill in for that.

2.6.2 Structural and Non-Structural Members Analyses:

The structural members' fire protection systems employ schemes like insulation, flame shielding and heat sinks, and non-structural protection schemes include detection and sprinkler systems, fire-proof doors, and fire extinguishing systems like hydrant and emergency exits. Fire protection systems also contain active mechanisms like automatic sprinklers and passive mechanisms like insulation of structural members and emergency egress. However, high likelihood of failure of active and passive fire safety systems that

have been experienced in the past earthquake occurrences is one of the prominent concerns. Therefore, a redundant fire protection system must be employed.

One of the very essential agents of fire protection systems, as mentioned earlier, is passive protection system. However many of such systems like gypsum plasterboard walls are very vulnerable when they undergo deformation caused by earthquakes. Gypsum plasterboard has superior fire resisting properties which can be further enhanced by some glass fiber reinforcing (Chu Nguong, 2004). The level of risk due to PEF may be evaluated by calculating factor of safety, which is the ratio of available and actual escape times, and assessing the effect of damage to plasterboard walls and protecting escape paths. It was found by Chu Nguong (2004) that in buildings higher than ten-story, in which sprinklers are inoperative, the expected escape time is bigger than the expected failure time of the fire rated surrounding walls of the escape routes. The damage influences the fire performance of the wall at drifts close to 0.6% that is considerably less than the magnitude allowed by most building codes. For instance, in the New Zealand code the allowable inter-storey drift ranges from 1.5% to 2% depending on the story height (Sharp, 2003). This limit in the National Building Code of Canada (NBCC 2005) ranges from 1% to 2.5% of the building height, depending on the building use.

Fundamental factors that should be kept in mind when determining the required fire resistance for floors, roofs, and structural frames are: building use and occupancy, building height and area, combustibility of construction, accessibility by fire department,

distance from other buildings, and presence of sprinkler and other active fire protection systems (Alkhrdaji, 2004).

The categories of the fire rating are usually specified by the building codes (e.g. IBC, 2003, NBCC 2005, NZS, 2006). Normally, increase in building height, area, combustibility, limitation of access, the closeness to adjacent buildings, and the lack of a sprinkler system require a larger magnitude of fire resistance rating.

2.6.3 Selection of Construction Materials:

Construction materials lose their strength and stiffness properties, at varying rate, when subjected to high temperatures encountered in fire exposures. To minimize the fire induced loss properties appropriate measures have to be taken during the design, construction or retrofitting stage. One or a combination of the following factors should be considered in choosing the building materials or construction process to achieve such delay in temperature rise: (i) low thermal conductivity, (ii) high effective heat capacity, (iii) heat absorbing physical (e.g., transpiration, evaporation, sublimation, and ablation) or chemical (e.g., endothermic decomposition, and pyrolysis) reactions, (iv) intumescences, i.e., formation of thicker foam upon heating, and (v) radiation or reflection.

The traditional enclosure materials used in fire protecting steel structural components are plaster, concrete, and masonry. However, nowadays there are several other types of materials like ceramic wool wraps are being used. It is worthwhile to note that even steel itself could be an efficient fire protective material where is used in form of sheets; in such cases it works as protective and reflective protection shield, or it may be employed in form of mesh or wrap in order to prevent other materials from disintegration.

Structural members' protection is to decrease the heat transfer to the structural component; the usual means are using protective boards, concrete encasement and spray–applied materials. However, these protective systems could potentially be damaged by earthquake or fire. Shielding falling, peelings off of the sprayed insulation or spalling of the concrete are some of the possible damages that could occur. In order to evaluate the fire performance of a building following an earthquake, it is important to know the state of damage in the building structure and its fire protection system due to the seismic event. It is important to take into account the damage to fire protection system of structural members and of all other non-structural components by which fire hazard status would be affected.

The integrity of the building as a whole is a paramount factor in preventing a progressive collapse, so that the building would be capable of withstanding high temperature for at least for some time, and the spread of a structural failure in a chain reaction form will not occur. The least resistance time against fire is referred as fire rating time for structural

members that are normally regulated by codes and is a function of the features of building and occupancy type. These time periods should provide occupants with adequate time to evacuate the building, fire fighters to put out the fire, and to avoid any possible progressive collapse. Also, other objectives such as the reduction of downtime should also be achieved. To comply with fire resistant structural design requirements, it is essential to know the characteristics of the building materials used in the construction of structural elements while they are exposed to fire.

Following three materials are commonly used in constructions of structural elements these days: concrete, steel, and Fiber Reinforced Polymer (FRP). The behavior of these materials could be categorized in two groups as, thermal and mechanical. Basically, the evaluation of the serviceability limit state such as, "temperature growth on an unexposed face" depends on thermal properties (except thermal expansion), while ultimate limit state design assessment depends on mechanical properties of the material. Stress-strain and strength-temperature relationship for ASTM A36 Steel as reported by (Harmathy, 1978) shows that the rate of strength loss for steel is far greater than concrete, and the concrete cover could provide acceptable fire rate protection provided that the cover is thick enough. Experimental results on compressive strength of concretes at high temperature by Anchor et al., (1986) showed a significant reduction in the compressive strength of normal density concrete after almost 300°C.

FRP composites are materials that are being increasingly used in the construction and rehabilitation of bridges and offshore structures. However, FRP composites are vulnerable when attacked by fire since plastic based substances are combustible in nature at high temperature. Although, there are some guidelines for the use and protection of these materials in fire-sensitive applications, the lack of standardized design information is a reason for which FRPs have so far been employed in cases where the fire risk is low (e.g. bridges). The threshold temperature of the epoxy resin used in building up FRP composite, which is known as the glass transition temperature which for most types of epoxy resins used in the composite's construction is between 60°C (140°F) and 82°C (180°F), although the fibers themselves can endure higher temperatures (Kumahara et al., 1993; Wang and Evans, 1995).

2.6.4 Damage Analysis:

Damage condition of the building can be categorized as minor, moderate, or major damage, and collapse. The damage to non-structural fire protection system may be defined as undamaged, loss of the functionality in percentage (e.g., 25%, 50%, 75%, etc.), and non-functional. Damage analysis could be either analytical or qualitative (based on inspection). When a strong earthquake takes place, there usually is not a rapid access to the buildings' interior. So, the most feasible and fast way for the qualitative evaluation would be by inspection of the building from the exterior. The purpose of such assessment is to address the abrupt high risk situations in post earthquake environment and the subsequent fire, knowing the fact that most PEFs are a direct product of primary earthquakes, not the aftershocks. The risks can be identified as falling hazards,

incomplete collapse, and collapse (Wastney, 2002). Fundamental variables of damage assessment in analytical approach include the followings (Taylor, 2003):

(i) earthquake intensity, (which is usually measured using the two following scales: (i) Modified Mercalli Intensity (MMI) Scale, and (ii) Richter scale),

(ii) subsoil dynamic properties that affect building response to seismic loads,

(iii) ground status that can affect services (water, gas, oil etc.) such as in case of ground dislocation,

(iv) building type in terms of the configuration and structural characteristic that will influence dynamic properties of the building like the magnitude of displacement and acceleration affecting that could affect non structural components,

(v) building age which reflects the code and standards used in design of the building and possible deterioration of structural, and

(vi) nonstructural components including fire protection over time.

2.6.5 Loss Analysis:

One of the methods in loss estimation is using square grids simulation. This technique consists of three sub-models that are: (i) outbreak of fire in which the probability of fire occurrence is considered (ii) spread of fire in the area which is expressed by elliptic equation, and (iii) refuge action that would be obtained from the actual condition of the earthquakes taken place in the past. This technique is capable of providing an assessment

over the average fire damage, the human loss, and also beneficial in optimizing operation of fire-extinguishing with respect to various fire patterns (Chang, 2003).

Loss analyses include life loss and injuries, direct financial loss, and indirect financial loss due to downtime. Evaluation of fatalities and injuries is not easy; since in addition to earthquake magnitude and fire intensity, it is a function of parameters like usage of the building, architectural configuration consisting of emergency exits condition, occupants' age pattern and their reaction when they are exposed to the hazards. Direct financial loss comprises the properties repair and replacement costs. The indirect financial loss is difficult to identify too, as it must a reflect the loss of building services due to repair or replacement, and the influence of both physical and emotional trauma of people involved in the disaster in any way (Chen et al., 2004, Williamson, 1999).

2.7 Computer Programs for Analysis and Simulation:

Currently there a few of software tools in commercial level and research level that can be used in analysis of fire hazard, loss estimation and structural response. Although some of the software packages like SAFIR (Franssen et al., 2000; Kosaka, 2004), FIRECAM (NRC, 2008), and VULCAN (Grosshandler, 2002) are capable of performing the analysis a structure under fire, a complete coupled analysis of the structural response under a PEF event is not possible, yet. Majority of the software tools available in this area are used for fire and smoke modeling, and fire risk analysis. Some of them are NIST (National Institute for Standards and Testing) Fire Dynamics Simulator (FDS) and Smokeview

(NIST, 2006), ANSYS CFX – Fire and Safety Analysis (ANSYS 11), FLUENT - Fire and Smoke Modeling (FLUENT, 2006), HAZUS-MH MR2 is a risk assessment software (FEMA, 2006).

Although, there are some computer programs that offer design, management and other facilities, there is no comprehensive and sophisticated software for PEF performance evaluation of structures. For instance, SAFIR in research level and Vulcan in both research and commercial level software programs that offer fire engineering design facilities. But, they do not have, the sophistication of ANSYS CFX to expose the building to more realistic fire scenarios. Such scenarios could involve structural, non-structural damages due to earthquake, ignition of fire at a particular location, and its evolvement across and along the height of the building, the stack effect, and breakage of windows.

2.8 Design Strategies and Research Needs:

To minimize the devastating effect of post-earthquake fires, appropriate hazard mitigation technique are to be accounted for both at regional and individual building level. One of the key considerations for ensuring the safety of the building following an earthquake is to provide for structural fire safety measures to withstand the effect of fire under seismic loads. One of the clear gaps identified here is the lack of a standard, or a set of integrated and practical guidelines for the design of structural and non-structural elements to ensure an acceptable level of PEF performance of structures. Significant research effort must be expended towards numerical studies and simulation of PEF scenarios to structural performance and damage. In general, the building codes,

including NBCC (2005), do not distinctively consider the effect of PEF in evaluating fire safety; instead, some of them like New Zealand's code (NZS, 2006) have provided a part as Acceptable Solution which may actually produce inconsistent performance of structures (Taylor, 2003).

The main steps involved in developing a rational approach for overcoming PEF hazard are:

a) identifying proper design (realistic) fire scenarios and realistic loading levels on structural members in a post-earthquake scenarios;

b) carrying out detailed thermal and structural analysis by exposing the structural members to fire conditions; and

c) developing relevant practical solutions, such as use of fibers in high strength concrete for mitigating spalling under earthquake loads or better insulations that can withstand the vibrations effect, to achieve required fire resistance.

The design fire scenarios for any given situation should be established either through the use of parametric fires (time-temperature curves) specified in Eurocodes or through actual calculations based on ventilation, fuel load and surface lining characteristics (EC 1, 1994; SFPE, 2004). Figure 5 shows typical standard and real fire exposure curves that can be used for performance based fire safety design. The loads that are to be applied on structural members, in the event of fire, should be estimated based on the guidance given in ASCE-07 standard (ASCE-07, 2005) (dead load + 50 % live load) or through actual

calculation based on different load combinations, including expected post earthquake ground motions. Incorporation of appropriate monitoring systems in buildings and other fire-sensitive structures can provide the response history records for regular fire and PEF events.

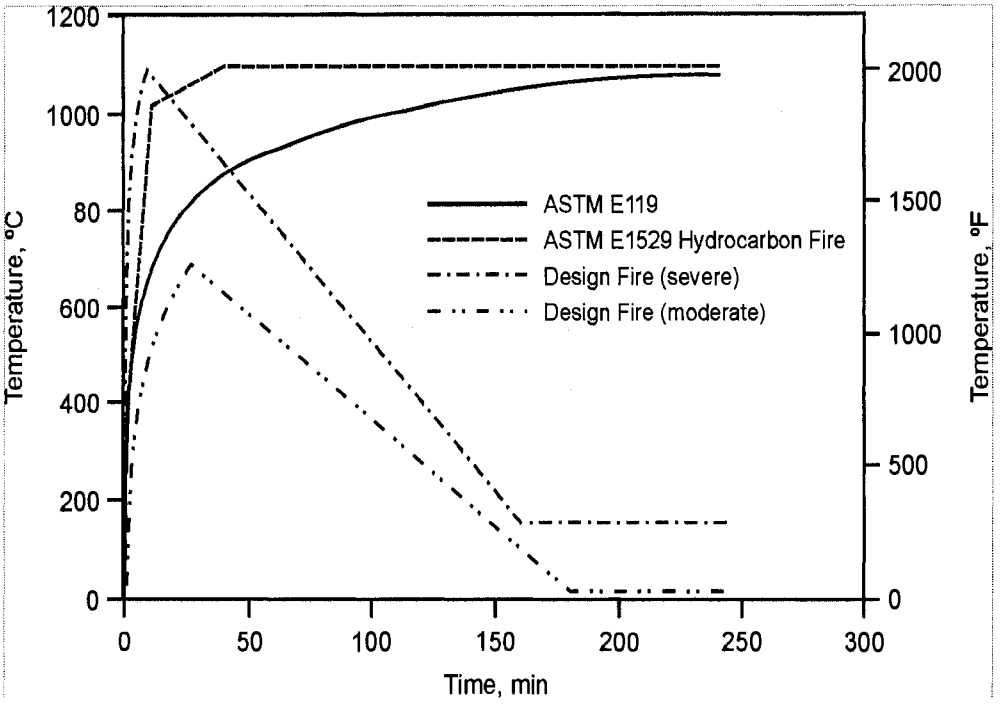

Figure 2-1 Typical Fire Exposure Scenarios for Performance Based Design

Once the fire scenarios and load level are established, the next step is to avail of a computer program for the analysis of structural members exposed to fire scenarios. The computer program should be able to trace the response of the structural member in the entire range of loading (including seismic loads) up to collapse under fire. Using the computer program, a coupled thermal-structural analysis shall be carried out at various

time steps. In each time step, the fire behavior of a structural member is estimated using a complex, coupled heat transfer/strain equilibrium analysis, based on theoretical heat transfer and mechanics principles. The analysis shall be performed in three steps: namely, calculation of fire temperatures to which the structural members are exposed, calculation of temperatures in the structural members, and calculation of resulting deflections and strength, including an analysis of the stress and strain distribution.

The program, used in the analysis, should be capable of accounting for nonlinear high temperature material characteristics, complete structural behavior, various fire scenarios, different loading (including lateral loads) scenarios, high temperature creep, different materials types and failure criteria. In the analysis, geometric nonlinearity which is an important factor for slender columns (that are used in many practical applications), shall be taken into consideration. Thus, the fire response of the structural members shall be traced in the entire range of behavior, from a linear elastic stage to the collapse stage under any given fire and loading scenarios. Through this coupled thermal-structural analysis, various critical output parameters, such as temperatures, stresses, strains, deflections and strengths, have to be generated at each time step.

The temperatures (in the structural members), strength capacities and computed deflections shall be used to evaluate failure of the structural members at each time step. At every time step the failure of the structural members shall be checked against a pre-determined set of failure criteria, which include thermal and structural considerations.

The time increments continue until a certain point at which the thermal failure criterion has been reached or the strength or deflection reach the limiting state. At this point, the structural members become unstable and will be assumed to have failed. The time to reach this failure point defines the fire resistance of the structural element or the system.

The development of relevant strategies for ensuring structural fire safety under seismic loads will effectively minimize PEF hazard. This will enhance the safety and security of built infrastructure and also will reduce the significant human and property losses. Further, the output from structural safety models can be input to risk models to assess the overall risk due to PEF hazard. Such risk studies will also help policy makers and insurance industry to assess the realistic estimate of impact of earthquake on society. A summary of possible analysis methodology as proposed by Mousavi et al. (2008) is presented in Figure 2-2.

The systematic way shown in Figure 2-2 proposed a seismic hazard analysis to be performed initially as a first step in the PEF analysis course. The seismic hazard analysis involves a seismic structural analysis which gives the post-earthquake residual lateral deformation in the structure as an output. The new condition of the structure after earthquake will be the input for the fire hazard analysis. In this stage the structure would be exposed to a standard fire curve as a thermal load. Following that a coupled thermal-structural analysis should be performed. The aim of this stage is to calculate the stresses in the structure due to the thermal load i.e. the fire and determine the collapse time of the structure which is called the fir resistance rate.

It can be concluded from the previous revision that a small attention has been given to study structures performance under post earthquake fire. Most of the studies concerned about the fire safety systems' integrity after the earthquake. Others were about risk analysis and statistical analysis. In the present research, a direct attention has been given to the performance of the structure in PEF and a proposed analysis methodology has been discussed. A comprehensive research program is needed for developing validated tools and computer programs for analyzing the PEF hazards.

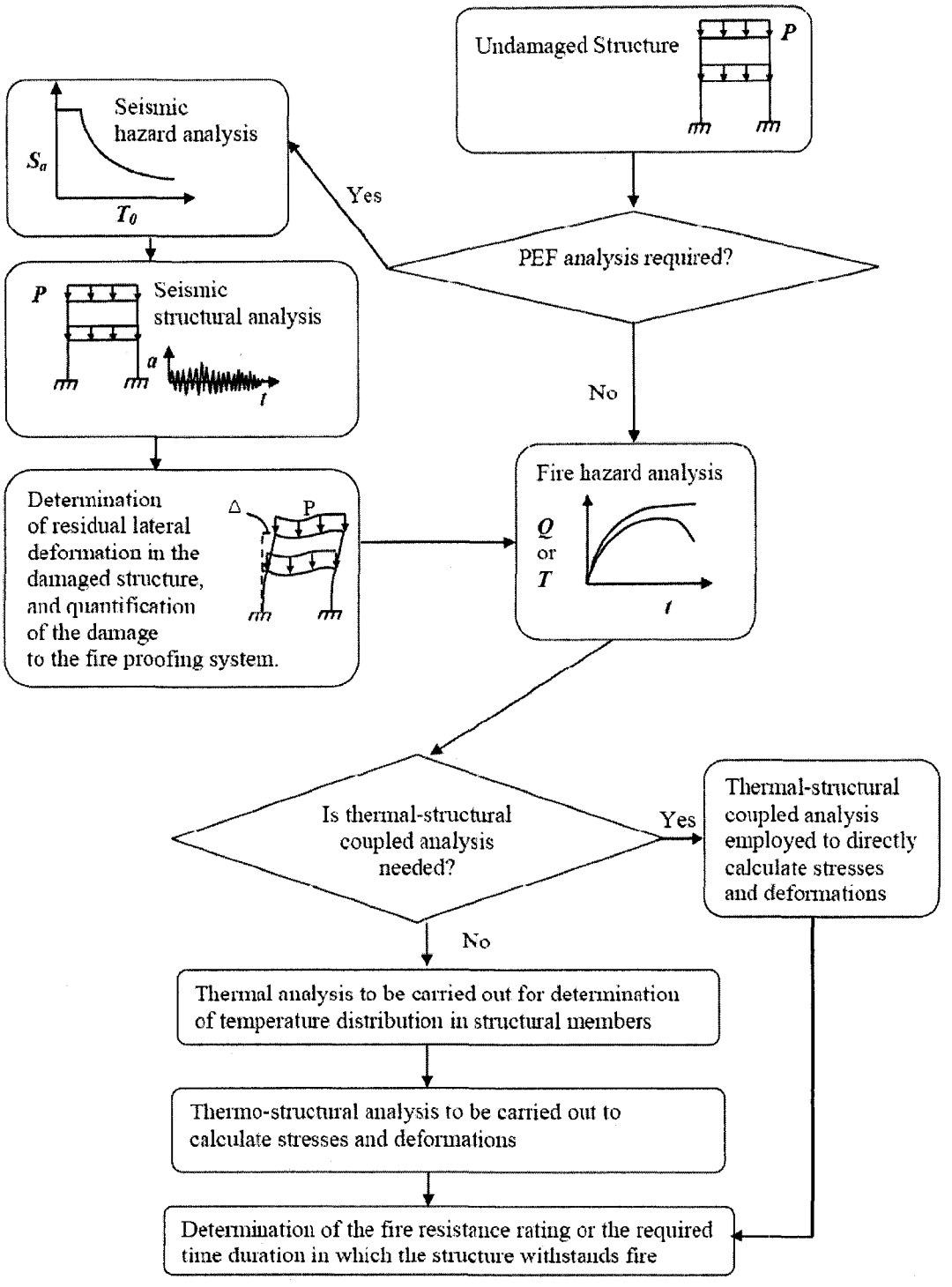

Figure 2-2 Flow-chart for the post-earthquake fire performance evaluation of building frames (Mousavi et al. 2008)

Chapter 3

Structures Response in the Earthquake Event

3.1 Overview

Seismic Analysis is part of the structural analysis procedure which focuses on the calculation of the response of the structure to earthquakes. It is part of the process of structural design, earthquake engineering or structural assessment and retrofit in regions where earthquakes are common.

A building has the potential to 'wave' back and forth during an earthquake. The basic vibration pattern of a structure is called the 'fundamental mode' or mode 1, which represents a structure's response when it vibrates in its lowest frequency, i.e. longest period. Most buildings, however, have higher modes of response, which are uniquely activated during earthquakes.

Structural analysis methods can be divided into the following five methods, and choosing an appropriate method of analysis depends on the type and importance of the structure (Chopra 1995).

3.1.1 Equivalent Static method:

This approach defines a series of forces acting laterally on a building to represent the effect of earthquake ground motion, typically defined by a seismic design response spectrum. It assumes that the building responds in its fundamental mode. Or more accurately the contribution to the respond of the structure comes mainly (90%) from the first mode. For this to be true, the building must be low-rise and must not twist significantly when the ground moves. The response is obtained from a design response spectrum, given the natural frequency of the building (either calculated from modal analysis or defined by the building code; i.e based on the construction materials). The applicability of this method is extended in many building codes, including NBCC 2005, by applying factors to account for higher buildings with some higher modes, and for low levels of twisting. To account for effects of "yielding" of materials in the structural elements, many codes apply modification factors that reduce the design forces.

3.1.2 Response Spectrum Analysis:

In this method a modal analysis should be done as a first step to get the main modes, then the multiple modes of response of a structure will contribute, in the frequency domain, to the total response of the structure. This is recommended in many building codes for all cases except for very simple or very complex structures. The response of a structure can be defined as a combination of many special shapes (modes) that in a vibrating string correspond to the "harmonics". Computer analysis can be used to determine these modes for a structure. For each mode, a response is read from the design spectrum, based on the

modal frequency and the modal mass, and they are then combined to provide an estimate of the total response of the structure. Most of combination methods include the following:

- Absolute - peak values are added together.
- Square root of the sum of the squares (SRSS).
- Complete quadratic combinations (CQC) method.

The result of a response spectrum analysis using the response spectrum from a ground motion is usually different from that which would be calculated directly from a linear dynamic analysis using specified same ground motion records. This is because the phase information is lost in the process of generating the response spectrum.

The limits of this method does not include the cases where structures are either too irregular, too tall or of significance to a community in disaster response. In those cases, more complex analysis is often required, such as linear or non-linear dynamic analysis.

3.1.3 Linear Dynamic Analysis:

Static procedures are appropriate when higher mode effects are not significant. This is generally true for short, regular buildings. Therefore, for tall buildings, buildings with torsional irregularities, or non-orthogonal systems, a dynamic procedure is required. In the linear dynamic procedure, the building is modeled as a multi-degree-of-freedom (MDOF) system with a linear elastic stiffness matrix (Wikepedia 2008) and an equivalent viscous damping matrix for the whole system is considered in the solution.

The ground motion response is represented here through considering the multiple levels of modes. Time history data or modal spectral analysis input to the solution and in both cases, the corresponding internal forces and displacements are determined using linear elastic analysis. The advantages of these linear dynamic procedures with respect to linear static procedures are that higher modes can be considered.

3.1.4 Non-linear Static Analysis (pushover analysis):

When linear analysis is not achieving the acceptable accuracy or uncertainty is governing the results of linear analysis, a more accurate analysis procedure should be conducted to address the nonlinear behavior of structure in earthquake. Therefore, procedures incorporating inelastic analysis can reduce the uncertainty and conservatism results in the linear methods. In this method a pattern of forces is applied to a structural model that includes non-linear properties, and the total force is plotted against a reference displacement (usually the roof displacement or lateral drift) to define a capacity curve. This can then be combined with a demand curve (typically in the form of an acceleration-displacement response spectrum (ADRS)). This essentially reduces the problem to a single degree of freedom system.

Nonlinear static procedures use equivalent SDOF structural models and represent seismic ground motion with response spectra. Story drifts and component actions are related subsequently to the global demand parameter by the pushover or capacity curves that are the basis of the non-linear static procedures.

3.1.5 Non-linear Dynamic Analysis:

When a structure is expected to reach the yielding point or when we want to achieve accurate time-history results about the performance of a structure during the period of an earthquake event, nonlinear dynamic analysis is necessary to be performed. Nonlinear dynamic analysis Utilizes the combination of ground motion records with a detailed structural model therefore is capable of producing results with relatively low uncertainty. In nonlinear dynamic analyses, the detailed structural model subjected to a ground-motion record produces estimates of deformations for each degree of freedom in the model. The non-linear properties of the structure materials are considered in the time domain

For the purpose of achieving accurate permanent plastic deformation in the structure after an earthquake and before fire starts the nonlinear dynamic analysis is performed in this study.

3.2 Seismic Behavior of Structures:

3.2.1 Wood structure:

Wood frame structures can resist earthquake if they are designed adequately. The main structural components in wood frame structures that resist earthquake are typically shear walls and diaphragms. The induced lateral load by earthquake or wind are transferred from the roof and floors, as depicted in Fig. 3.1, through diaphragm action, to supporting shear walls and eventually into the foundation (Judd 2005). A typical shear wall and diaphragm structure is shown in Figure 3-2. Wood-stud framing and sheathing panels are connected using fasteners (nails or screws). Conservatively, sheathing panels consist of a wood material, such as plywood or Glass Fiber Reinforced Polymer (GFRP) or oriented strand board (OSB).

The system of wood shear walls and diaphragms has commonly shown very good performance in earthquakes, in terms of preserving life (Zacher 1994). Despite this performance, the costs of building hazard to wood structures—for example, in the Northridge 1994 earthquake and 1992 Hurricane Andrew—has prompted an interest in shifting design emphasis from life safety to damage control (Rosowsky et al. 2002). Limiting such type of damage and loss is the main objective for future performance-based design procedures (FEMA 349). In low rise wood frame structure the main objective is to control the inter-story drift, therefore the term displacement-based design methodology is more adequate.

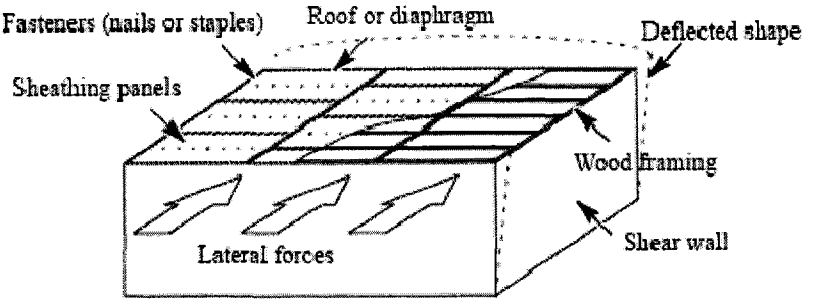

Figure 3-1 lateral force resisting system in wood structures (Judd 2005)

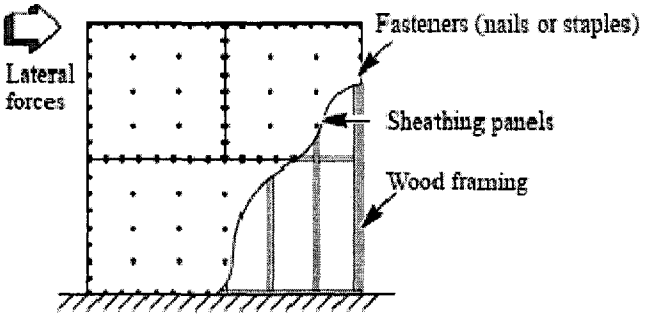

Figure 3-2 primary structural components of wood frame shear walls (Judd 2005)

The characteristics of a whole building differ from that of its components. To investigate the dynamic characteristics of wood-frame structures, Medearis (1987) subjected 63 wood homes to low amplitude vibrations. These tests indicated a building frequency range of 4 to 18 hertz, depending on building height. Sugiyama (1985) tested wooden homes constructed of plywood shear walls and found that natural frequencies ranged from about 3 to 7 hertz. Wood buildings subjected to earthquake motion often undergo torsional motion which is not resisted by wood components very well.

The greatest deficiency of wood-frame construction was found to be the lack of resistance to torsional racking. The basic cause of this motion is the eccentricity between the centers of mass and resistance at various floors of the building. Theoretical models for the lateral torsional analysis of low-rise timber structures have been developed by Naik (1982) using nonlinear springs to model the racking walls, He analyzed a two-story house and found that the first mode frequencies of the building is between1.79 and 4.0 Hertz. Using a similar model, Moody (1986) found reasonable agreement between experimental results and analytical predictions of lateral response for several wood buildings.

For the present study the displacement-based modeling is used to simulate the damage in the wood frame after earthquake. This study is performed in the 2D plane direction which does not include torsional analysis.

3.2.2 Steel structures:

The use of steel for construction has relatively increased within the last ten decades. Several elements have contributed to the growth of this domain. The general favorable performance of steel buildings in earthquakes prior to 1994 played a significant role. Specifically four earthquakes in California and Japan (San Francisco1906, Kanto 1923, Santa Barbara 1925 and Long Beach 1933) during the first part of the last century gave engineers confidence in steel as a reliable material for earthquake resistant design. During

these events, there were typically fewer problems observed in steel structures as compared with concrete and masonry buildings of similar size and scale.

An essential requirement for the integrity of any structure is to withstand the gravity and lateral loads. Steel structures should be designed adequately to resist these loads. Ignoring the effect of the lateral loads caused by wind or earthquake during the design procedure may lead to extremely large deformations or even collapse of the structure, and cause humanitarian and financial losses. But it is an obvious fact that a structural failure does not take place by itself without a technical reason. These failures may happen due to an earthquake effect, a fire, underestimated excess loading, severe wind effects or similar natural events. However, it is possible to design and construct steel buildings to resist these load effects and prevent failure. Nowadays, engineers can design any type of steel structure by considering the different types of acting loads and materials properties; a sound prediction of building loads at an acceptable level of safety defined by the codes and structural standards.

In seismic design of steel or reinforced concrete structures, it is very important to assess the ability of a structure to develop and maintain its resistance capacity in the inelastic range. A measure of this ability is called ductility, which is a mechanical property used to describe the extent to which materials can be deformed plastically without fracture (Beer and Johnston 2005). This property may be observed in the material itself, in a structural

element, or to a complete structure. At the element level μ_q is defined as the ratio of the maximum displacement (D_u) to the yield displacement (D_y). the ductility In science of structures there are three types of ductility; these three kinds are very different in their numerical values, and each one plays a significant role in seismic design.

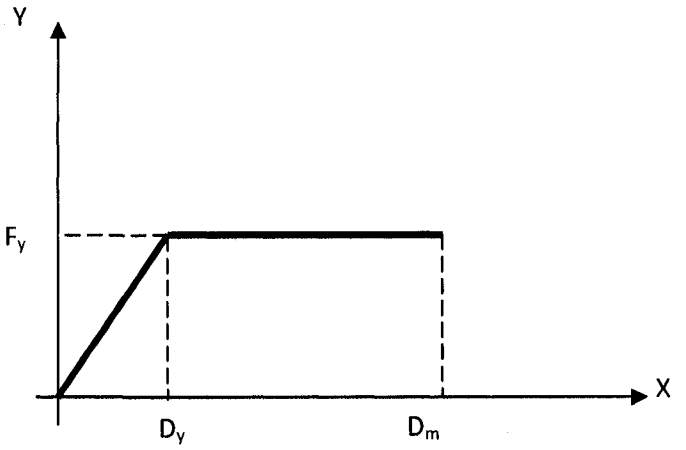

Figure 3-3 yielding and maximum displacement

a) Material ductility -μ_e, measures the ability of the material to undergo large plastic deformations. A high value of -μ_e characterizes a ductile material, a low value a brittle one.

b) Structural element or joint ductility -μ_q, characterizes the behavior of a member or joint, and particularly its ability to transmit stresses in the elastoplastic range without loss of resistance. For instance a frame structure cannot exhibit ductile behavior if the plastic hinges are not able to redistribute the bending components.

c) Structural ductility -μ_d, is an index of the global behavior of the structure, i.e. the ability of a structure to deform in the inelastic range after some of its parts have

exceeded their linear elastic range. The ductilities μ_e, μ_q and μ_d must meet the condition: $\mu_e > \mu_q > \mu_d$.

For the present study the damages caused by an earthquake has been modeled using two approaches. In the first approach an equivalent static lateral load has been applied to the structure to cause lateral deformation, and the fire load is applied subsequently. However, in the second approach a time history ground motion data has been used to the analyze structure before applying the fire load.

Chapter 4

Heat Transfer Analysis and Mechanism

4.1 General:

Heat transfer is the means of accessing the thermal energy from a hot body to a colder body. When a physical body is at a different temperature than its surrounding environment or another body that is or is not in contact with it, a *transfer of thermal energy* takes place in such a way that the body and the surroundings reach thermal equilibrium.

Heat transfer analysis is an important aspect in the study of structural performance due to a fire event, because it gives a clear prediction of the temperature and load bearing capacity of structural components as well as the burning behavior of the materials.

The modeling of the Heat transfer mechanisms involves numerous mathematical equations that describe the temperature distribution through a structure/material. The mechanisms of heat transfer are categorized mainly in the followings:

1. Conduction
2. Convection
3. Radiation

4.2 Conduction:

Conduction is the transfer of thermal energy from a region of higher temperature to a region of lower temperature through direct molecular communication within a medium or between mediums in direct physical contact without a flow of the material medium. Conduction is greater in solids, where atoms are in constant contact. In liquids (except liquid metals) and gases, the molecules are usually further apart, giving a lower chance of molecules colliding and passing on thermal energy. Thus conduction occurs within solids on a molecular scale without any movement of solid matter relative to one another. Figure 4.1 represents the conduction process occurring through an element of thickness x having constant thermal conductivity, k.

Figure 4-1 conduction occurring through an element of thickness x

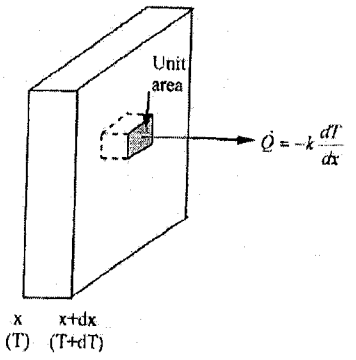

The basic equation for conductive heat transfer is given by Fourier's law as shown by Equation 4-1. The negative sign in the equation indicates that the heat flows from the higher temperature side to the lower temperature side.

$$Q = -k\left(\frac{dT}{DX}\right) \quad \text{..... 4-1}$$

Where, dT = temperature difference across a thickness of dx

Q= rate of heat transfer across material thickness of dx

k = thermal conductivity of material

So, for a material of thickness Δx with different temperatures T_1 and T_2 at its two faces, as shown in Figure 4.1, the conductive heat transfer can be written as Equation 4-2.

$$Q = -k\frac{(T_2 - T_1)}{\Delta x} \quad \text{..... 4-2}$$

4.3 Heat Conduction in a Solid in Contact with Fluid at Elevated Temperatures:

When the exposed surfaces of a solid body are in contact with fluids at elevated temperatures, the fluid temperatures are used as the boundary conditions for determining the temperature distribution in the solid body.

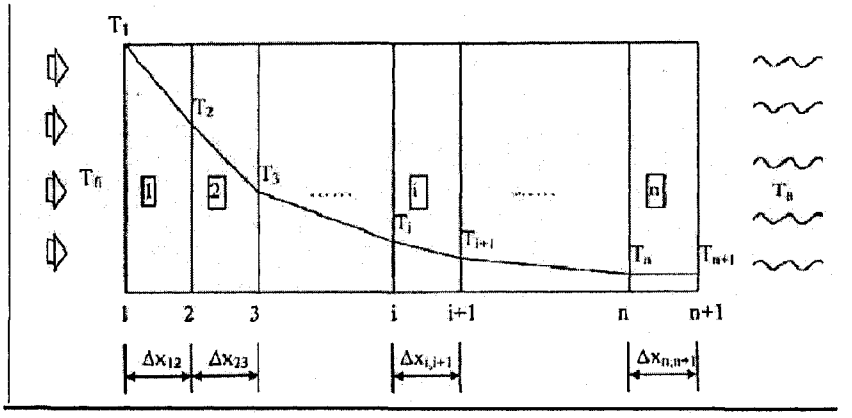

Figure 4-2 conduction through solids in contact with hot fluid layer

(Wang 2002)

Referring to Figure 4-2, the rate of heat transfer at the interface between the temperature T_{fi} and the material surface T_i is given by,

$$\boldsymbol{Q = h_{fi}(T_{fi} - T_1)} \quad \text{4-3}$$

On the ambient air side,

$$\boldsymbol{Q = h_a(T_{n+1} - T_a)} \quad \text{4-4}$$

Where:

T_{fi} = fire temperature, T_a = air temperature.

h_{fi} , and $h_a$are the overall surface heat exchange coefficients on the fire and air side respectively which depend on convective and radiative heat transfer.

4.4 Convection:

Convection is defined as the transfer of heat by motion of or within a fluid. It may arise from temperature differences either within the fluid or between the fluid and its boundary, or from the application of an external motive force. Convection heat transfer is one of the very complex problem types in engineering science. Convection is difficult to study because it is highly unpredictable in nature, and one can only make the best effort to assume certain parameters to achieve the goal of safety from the view point of flame spread (Wang 2002).

There are two types of flows:

1) Laminar

2) Turbulent

The type of flow would be an important area of study when the heat transfer process occurs through a fluid medium. In this case the heat transfer process occurs through the medium of air.

The study of convective heat transfer involves dimensionless parameters such as Nusselt number as defined below:

$$N_u = \frac{h_c L}{k} \quad \text{..... 4-5}$$

Here, L = length of solid surface

h_c = convective heat transfer coefficient

k = thermal conductivity of fluid

There are primarily two types of convection processes,

1. Forced Convection

2. Free Convection

The following two sections explain in detail the different types of convection processes.

4.5 Heat Transfer Coefficients for Forced Convection:

Heat transfer coefficients for different types of flow conditions can be found in Table 4-1 based on the values of Reynolds Number R_e, and Prandtl Number P_r, which are defined in Equations 4-6 and 4-7, respectively

$$\boldsymbol{R_e = \frac{\rho L U_O}{\mu}} \quad \text{..... 4-6}$$

$$\boldsymbol{P_r = \frac{\mu C}{k}} \quad \text{..... 4-7}$$

where, ρ = fluid density

U_o = flow velocity

μ = absolute viscosity of fluid

k = thermal conductivity

C = specific heat of air.

Table 4-1 convection coefficient (Wang 2002)

Flow type	*Condition*	*Characteristic length*	*Nu(=hL/k)*
Laminar flow, parallel to a flat plate of length L	$20 < Re < 3 \times 10^5$	L	$0.66Re^{1/2} Pr^{1/3}$
Turbulent flow, parallel to a flat plate of length L	$Re > 3 \times 10^5$	L	$0.037Re^{4/5} Pr^{1/3}$
Flow round a sphere of diameter L	General equation	L	$2 + 0.6Re^{1/2} Pr^{1/3}$

4.6 Heat Transfer Coefficients for Free Convection:

Natural convection is caused by buoyancy forces due to density differences arising from temperature variations in the fluid. At heating the density change in the boundary layer will cause the fluid to rise and be replaced by a cooler fluid that also will heat and rise. This phenomenon is called natural or free convection. Boiling or condensing processes are also referred to as convective heat transfer processes. The heat transfer per unit surface through convection was first described by Newton, and the relation is known as the Newton's Law of Cooling. The equation for convection can be expressed as:

$$\boldsymbol{Q = kAdT} \quad \text{..... 4-8}$$

Where, q = heat transferred per unit time (W)

A = surface area for heat transfer (m^2)

k = convective heat transfer coefficient for the process (W/m^2-K or W/m^2-°C)

dT = temperature difference between the exposed surface and the bulk fluid (K or °C)

Air acts as a thermal barrier and thus provides protection to the main component or material. By modeling the thermal properties of air the process of precise model building in case of finite element techniques can be facilitated. Table 4-2 presents the variation in values properties of air with increasing temperature. The general equation for Nusselt Number N_u, for the case of free convection is given by,

$$\boldsymbol{N_u = BRa^m} \quad \text{..... 4-9}$$

The values of unknowns *"B"* and *"m"* depend upon the type of flow, surface configuration, flow type and dimensions.

Where R_a is the Raleigh number and is given by the following equation,

$$\boldsymbol{R_a = Gr\ Pr} \quad \text{..... 4-10}$$

where, Pr is the Prandtl number (Equation 4-11), and *Gr* is known as the Grashof Number, which is given by,

$$\boldsymbol{G_r = \frac{gL^3\beta\Delta T}{v^2}} \quad \text{..... 4-11}$$

Where , g = acceleration due to gravity m/sec^2

β is the coefficient of thermal expansion for the fluid

ΔT is the temperature difference between fluid and solid surface °C

and v is the relative viscosity of the fluid

Table 4-2 Air properties at atmospheric pressure (engineeringtoolbox.com 2008)

Temperature - t -(^oC)	Density $\rho(kg/m^3)$	Specific heat capacity- c_p - $(kJ/kg.K)$	Thermal conductivity - l $(W/m.K)$	Kinematic viscosity - ν (m^2/s) x 10^{-6}	Expansion coefficient - b $(1/K)x10^{-3}$	Prandtl's number P_r
-150	2.793	1.026	0.0116	3.08	8.21	*0.76*
-100	1.980	1.009	0.0160	5.95	5.82	0.74
-50	1.534	1.005	0.0204	9.55	4.51	0.725
0	1.293	1.005	0.0243	13.30	3.67	0.715
20	1.205	1.005	0.0257	15.11	3.43	0.713
40	1.127	1.005	0.0271	16.97	3.20	0.711
60	1.067	1.009	0.0285	18.90	3.00	0.709
80	1.000	1.009	0.0299	20.94	2.83	0.708
100	0.946	1.009	0.0314	23.06	2.68	0.703
120	0.898	1.013	0.0328	25.23	2.55	0.70
140	0.854	1.013	0.0343	27.55	2.43	0.695
160	0.815	1.017	0.0358	29.85	2.32	0.69
180	0.779	1.022	0.0372	32.29	2.21	0.69
200	0.746	1.026	0.0386	34.63	2.11	0.685
250	0.675	1.034	0.0421	41.17	1.91	0.68
300	0.616	1.047	0.0454	47.85	1.75	0.68
350	0.566	1.055	0.0485	55.05	1.61	0.68
400	0.524	1.068	0.0515	62.53	1.49	0.68

4.7 Radiation:

In the case of radiative heat transfer, there exists the phenomena of absorptivity α, reflectivity ρ, and transmissivity τ that represent the fractions of incident thermal radiation that a body absorbs, reflects and transmits, respectively.

$$\alpha+ \tau+ \rho=1 \quad \text{..... 4-12}$$

A blackbody is a perfect emitter of heat. The total amount of thermal radiation emitted by a blackbody is given by

$$E_b = \sigma T^4 \quad \text{..... 4-13}$$

Where, σ = Stefan-Boltzmann constant = $5.67*10^{-8}$ W/ m^2 K^4

T = absolute temperature in K.

For analytical purposes, the radiant thermal exchange between two blackbodies as shown in Figure 4-3, can be calculated on the basis of the following equation (Wang 2002),

$$d\dot{Q}_{dA1\rightarrow dA2} = E_{b1}\frac{\cos\theta_1 \cos\theta_2}{\pi r^2} dA_1 dA_2 \quad \text{..... 4-14}$$

Where, dA_1, dA_2 are areas of radiating and receiving surfaces respectively.

θ_1 and θ_2 are the respective angles,

E_{b1} is the thermal radiation per unit surface of $A1$

r is the distance between the two surfaces.

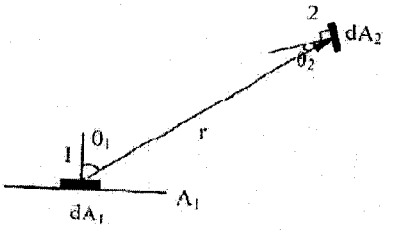

Figure 4-3 radiation between tow surfaces (Wang 2002)

4.8 View Factor:

As shown in Figure 4-3, consider two surfaces A_1 and dA_2 where A_1 is the emitting surface. The total thermal radiation from A_1 to dA_2 is given by Equation 4-15 (Wang 2002), as given below.

$$Q_{A1-dA2} = \int \left(\frac{E_{b1}\cos\theta_1 \cos\theta_2}{\pi r^2}\right) d_{A1} d_{A2} = \Phi\, E_{b1} dA_2 \quad \text{..... 4-15}$$

The configuration factor or view factor, Φ represents the fraction of thermal radiation from A_1 to dA_2. The configuration or view factor has a maximum value of 1.0, and it is additive in nature. For the case of a complex structure, individual view or configuration factors can be found for different elements broken down into smaller parts. The resultant view or configuration factor can then be obtained by summation of all the corresponding factors. The factor "Φ" plays an important role in numerical modeling of heat transfer as it determines the overall thermal response of a structure. Radiation plays a key role as the amount of heat that is emitted from a surface contributes towards the overall fire event, and thus the temperature rise within supporting members.

4.9 Heat Transfer in Fire:

In case of a fire, the heat is transferred from combustion and hot gases to solid surfaces by radiation and convection (Wickstrom et al. 2007). the two contributions make up the *net* total heat flux,

$$Q_{tot} = Q_{rad} + Q_{con} \quad \text{4-16}$$

The radiation term in the above formula is the difference between the absorbed incident radiation and the radiation emitted from the surface. The heat transmitted through the surfaces is neglected, and no consideration is given to the influence of various wavelengths. Thus, as the absorptivity and emissivity are equal, the net heat received by the surface may be written as:

$$Q_{rad} = \varepsilon(Q_{inc} - \sigma T_s^4) \quad \text{4-17}$$

Where Q_{inc} is the incident radiation, σ the Stefan Boltzmann constant, and T_s is the surface temperature.

The emissivity, ε, is a material property related the surface condition. It can be measured, but, in most cases of structural materials being exposed to fire, it can be assumed equal to 0.8 (Wickstrom et al. 2007). Because fires are characterized by non-homogeneous temperature distributions, the incident radiation heat flux should ideally include contributions from nearby flames, hot gases, and surfaces, in which case the incident radiation may be written as the sum of the contributions from all of the radiating sources:

$$\boldsymbol{Q_{inc} = \sum_i \varepsilon_i \Phi_i \sigma T_i^4} \quad \text{..... 4-18}$$

Here ε_i is the emissivity of the i^{th} flame or surface, and σ is the Stefan-Boltzmann constant. Φ_i and T_i are the corresponding view factor and temperature, respectively. To obtain the incident radiation using Eq.4-18 is in general very complicated, but current generation fire models all have various algorithms for calculating it.

The convective heat flux depends on the difference between the surrounding gas temperature and the surface temperature. It is often assumed proportional to this difference and is then written:

$$\boldsymbol{Q_{con} = h(T_g - T_s)} \quad \text{..... 4-19}$$

where h is the heat transfer coefficient and T_g the gas temperature adjacent to the exposed surface.

From the discussion above, the total net heat flux to a surface can be expressed:

$$\boldsymbol{Q_{tot}} = \varepsilon(\boldsymbol{Q_{inc}} - \boldsymbol{\sigma T^4}) + \boldsymbol{h}(\boldsymbol{T_g} - \boldsymbol{T_s}) \quad \text{4-20}$$

Chapter 5

Material Properties at Elevated Temperatures

5.1 General:

Materials properties change significantly when it is exposed to high temperature, these changes including the mechanical and thermal properties; affect the behavior and the total capacity of the structure dramatically. High temperature usually cause an increase in some thermal properties such as the conductivity and the specific heat, while it reduces the mechanical properties, like the modules of elasticity, yield stress and the overall structural capacity.

5.2 Mechanical Properties:

5.2.1 Modulus of elasticity:

Modulus of elasticity is the mathematical description of an object or substance's tendency to be deformed elastically when a load is applied to it. The elastic modulus of an object is defined as the slope of its stress-strain curve in the elastic deformation region.

The stress strain relationship in the elastic domain is presented through Hook's law as given in Equation 5-1,

$$\sigma = E.\varepsilon \quad \text{.....Eq. 5-1}$$

Where

σ Is the stress [force /area]

ε is the strain; the strain is a dimensionless number equals to the ratio of the change in dimension to the original dimension.

and E is the elastic modulus of elasticity.

When a substance is expose to extremely high temperature, the modules of elasticity decreases significantly until it reaches zero when the material melts (e.g. in steel), or chars (e.g. in wood).

5.2.2 Thermal Expansion:

Thermal Expansion is the tendency of matter to change its dimensions in response to temperature changes. Most materials expand when they are heated and contract when they are cooled down.

The tendency of a material to change its size with respect to the changes in its temperature is measured by a coefficient called the coefficient of thermal expansion α. This coefficient is very important in calculating the thermal expansion and the thermal stresses of an element.

For example for a beam or truss element; the change in length due to temperature change is given by the following equation:

$$\delta_T = \alpha(\Delta T)L \quad \text{.....Eq. 5-2}$$

Where : δ_T is the change in length.

α is the thermal coefficient of the material.

ΔT is the change in temperature

and L is the length of the element.

Where thermal strain can be calculated then form Equation 5-2:

$$\varepsilon_t = \alpha \Delta T \quad \text{.....Eq. 5-3}$$

and the thermal stress can be found as:

$$\sigma = -E\alpha\Delta T \quad \text{.....Eq. 5-4}$$

Where E is the modulus of elasticity.

This coefficient is relatively constant in temperatures below 100^0C, however it changes notably in high temperatures above 500^oC.

5.3 Physical properties:

5.3.1 Density of material (ρ):

The density is the measure of how dense the matter is, and is defined as the mass per unit volume of the material (Equation 5-5).

$$\rho = \frac{m}{V} \quad \text{.....Eq. 5-5}$$

Where m is the mass, and V is the volume.

Generally density changes with temperature, and this change is due either to the physical change in the material phase or because of the losing of some components like water, or even by changing to another material for example when it burns to char.

The change in material density due to fire exposure is sometimes represented by the mass loss, which is the measurement of loss in weight because of burning or dehydration reactions.

5.4 Thermal Properties:

5.4.1 Thermal Conductivity:

Thermal Conductivity k, is the property of a material that indicates its ability to conduct heat, and is calculated by the heat flow across a surface per unit area per unit time, divided by the negative of the rate of change of temperature with distance in a direction perpendicular to the surface.

5.4.2 Emissivity of a Material (ε):

Emissivity of material is the ratio of energy transferred by radiation from a particular material to energy radiated by a black body at the same temperature, so it is a dimensionless quantity. It is a measure of a material's ability to radiate absorbed energy.

A true black body would have an $\varepsilon = 1$ while any real object would have $\varepsilon < 1$. Emissivity is very important in heat transfer during fire since the biggest portion of thermal energy transferred to exposed members comes from radiation.

5.4.3 Specific Heat:

Special heat (C) is the quantity of heat energy per unit mass required to elevate the temperature by one degree. The correlation between heat and temperature change is usually expressed in the equation shown below (Eq. 5-6) where c is the specific heat.

$$Q=C.m.\Delta T \quad \text{.....Eq. 5-6}$$

Some Materials properties are collected from the NRC (National Research Council of Canada) fire tests reports (Bénichou et al. 2001), others are considered from SAFIR user manual (Franssen ct al. 2000). Wood, gypsum boards and insulation fibers are taken from NRC reports where steel properties in fire are taken from SAFIR code. For plywood properties are taken from Canadian plywood manual (CANPLY 2008).

For gypsum boards and insulation, no mechanical properties are considered, only their thermal properties are used.

5.5 Properties of used Materials in this study:

5.5.1 Steel Properties:

5.5.1.1 Thermal properties:

5.5.1.1.1 Thermal capacity: C_a: The following ranges of temperature (θ_a) dependent values of the thermal capacity, C_a has been defined in SAFIR (Franssen et al. (2000):

for $20°C \leq \theta_a < 600°C$:

$$ca = 425 + 7.73 \text{ x } 10\text{-}1\theta_a - 1{,}69 \text{ x } 10\text{-}3\theta_a^2 + 2{,}22 \text{ x } 10^{-6}\ \theta_a^3 \text{ J/kgK}$$

for $600°C \leq \theta_a < 735°C$:

$$c_a = 666 + \frac{13002}{738 - \theta_a} \text{ J/kgK}$$

for $735°C \leq \theta_a < 900°C$:

$$c_a = 545 + \frac{17820}{\theta_a - 731}$$

for $900°C \leq \theta_a \leq 1200°C$:

$$c_a = 650 \text{ J/kgK}$$

where θ_a is the steel temperature [°C].

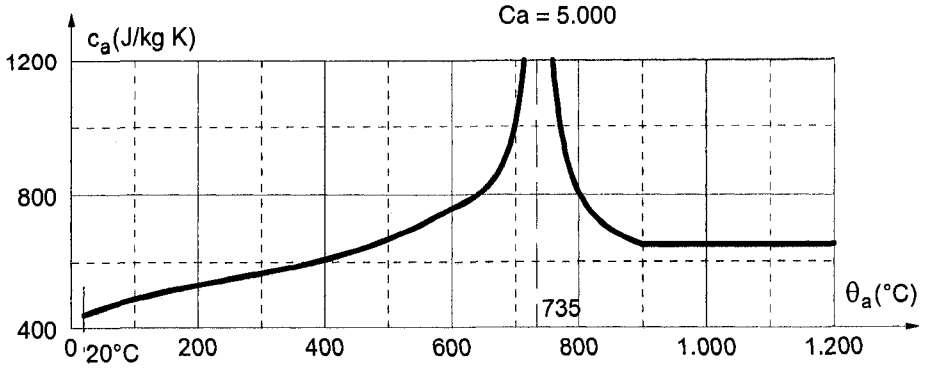

Figure 5-1 Thermal capacity of steel in high temperature

5.5.1.1.2 Thermal conductivity, λ_a:

for $20°C \leq \theta_a < 800°C$:

$$\lambda_a = 54 - 3{,}33 \times 10^{-2}\ \theta_a \text{ W/mK}$$

for $800°C \leq \theta_a \leq 1200°C$:

$$\lambda_a = 27{,}3 \text{ W/mK}$$

Thermal Conductivity [W/mK]

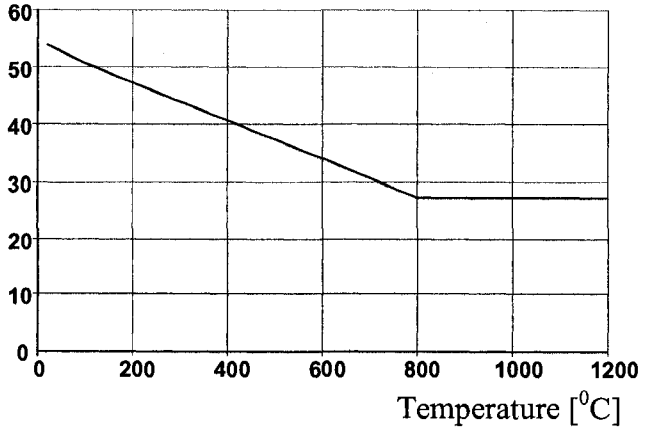

Figure 5-2 thermal conductivity of steel

5.5.1.2 Physical and Mechanical properties:

5.5.1.2.1 Stress-strain relation: is presented through the table 5-1 and figure 5-3.

Table 5-1 stress strain Relationship equation (Franssen et al. 2000)

Strain domain	Stress σ	Tangent modulus
$\varepsilon \le \varepsilon_{p,\theta}$	$\varepsilon E_{a,\theta}$	$E_{a,\theta}$
$\varepsilon_{p,\theta} < \varepsilon < \varepsilon_{y,\theta}$	$f_{p,\theta} - c + (b/a)[a^2 - (\varepsilon_{y,\theta} - \varepsilon)^2]^{0,5}$	$\frac{b(\varepsilon_{y,\theta} - \varepsilon)}{a\left[a^2 - (\varepsilon_{y,\theta} - \varepsilon)^2\right]^{0,5}}$
$\varepsilon_{y,\theta} \le \varepsilon \le \varepsilon_{t,\theta}$	$f_{y,\theta}$	0
$\varepsilon_{t,\theta} < \varepsilon < \varepsilon_{u,\theta}$	$f_{y,\theta}[1 - (\varepsilon - \varepsilon_{t,\theta})/(\varepsilon_{u,\theta} - \varepsilon_{t,\theta})]$	$- f_{y,\theta} / (\varepsilon_{u,\theta} - \varepsilon_{t,\theta})$
$\varepsilon = \varepsilon_{u,\theta}$	0	0
Parameters	$\varepsilon_{p,\theta} = f_{p,\theta}/E_{a,\theta}$; $\varepsilon_{y,\theta} = 0,02$; $\varepsilon_{t,\theta} = 0,15$; $\varepsilon_{u,\theta} = 0,20$	
Functions	$a^2 = (\varepsilon_{y,\theta} - \varepsilon_{p,\theta})(\varepsilon_{y,\theta} - \varepsilon_{p,\theta} + c/E_{a,\theta})$ $b^2 = c(\varepsilon_{y,\theta} - \varepsilon_{p,\theta})E_{a,\theta} + c^2$ $c = \frac{(f_{y,\theta} - f_{p,\theta})^2}{(\varepsilon_{y,\theta} - \varepsilon_{p,\theta})E_{a,\theta} - 2(f_{y,\theta} - f_{p,\theta})}$	

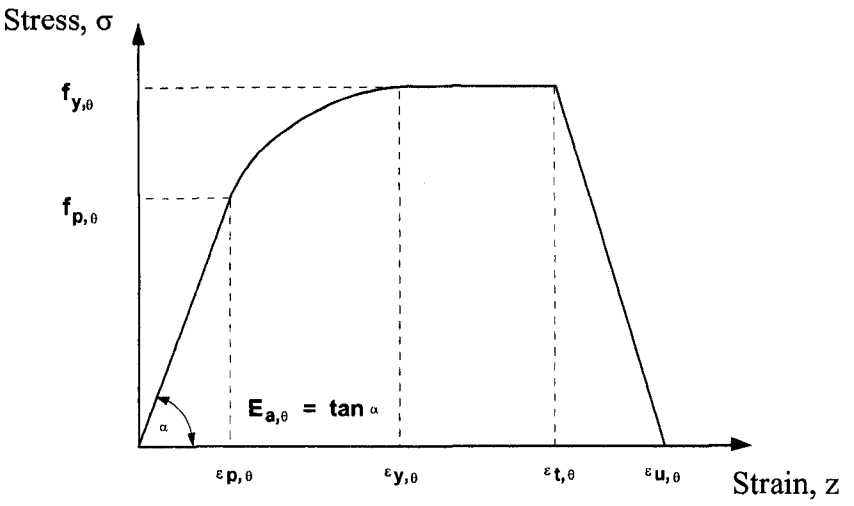

Figure 5-3 stress-strain relationship in normal temperature (Franssen et al. 2000)

Where:

$f_{y,\theta}$ is the effective yield strength

$f_{p,\theta}$ is the limit of proportionality

$E_{a,\theta}$ is the slope of the elastic domain

$\varepsilon_{p,\theta}$ is the strain at the limit of proportionality

$\varepsilon_{y,\theta}$ is the strain at the effective yield strength

$\varepsilon_{t,\theta}$ is the limit plastic strain

$\varepsilon_{u,\theta}$ is the ultimate strain

The modulus of elasticity of steel reduces with temperature; the reduction factor is shown in figure 5-4.

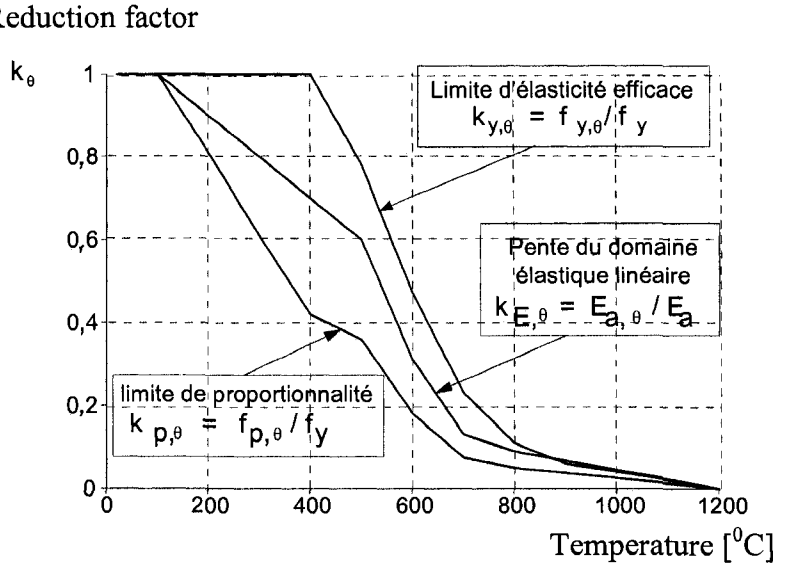

Figure 5-4 reduction factor for modulus of elasticity (Franssen et al. 2000)

5.5.1.2.2 Specific mass:

$\rho_a = 7850$ kg/m^3

5.5.1.2.3 Thermal expansion:

The thermal strains ($\Delta l / l$) or the rate of change in length due to temperature is dependent on temperature θ_a.

for $20°C \leq \theta_a < 750°C$:

$$\Delta l / l = 1{,}2 \times 10^{-5}\theta_a + 0{,}4 \times 10^{-8}\theta_a^2 - 2{,}416 \times 10^{-4}$$

for $750°C \leq \theta_a \leq 860°C$:

$$\Delta l / l = 1{,}1 \times 10^{-2}$$

for $860°C < \theta_a \leq 1200°C$:

$$\Delta l / l = 2 \times 10^{-5}\theta_a - 6{,}2 \times 10^{-3}$$

where : l is the length at 20°C

Δl is the length variation dur to temperature variation

θ_a is the steel temperature [°C]

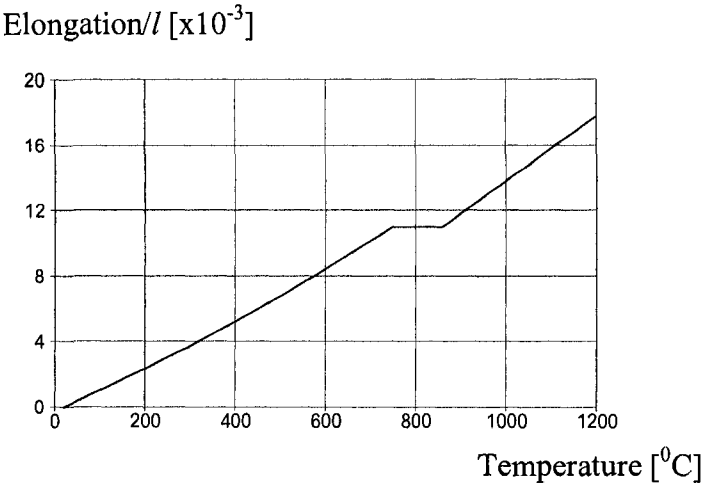

Figure 5-5 thermal strain of steel (Franssen et al. 2000)

5.5.2 Wood Properties:

5.5.2.1 Thermal properties:

5.5.2.1.1 Thermal Conductivity of wood:

Thermal conductivity of wood generally increases with temperature rise. However, this change is not same for all wood species and it is moisture dependent. The change in thermal conductivity of wood with temperature is shown in Figure 5-6.

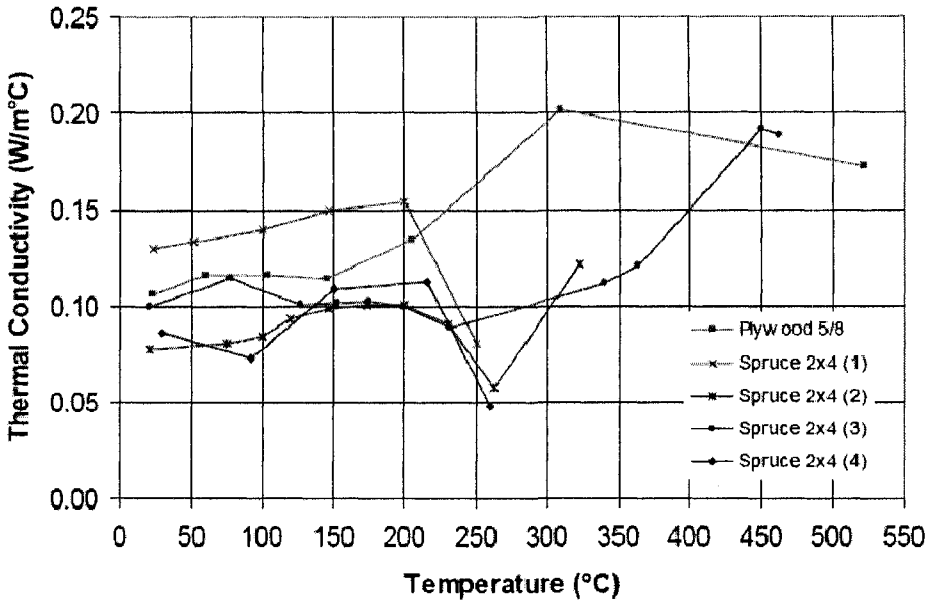

Figure 5-6 thermal conductivity of wood (Bénichou et al. 2001)

5.5.2.2 Physical and Mechanical properties:

5.5.2.2.1 Modulus of elasticity:

Wood is an orthotropic material which means it has two or three mutually orthogonal two-fold axes of rotational symmetry, so that its mechanical properties are different along the directions of each of the axes. Generally wood has two different modulus of elasticity corresponding to the two directions; the grain direction and normal-to-grain direction; in the present analysis the parallel to grain direction modulus of elasticity has been considered since the main applied load and action in the present model is parallel to grain.

Wood modulus of elasticity reduces as temperature increases. Many numerical and experimental models are available to represent this change. The model considered here is

shown in equation 5-7, which has been verified and used by Benichou and Morgan (2003). The modulus of elasticity at a particular time is given by the following equation:

$$E_i=E0*10^6*[1-(0.4*(T-20)/(T_c-20))] \quad \text{.....Eq. 5-7}$$

Where:

E_i: is the modulus of elasticity of wood at instant t [MPa].

E_0: is the modulus of elasticity of wood at normal ambient temperature [MPa].

T: is the stud temperature at moment t [^{0}C].

T_c: the Charring temperature of wood 288^{0}C.

5.5.2.2.2 Density:

The density of wood is about 500 kg/m^3 and it changes with temperature because of the dehydration within the first 100 degrees. Then when wood reaches charring temperature which is in range of 288-320 °C, it turn into burned substance which is quietly lighter than wood. This loss in mass is presented usually through the charring rate. The charring rate for wood according to the NBCC is 0.6 mm per minute. The change in mass because of the dehydration is not considered in this analysis since it is much smaller than the charring effect and it does not affect the accuracy of our study.

5.5.3 Plywood properties:

5.5.3.1 Thermal properties:

Plywood thermal properties are considered to be similar that of wood.

5.5.3.2 Physical and Mechanical properties:

5.5.3.2.1 Density is assumed to be 450kg/m^3 and it assumed to change a in similar way as wood.

5.5.3.2.2 Modulus of elasticity is assumed to be 12.4 GPa and considered to change according to the model in Equation 5-7.

5.5.4 Gypsum Properties:

5.5.4.1 Thermal properties:

5.5.4.1.1 Thermal conductivity:

Thermal conductivity if gypsum generally increases with temperature, as shown in Figure 5-7.

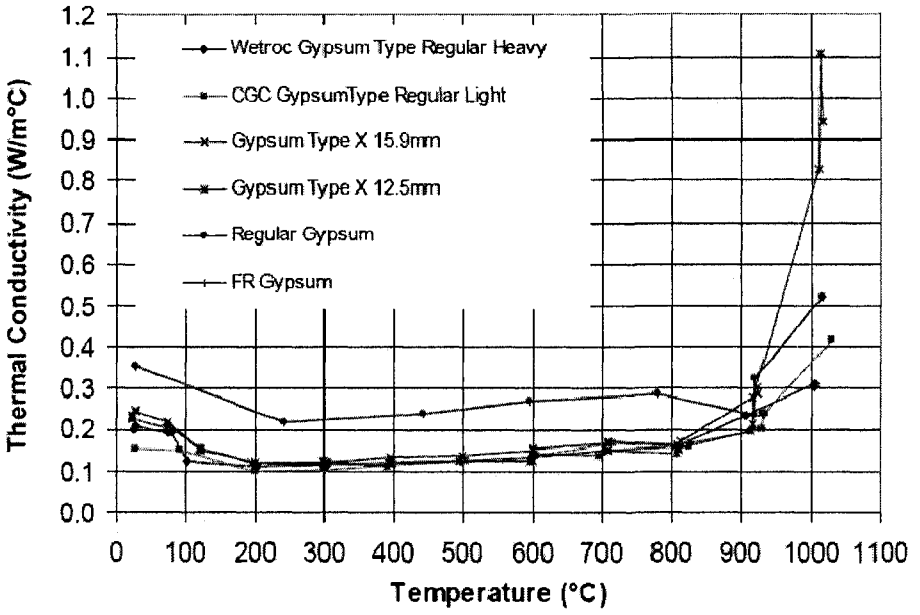

Figure 5-7 Thermal conductivity of gypsum wallboard (Bénichou et al. 2001)

5.5.4.1.2 Specific heat:

Specific heat, C of gypsum increases in the first 120 °C due to the energy released in the dehydration reaction. Then it goes back to the normal level after the gypsum is completely dry as presented in Figure 5-8.

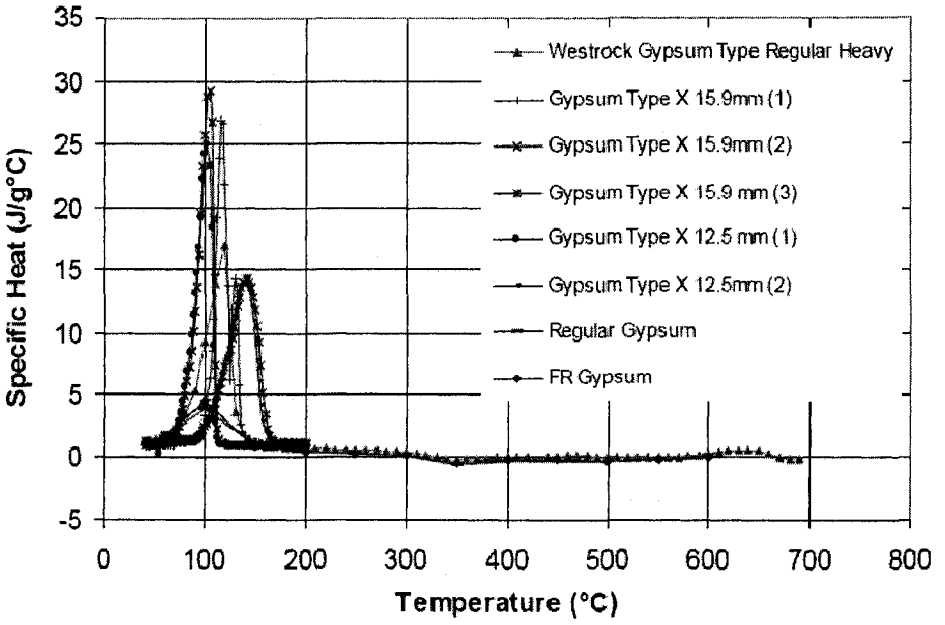

Figure 5-8 Specific heat of gypsum wallboard (Bénichou et al. 2001)

5.5.4.1.3 Mass loss:

Mass loss of gypsum appears to be independent of gypsum types as can be seen in Figure 5-9.

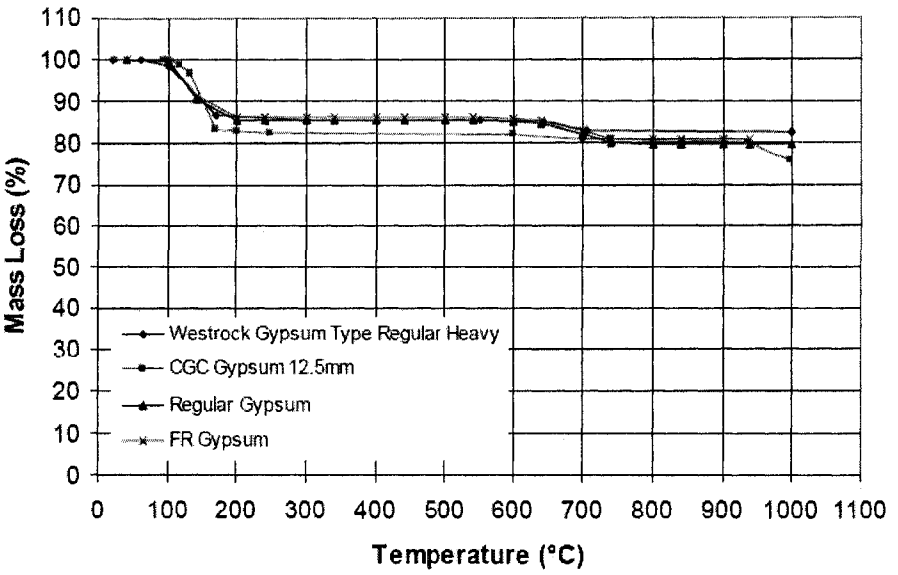

Figure 5-9 Mass loss of gypsum wallboard (Bénichou et al. 2001)

5.5.5 Insulation:

5.5.5.1 Thermal properties:

5.5.5.1.1 Thermal conductivity:

Thermal conductivity of insulation materials is very small and it does not change significantly until the material reaches high temperatures. The change in thermal conductivity of different types of gypsum is presented in Figure 5-10.

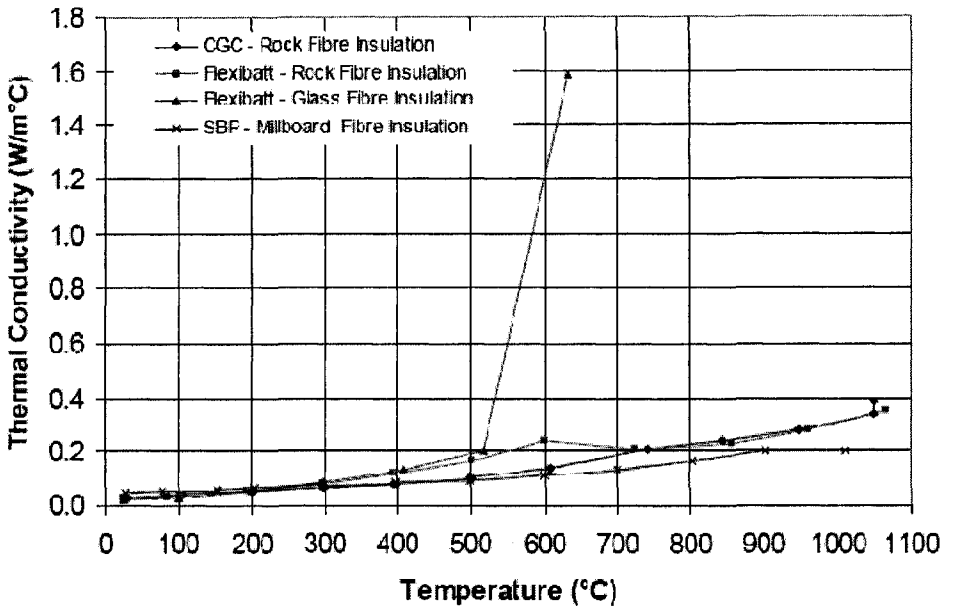

Figure 5-10 Thermal conductivity of insulation (Bénichou et al. 2001)

5.5.5.1.2 Specific heat:

Specific heat of different types of insulation is shown in Figure 5-11.

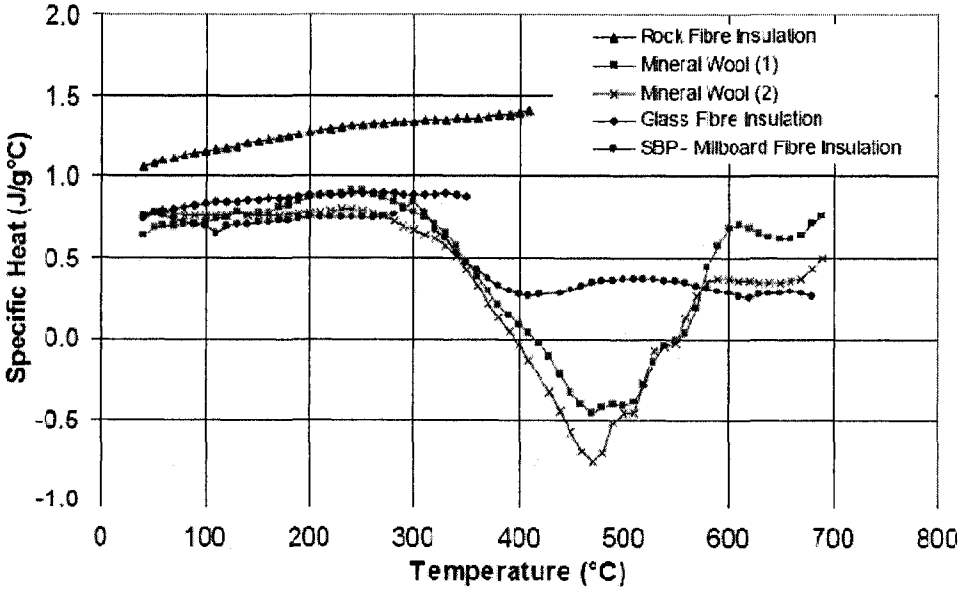

Figure 5-11 Specific heat of insulation (Bénichou et al. 2001)

5.5.5.1.3 Mass loss

Mass loss of insulation is highly dependent on the type of insulation as shown in Figure Figure 5-12 Mass loss of insulation (Bénichou et al. 2001). Glass fiber insulation looses mass at a faster rate as compared to the rock-fiber insulation.

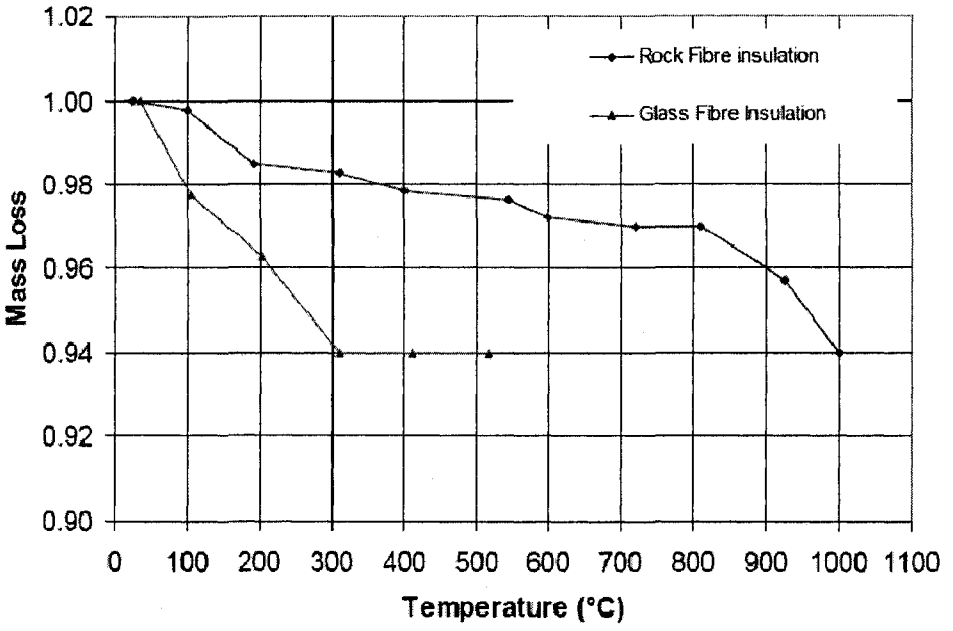

Figure 5-12 Mass loss of insulation (Bénichou et al. 2001)

Chapter 6

Structures in Fire

6.1 Wood Structure Behavior in Normal and Post-Earthquake Fires:

Wood is a combustible material and hence, fire safety is a concern in wood-frame structures which is common in residential housing in North America. Light wood frame structures can have good fire resistance if an appropriate designing and protection methods have been considered. Previous fire events in such building show that providing the structural members with enough Gypsum boards covering would prevent the spread of fire between compartments and keep on the load-bearing capacity of light steel frame or light timber frame for the duration if a severe fire (Buchanan 2001) .

When gypsum board lining is exposed to fire the surface temperature of the exposed side would rise up to 100°C, and at this point the temperature would slowly go up. The reason of this delay is the degradation of the gypsum molecules. The crystallized water begins to drive off and immigrate through the gypsum board thickness away from the fire. This process continues slowly until the entire board has been dehydrated. After that the temperature gradient through the wall will increase steadily with time.

Dehydration of gypsum boards will turn it to gypsum powder and the cavity then would be exposed directly to fire without any protection. This process is called *calcination* of gypsum board. The type of cavity insulation plays an important factor after the calcination take place. According to the NRC fire test reports (Kodur et al. 1996), the failure of the glass fiber insulated wall assembly occurred at 42 minutes, while the failure of the rock fiber insulated assembly occurred at 54 minutes. Therefore the use of rock fiber insulation provides a better fire resistance compared to glass fiber insulation. This is very important in the case of PEF since the gypsum board will suffer so many cracks and damages after the earthquake (Judd 2005) and the cavity then should face the elevated temperatures with no protection.

The location and type of shear membrane also affect the fire resistance of the stud-wall. As reported by Kodur et al. (1996), the wall assembly with the shear panel of ply wood on the exposed side endured fire for 48 minutes while the assembly with the shear panel on the unexposed side lasted 42 minutes. On the other hand, the fire resistance rating obtained for the shear wall assembly with OSB was 47 minutes.

As fire continues the following two main phenomena might lead to complete failure in the assembly; changes in the mechanical properties of construction materials, and charring in wood. The mechanical properties of wood will decrease and change rapidly. The modulus of elasticity of wood decreases, while the thermal stresses in the stud due to the thermal expansion of wood increases, and eventually the charring in wood starts.

These three physical events significantly weaken the wood member. The charring temperature is usually between 280 and 300°C. The cross sectional area and moment of inertia of the stud and the sheathing change due to charring. This change in the cross section properties depends on the charring rate. A typical value of the charring rate of wood is approximately 0.5 - 1 mm/min as suggested in Euro code (EN 1995). Table 6-1 shows design values of charring rate for various wood products as presented in the European design standards EN 1995-1-2.

In Canada, analytical expressions for the fire performance of glue-laminated beams and columns are described in Appendix D-2.11 of the National Building Code of Canada (NBCC 2005). These expressions imply a charring rate of 0.6 mm/min.

Table 6-1 charring rate for different types of wood (EN 1995-1-2)

Product	β_0 (mm/min)	β_n (mm/min)
a) Softwood and beech		
Glued laminated timber with $\rho_k \geq 290$ kg/m^3	0.65	0.7
Solid timber with $\rho_k \geq 290$ kg/m^3	0.65	0.8
b) Hardwood		
Solid or glued laminated hardwood with $\rho_k = 290$ kg/m^3	0.65	0.7
Solid or glued laminated hardwood with $\rho_k \geq 450$ kg/m^3	0.50	0.55
c) LVL		
with $\rho_k \geq 480$ kg/m^3	0.65	0.7
d) Panels		
Wood panelling *)	0.9	–
Plywood *)	1.0	–
Wood-based panels other than plywood *)	0.9	–

*) The values apply to $\rho_k = 450$ kg/m^3 and $d = 20$ mm. For other densities ρ_k and thicknesses d, charring rates can be calculated by multiplying β_0 with correction factors $\sqrt{450/\rho_k}$ and $\sqrt{20/d}$.

Based on this rate of change in the cross sectional area, the section centriod, and the moment of inertia of the stud at each instance during the fire time can be calculated. These values of area and moment of inertia are then utilized in the calculation of the

buckling load in the sheathing stud wall assembly during fire. The buckling in the wood stud wall will occur mainly because of the degradation of the studs stiffness, due to high temperatures; i.e. degradation of modulus of elasticity of wood, adding to that the change in the cross sectional area and moment of inertia, as a result of charring, and the increasing in the applied vertical load on the studs which comes from the reaction of the frame toward the stud because of the thermal strain in these studs where the applied vertical load from the ceiling is constant.

6.2 Buckling Analysis:

The structural failure mode of wood stud in fire wall takes the form of buckling. Buckling happens when the thermal stresses becomes higher than the buckling capacity of the wall. Factors like changes in wood strength and section in elevated temperatures play an important factor in weakening of the wall. The critical load of wall has been calculated using linear and nonlinear analysis. Benichou and Morgan (2003) developed a simplified model for calculating the critical load of the wall by modeling the whole assembly with pined-pined beam. In their model they considered the degradation in the mechanical properties of wood during fire. In addition to that they considered the eccentricity of the load on the stud due to the continuous weakening of members. Results from simplified model were different from the experimental data. A justification then had to be made by considering the location of the stud in the wall and the opening of the gypsum board in calculating the overall critical load of the wall.

However, the NRC simplified model, (Benichou and Morgan 2003), was intended for the walls without shear membrane. The load bearing wood stud walls are usually supported by shear panels. In North America Plywood and OSP boards are commonly used in this type of construction.

The buckling analysis of the wood stud wall with shear membrane should consider the composite action between the sheathing and studs. Linear model based on the classic theory of buckling has been developed by Kamiya (1987) to address this issue.

This model has been developed originally for static load with constant material properties. In the present research the model of Kamiya (1987) has been modified to account for time dependent material properties in order to calculate the buckling capacity of the wood stud wall at each moment during fire. In the present formulation, the quantities representing the modulus of elasticity of wood and plywood boards, the cross sectional moment of inertia are expressed as functions of time or temperature.

The critical buckling load is calculated at each instance during the fire history based on the composite interaction between the shear membrane board, i.e. the OSP or Plywood board, and the studs frame. For this analysis an effective length through the wall length has been studied and following assumptions have been made (Kamiya 1987):

1. The effective width of the sheathing can be considered to be constant along the length and is the same as the effective width when the wall is bent by uniformly distributed loads.

2. Buckling of the sheathing does not occur.
3. The separation between the stud and the sheathing does not occur.
4. The elastic and geometric properties of the stud and the sheathing are constant along the length, and nails that fasten the sheathing to the studs have the same capacity and spacing.
5. The load-slip relationship of the connections between the stud and the sheathing is reversible and is not hysteretic.

The previous assumptions are valid for the normal static loading circumstances; however after the earthquake the wall could have a new geometry. The damage because of the seismic load should be considered and degradation in the fasteners' stiffness has to be accounted for. In other words, the connection between sheathing and studs might have been weakened, the sheathing might have some cracks and nail could slip partly or completely from the wall. The slip of the nails inside the thickness of the plywood makes them overdriven which reduce the wood shear wall from 5 to 22%, depending on the depth the nails are overdriven (Fonseca 2004). These factors are taken into account by decreasing the overall initial composite stiffness of the wall and modulus of elasticity of wood and shear membrane material in the calculations.

The following model has been developed by Kamiya (1987) for the linear analysis of the buckling of the sheathing in walls. Another nonlinear model has been developed by the same author. He obtained similar results from both models and thus for simplicity of modeling the linear model has been considered in this research.

The governing equation of the deflection at any point over the height of the wall is given in Equation 6-1.

$$-\frac{d^2y}{dx^2}=\frac{M_s}{E_sI_s}=\frac{M_p}{E_pI_p}=\frac{M_s+M_p}{E_sI_s+E_pI_p}=\frac{P(y+e)+N_p}{D} \qquad \text{..... 6-1}$$

Where:

$$D=E_sI_s+E_pI_p \text{ ..... 6-2}$$

In which E_s,E_p are the modulus of elasticity of stud and plywood board respectively. and I_s,I_p are the moments of inertia.

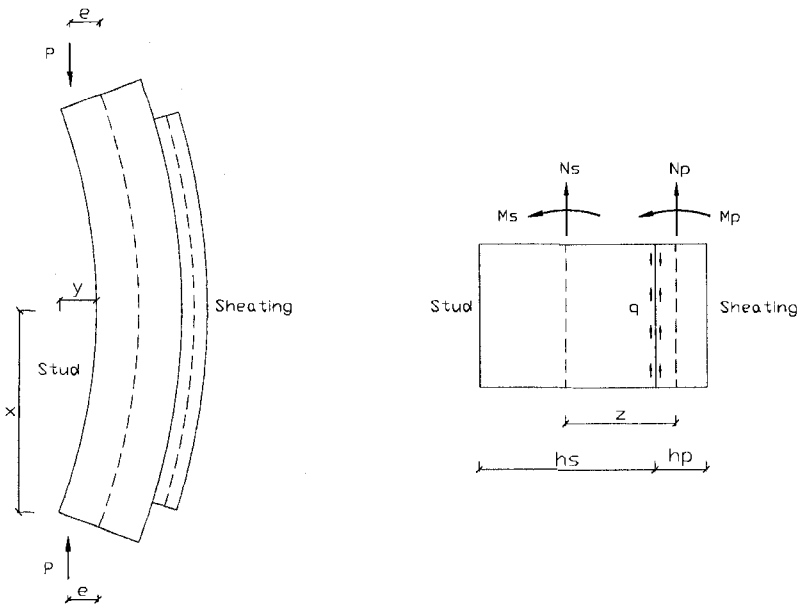

Figure 6-1 The sheathing to framing buckling model

By solving equation 6-1 we get the deflection y at the any point over the height of the stud.

$$y = \frac{b^2A+B}{a^2+b^2}\left(\tan\frac{aL}{2}\sin ax + \cos ax\right) - \frac{a^2A-B}{a^2+b^2}\left(\tanh\frac{bL}{2}\sinh bx - \cosh bx\right) - A \quad \text{6-3}$$

Where

$$A = e + (Z/E_sA_sC) \quad \text{6-4}$$

and

$$B = \frac{Pe}{D} \quad \text{6-5}$$

P is the applied load and e is the distance between the loading point and the centriod of the stud cross section.

We can get the deflection at the mid-height of the wall by substituting x by L/2.

The critical load for the wall is then calculated from the following equation:

$$P_{cr} = \frac{\beta D\pi^4 + L^2(CD+Z^2)}{\beta L^2\pi^2 + CL^4} \quad \text{6-6}$$

Where: $\beta = S_p/K$; in which Sp is the spacing between the fasteners and K is the stiffness of those fasteners.

D is calculated from equation 6-2

C is calculated from equation 6-7

$$C = 1/E_s A_s + 1/E_1 A_p \quad \text{..... 6-7}$$

L is the height of the wall.

and

$$Z = h_s/2 + h_p/2 \quad \text{..... 6-8}$$

where h_s,h_p are the depth of the stud and the sheathing respectively.

During the analysis of the stud wall the critical load with normal and PE fire can be calculated and compared with the applied one.

In the present research, parameters like A_s, K, I_s, etc are expressed as functions of time t or temperature (T).

6.3 Behavior of Steel Structure in Normal and Post Earthquake Fire:

When a steel structure is exposed to fire, the steel temperatures increase (Buchanan 2000) and consequently the strength and stiffness of steel are decreased. The degradation in members' stiffness due to high temperature and the increase in the thermal stresses due to the thermal expansion in steel members at the same time, would lead to structural failure. The time for the structure to fail due to the fire exposure is called the *fire resistance*. This duration is based on the following factors:

1. Severity of the fire.
2. Type of fire protection

3. Sections dimensions and geometry of the structure.

4. The internal stresses in the member sections due to the applied load before fire.

Unprotected steel structures have poor performance in fire compared with the protected ones. That is basically due to the thermal properties of steel. Steel like most metals has high thermal conductivity and thermal expansion factor. Thermal expansion of steel can cause damage in the building (Buchanan 2000).

For the present study it is assumed that no protection lasts after the earthquake since the usual fire protection for steal elements may be severely damaged due to seismic action. The most important factors in modeling the damage in the structure are the new geometry of the structure after earthquake due to the permanent deformations and the internal stresses in the sections in this new configuration. The plastic strains in the structure after earthquake will contribute significantly to the overall fire resistance of the structure.

The new system, after earthquake has less capacity, unstable deformed shape, and internal residual stresses. These factors besides the changes in the properties of steel in high temperatures are included in our nonlinear time history analysis in the fire regime.

6.4 Fire and Structural Modeling Issues:

After defining the structure's physical state after an earthquake, it is necessary to select a fire scenario and the model the fire resistance of structural components. As far as the fire scenario is concerned, it should be assumed in such a way that it produces the most severe effect on the earthquake-damaged structure (Cortea et al. 2003).

Fire assumed to happen at the center of the room space and temperature has been assumed uniform inside the compartment and monotonically increasing in accordance with the time–temperature curve suggested by the standard CAN/ULC-S101-M89 which is similar to ASTM E119 as shown in Figure (6-2).

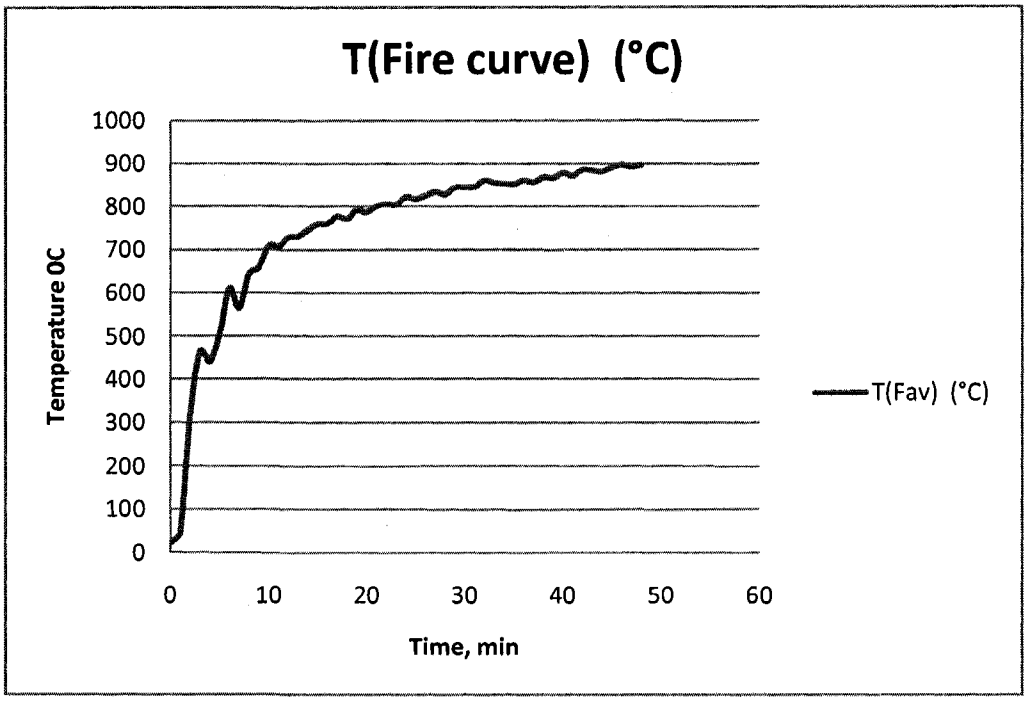

Figure 6-2 CAN/ULCS101 fire curve which is similar to ASTM E119 fire curve

The CAN/ULC-S101-M89 curve or the standard fire curve is a purely conventional fire action model, which does not represent any particular fire that could develop in real

buildings. The standard fire curve is mostly used for design purpose. The CAN/ULC-S101-M89 curve is used in the current study in order to reduce the already large number of parameters to be dealt with, and to simulate test condition similar to the NRC fire tests experiments.

The temperature is applied uniformly to the whole frame at each time step to get the thermal expansion and thermal stresses in members. The temperature distribution across the cross section of beam or column has been obtained from the 2D heat transfer analysis of the structural member sections. The temperature gradient inside the section is calculated by using FEM model using SAFIR. The average and gradient temperature of the section then can be calculated at each instance to use later for thermal stress analysis using ANSYS.

The steel behavior at high temperatures has been modeled according to the procedure described in the SAFIR user's manual (Franssen et al, 2002). More specifically, the steel stress–strain–temperature relationship used in the numerical analyses is shown in Figure 6-3 for several values of the temperature.

The potentially important effect of creep (Anderberg 1988) has not been explicitly taken into account. Thermal properties of steel have also been assumed according to SAFIR.

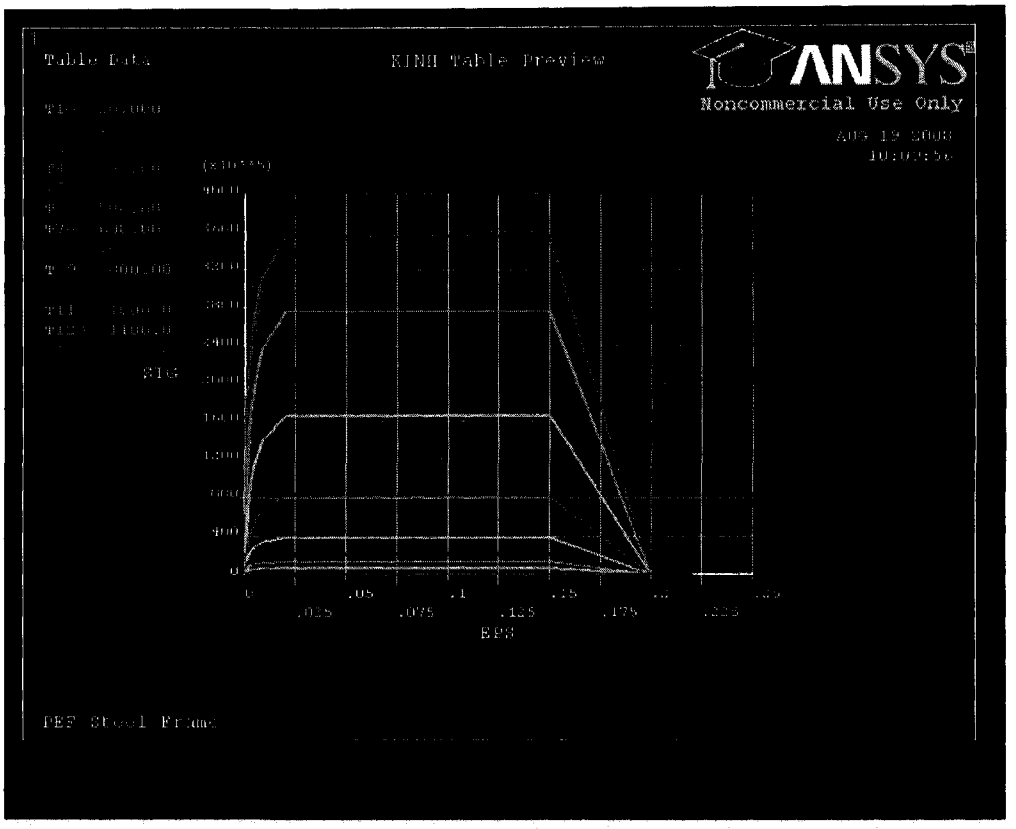

Figure 6-3 stress-strain relationship of steel elevated temperatures

Within this type of model the thermal analysis phase is based on the assumption that there is no heat transfer along the element length, so that the temperature field must be determined on the element cross-section. After obtaining the time-history distribution of the temperature field in the cross-section of the element, the mechanical analysis phase is started, by using ANSYS and applying the average gradient temperature at each minute during the fire period and by considering large displacements. The effect of thermal elongation of fibers is taken into account.

The structural fire-resistance analysis has been conducted in the time domain, by checking the stability either of the whole frame or of one of its members. The failure time

of the structure exposed to fire, which will be referred to in the following, has the meaning of the limiting time at which a structural instability occurs.

It is apparent that one main problem with fires following earthquakes is the damage to passive and/or active fire protection systems. But considering these types of damage would conceal the effect of structural damages and large modeling uncertainties must be faced due to the lack of sufficient experimental data. One possibility could be to consider a fire-protected structure before the earthquake and a completely fire un-protected one after a strong earthquake, which would certainly be a conservative assumption. On the other hand, it could be assumed that the fire protection systems are in-place and efficient after the earthquake (Cortea at el. 2003). In this way, the range within which the actual behavior clearly falls would be defined. However, the aim of the planned numerical analyses is to examine and quantify the fire resistance reduction exclusively attributable to earthquake-induced structural damage. This is the argument why the examined structures have been assumed to be unprotected against fire, both before and after the earthquake.

6.5 Thermal Stress Analysis:

The temperature distribution in a part can cause thermal stress effects (stresses caused by thermal expansion or contraction of the material). Thermal stress effects can be simulated by coupling a heat transfer analysis (steady-state or transient) and a structural analysis

(static stress with linear or nonlinear material models. The process consists of two basic steps:

1. A heat transfer analysis is performed to determine the temperature distribution across the cross section (i.e. the thermal gradient in the element), and then
2. The time history of temperature distribution is directly input as thermal loads in a structural analysis to determine the stress and displacement caused by the thermal and mechanical loads.

This methodology is employed in this study by using different types of solvers and simulators. In the case of wood-stud wall a fire dynamic simulator FDS (NIST, 2008) is used to determine the thermal gradient through the wall at each instance during the fire. The resulted temperature has been used in the buckling model described in section 6-1 to calculate the critical load at each instance. In the steel structures the heat transfer analysis is conducted through SAFIR; where a 2D transient heat transfer analysis has been done to determine the temperature through the member section at each instance during the fire. The average temperature is considered in the ANSYS model to calculate the thermal stresses later on.

Chapter 7

Post Earthquake Analysis of Wood Stud Wall

7.1 Description of Test Assemblies:

The wall unit considered here has been assembled and tested in the NRC fire testing lab by Kodur et al. (1996). The full-scale assembly was constructed in accordance with CAN/CSAA82.31-M91 (Gypsum Board Application 1991). Details on the assemblies for the test #F-19 from Kodur at el. (1996) are shown in Figures 7-1 and 7-2. These assemblies are used in the numerical study in the present research. The dimensions and the construction materials are described in the following;

1. **Dimensions:** The wood stud shear wall assembly is 3048 mm high by 3658 mm wide with depths of 127.1 mm. The specific dimensions of the assembly are given in Figure 7-1. The distances between the wood studs are 400 mm O.C. The 12.7 mm thick type X gypsum board is attached vertically to the wood studs on both the exposed and unexposed sides with Type S drywall screws, 41 mm long, and spaced at 400 mm O.C.

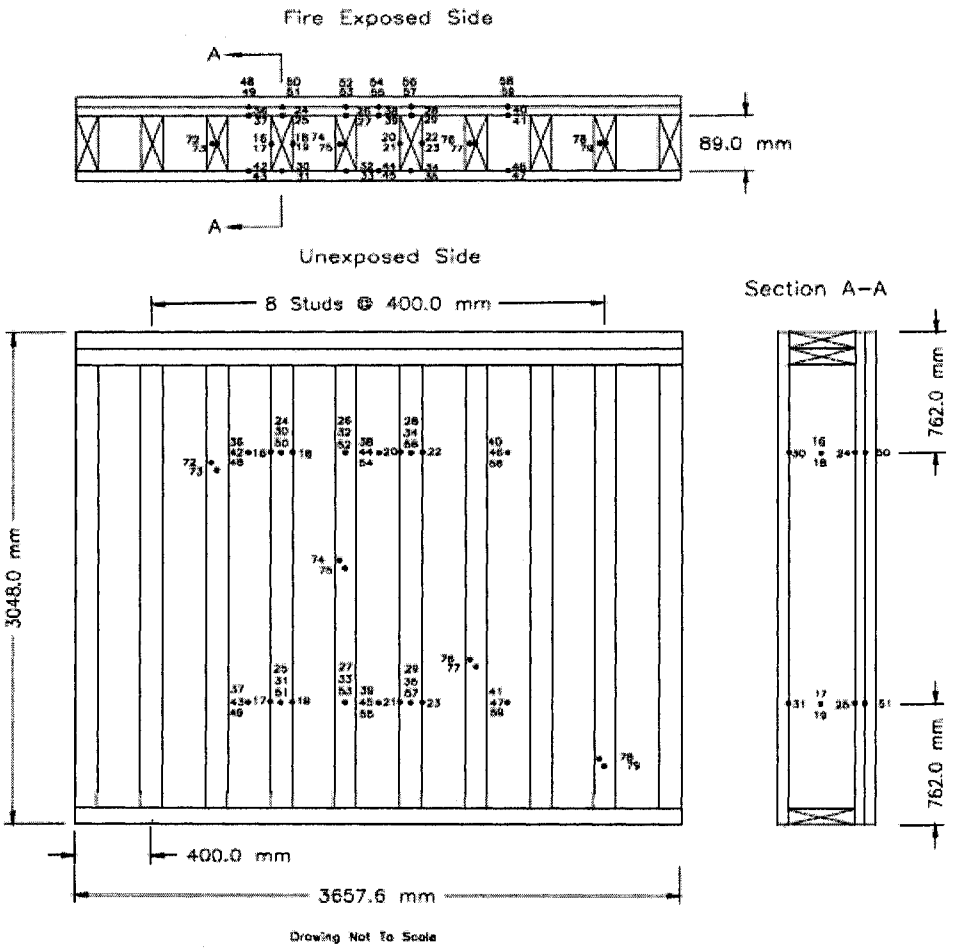

Figure 7-1 Wood stud assembly F-19, NRC fire test, Kodur and Sultan (1996)

2. **Construction Materials:** The materials used in the wall assembly are as follow:

   i. Gypsum Board: Type X gypsum board (Westroc "Fireboard" C/Type X), conforming to the requirements of CAN/CSA-A82.27-M91 (Gypsum Board-Building Materials and Products 1991) was used. The thickness of this Type X gypsum board was 12.7 mm.

   ii. Framing Materials: The wood studs used were nominal 2x4's (SPF No. 2, S-Dry, 38 mm thick by 89 mm deep) and conformed to CSA 0141-1970 (Softwood Lumber,1970).

iii. Shear wall panels: Plywood (12.5 mm thick).

iv. insulation : Glass Fiber- with a mass per unit area of 1.08 kg/m^2

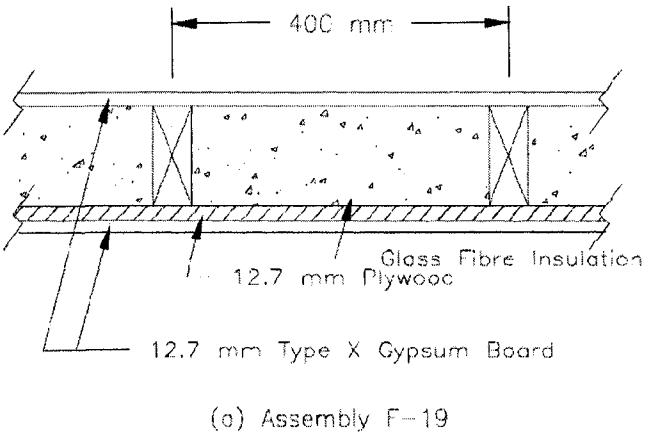

Figure 7-2 Section in the assembly F-19 (Kodur and Sultan 1996)

7.2 Fire Test Environment:

7.2.1 Loading System:

The loading device consists of 8 hydraulic jacks fitted at the top to simulate vertical structural loads. The applied loading on the wall assemblies used in this study is presented in 8.2 KN which is verified with the Canadian Wood Council calculations (Kodur et al. 1996.)

7.2.2 Test Conditions and Procedures:

7.2.2.1 Test Procedure:

The assembly exposed to heat in a propane-fired vertical furnace as shown in Figures 7-3 to 7-5. Ceramic fiber blankets were used to seal the assembly at the edges against the furnace. The furnace temperature was measured using nine (20 gauge) shielded thermocouples in accordance with the Standard Methods of Fire Endurance Tests of Building Construction and Materials CAN/ULC-S101-M89 (1989). The furnace temperature is controlled by considering the average of the measurements from nine thermocouples.

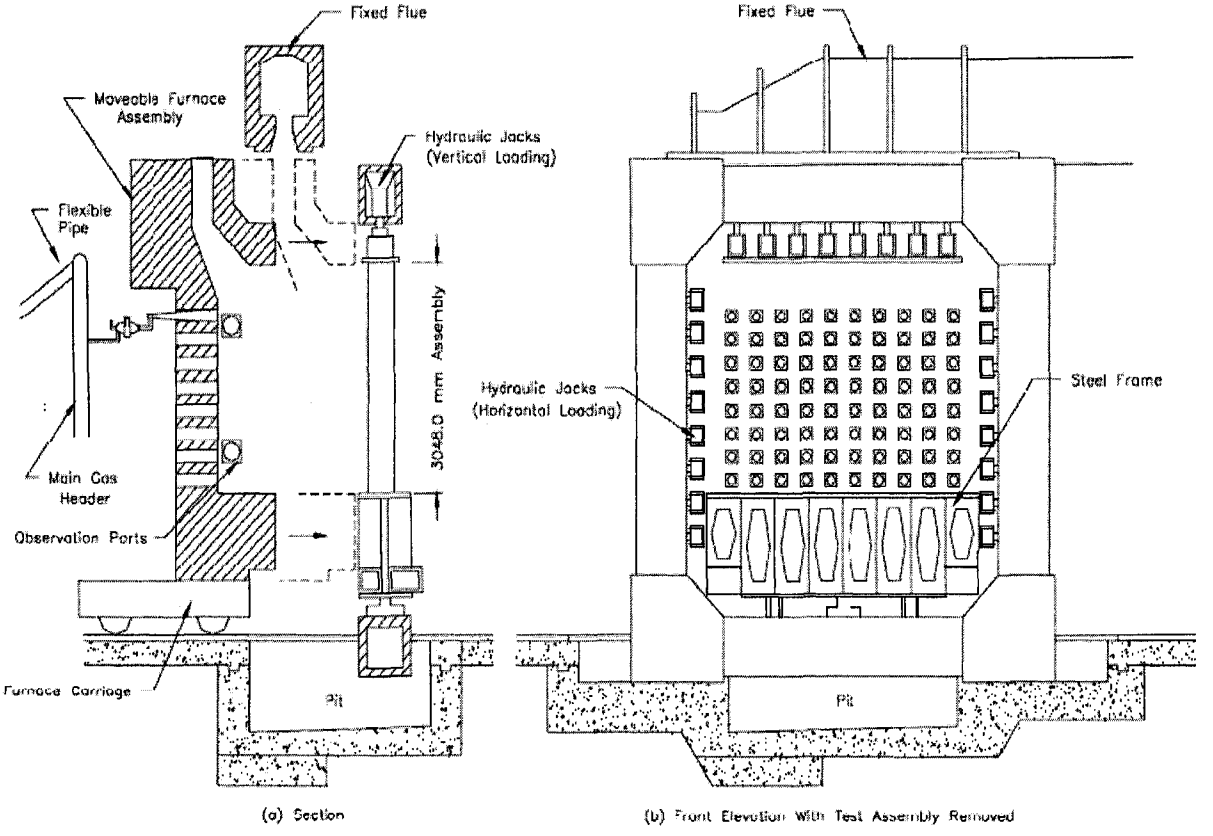

Figure 7-3 full-Scale Wall Test assembly Furnace (Kodur et al. 1996)

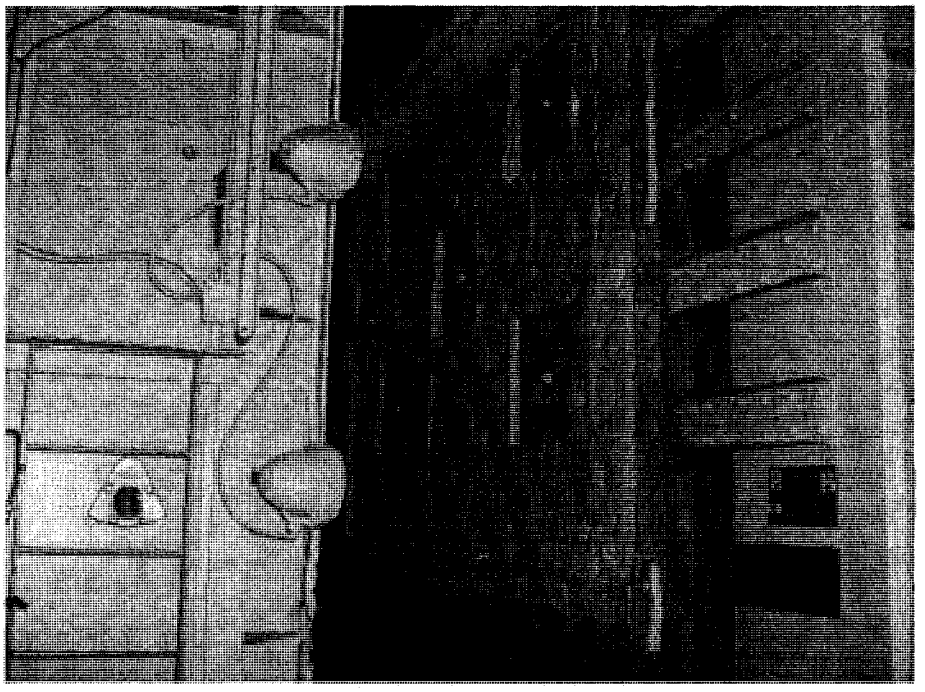

Figure 7-4 photographic view of the inside part of the furnace (photo is taken during our visit to the NRC fire lab 2008)

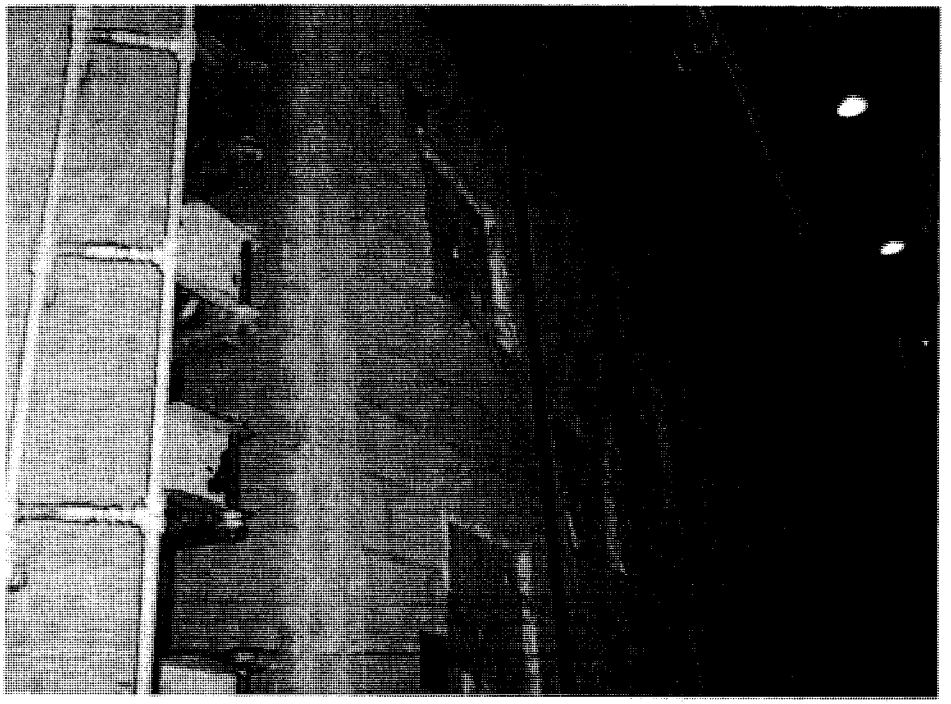

Figure 7-5 The outside part of the furnace. and part of the loading hydraulic jack system is shown on the top part of the photo. (Taken during our visit to the NRC fire lab 2008)

7.2.2.2 Fire Exposure:

At the beginning of the test the furnace temperature is about 21°C , then it starts to increase monotically with accordance to the CAN/ULCS101 (1989) standard temperature-time curve. The used fire curve is shown in Figure 7-6.

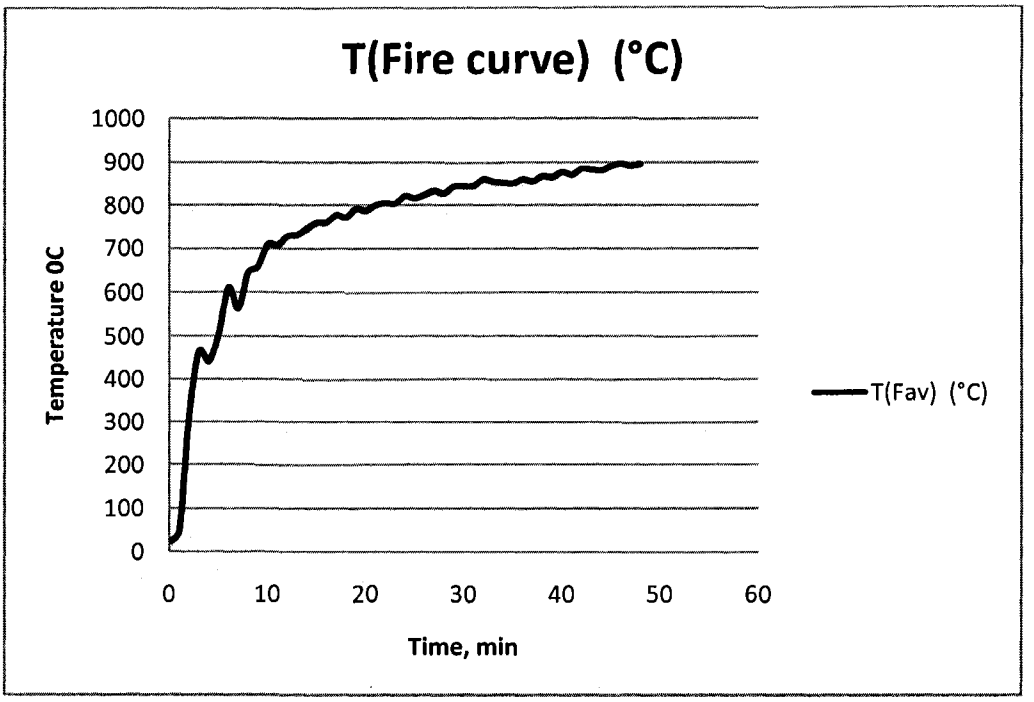

Figure 7-6 CAN/ULCS101 fire curve which is similar to ASTM E119 fire curve

7.2.2.3 Failure Criteria:

The failure criteria are divided into two categories; thermal failure and structural failure. In the thermal failure the member or its material reaches very high temperature in a way that it loses its ability to resist fire or to protect other materials from it. In the other type of failure the structural capacity of the member, or the whole structure, decreases to a

very low level it loses the ability to carry the applied loads or self weight any longer. The failure criteria in test were derived from CAN/ULC-S101-M89 (1989). The assembly was considered to have failed thermally if a single point thermocouple temperature reading on the unexposed face rose to 180 °C above ambient or the average temperature of the 9 thermocouple readings under the insulated pads on the unexposed face rose 140 °C above the ambient temperature, or there was passage of flame or gases hot enough to ignite cotton waste. The test assembly was also deemed to have structurally failed if there was excessive (>150 mm) deflection (Kodur et al. 1996).

However in the analytical model of Benichou and Morgan (2003) the structural failure in wall assembly is said to have happened when the applied load exceeded the critical buckling load. This concept has been also used in the buckling analysis model presented here to determine the time of failure of the wall.

7.2.2.4 Recording of the Results:

Temperatures and deflection are recorded from the gauge points at each minute during the test using Labtech Notebook data acquisition software and a Fluke Helios-I data acquisition system (Kodur et al. 1996). The average temperature calculated for each layer at each instance and considered to represent ht layer temperature at that instance.

7.2.3 Analysis stages and results:

7.2.3.1 Step 1:

Heat transfer analysis using FDS simulator: the model has been built for an effective length of the wall since the FDS runs 1D heat transfer analysis to determine the gradient through the wall. Hence there is no need to build the model for the whole wall. In other words, in FDS the heat transfers assumed to happen through the thickness of the wall layers not in the plane of the wall. This approach is acceptable in modeling the F-19 fire test since the average of temperature is calculated for each layer at of the wall at each moment and considered to be the layer temperature. Also, the temperature on th wall surface is found to be almost uniform.

The changes in the thermal and physical properties of the construction materials are considered as presented in Chapter 5.

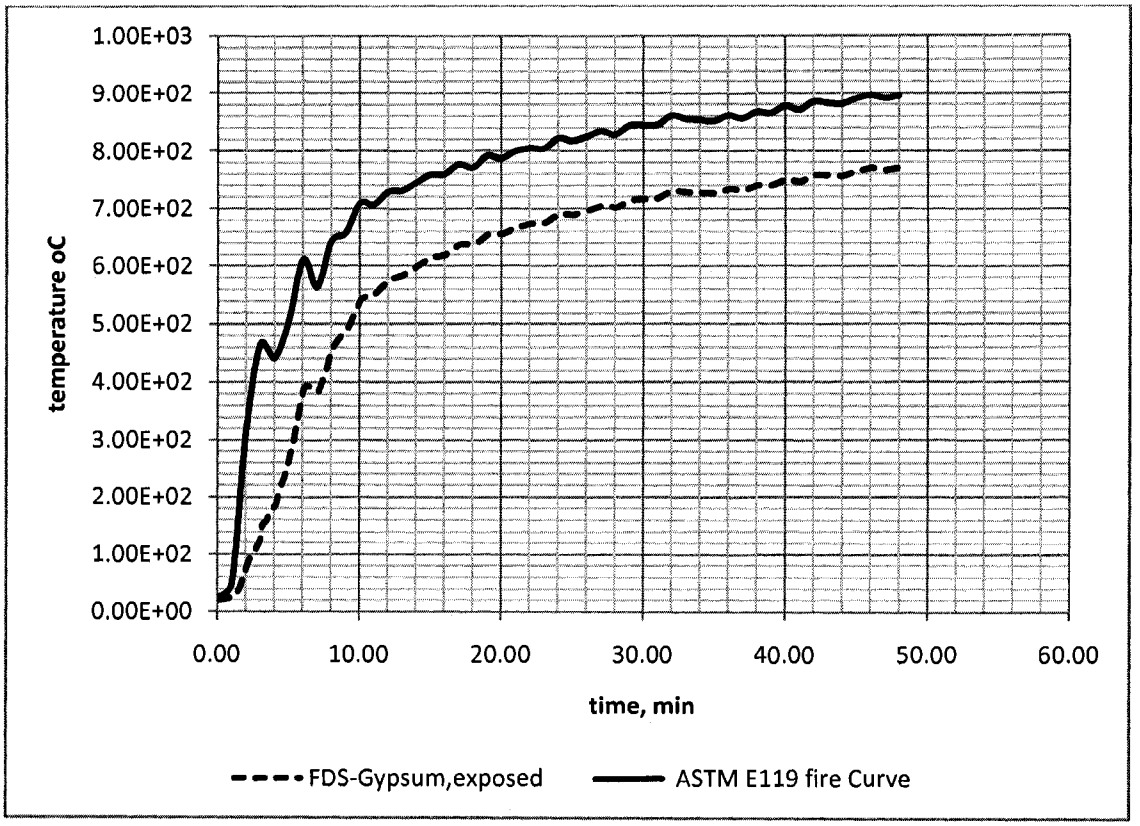

Figure 7-7 Temperature on the gypsum board, FDS analysis

Figure 7-7 presents the temperature of the exposed surface of gypsum board during the fire period of time. The lab measurements of this layer are not available from NRC test due to limitations in instrumentations. During the NRC fire test no thermocouples on the exposed surface have been installed, this is because they would melt in the early stage of the experiment.

Figures 7-8 and 7- 9 present the change in temperatures inside each layer through the wall with comparison to the experimental values from NRC test for the same unit. The

results from the heat transfer analysis shows reasonable matching with the experimental data as can be seen through previous figures.

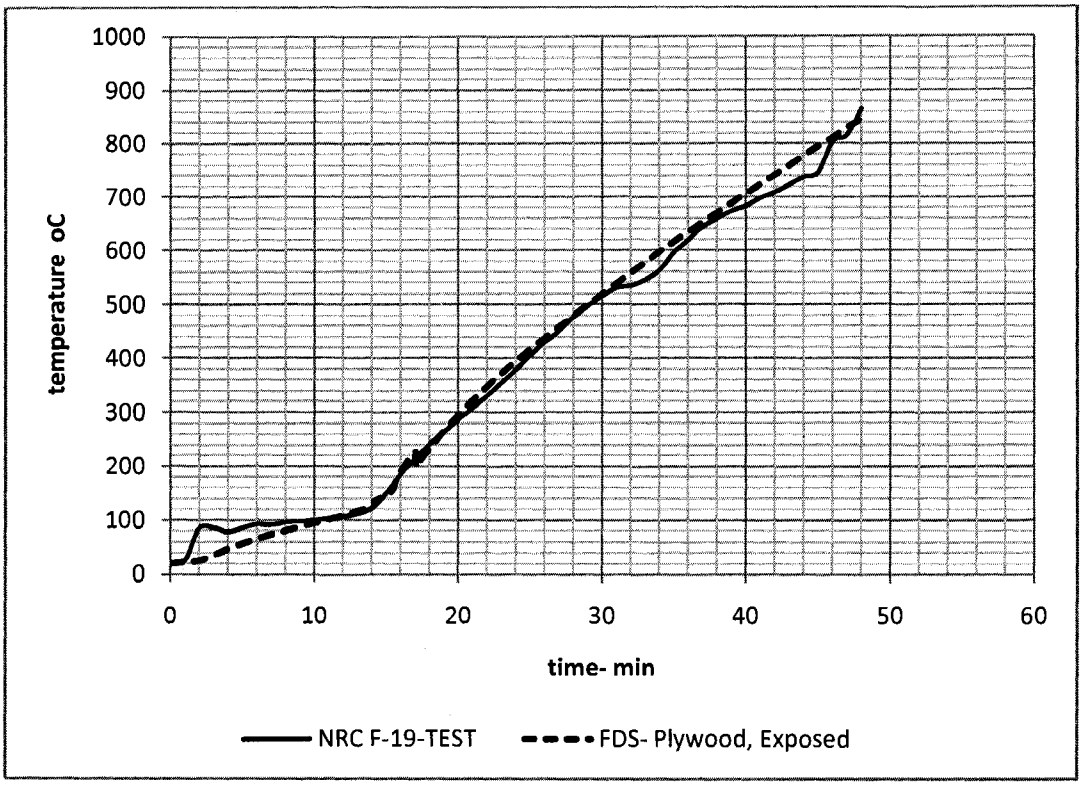

Figure 7-8 Temperature history results in the plywood layer

In Figure 7-8 the temperature inside the plywood layer from FDS model and NRC test is presented. The analytical model show nice matching with the experemantal one. NRC reported the temperature iside this layer by palcing a thermocouple inside the plywood board durig the fire test. similar approach has been considered during building the analytical model by palcing a device point inside this layer. A device in FDS model refers to a mathimatical integration point in the finite difference model. The value captured by the analytical divice could by any output result from the analysis such as temperature, pressure or heatflux.

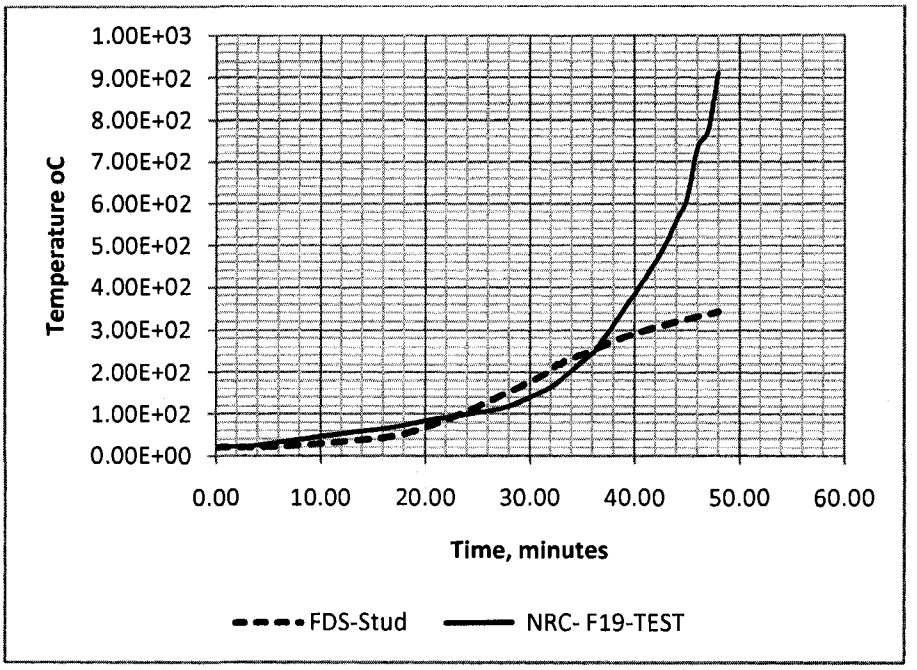

Figure 7-9 Temperature history results in the stud

In Figure 7-9 the analytical temperature result of the wood stud is presented with the experimental one as well. A similarity in the results can be observed in the diagram; however the imperfection in matching between the results is due to a trivial difference between the analytical and experimental models. In the real model the thermocouple is placed on the surface between the stud and the insulation layer because it is not possible to place it inside the stud. The technical difficulty in the analytical model does not exist; a thermocouple device could be placed anywhere in the wood layer and thus a more representative results for the element temperature can be achieved.

7.2.3.2 Step 2:

In this stage a fire resistance analysis in normal fire using the model described in section 6-1. The original analytical model has not been developed for fire event neither for

earthquake, however some modifications to the assumptions used to develop the original model has been implemented in this study to estimate the buckling capacity at each moment during fire. The original model assumed constant material properties uniform material distribution along the wall length. In our study we assumed that the properties of the materials are constant in each time interval. During the fire the mechanical and geometrical properties of the wall members change with time and theses changes has been calculated. The cross section, the moment of inertia, the eccentricity and the modulus of elasticity for wood and plywood become functions of time or temperature and their values have been calculated at each moment during the fire, then they have been used to calculate the buckling load at that moment of time.

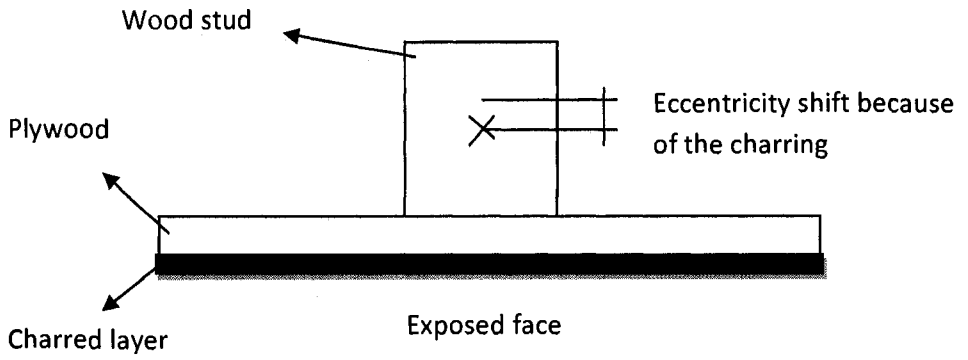

Figure 7-10 The effective length of the wood stud wall with charred layer.

The charred layer has no load capacity and thus the wood or plywood section losses material when the charring starts. This leads to shifting in the centroid of the section and as a result the eccentricity increases as presented in Figure 7-11. The increase of the eccentricity of the applied load accompanied with the mass loss because of the charring beside the degradation of the modulus of elasticity due to high temperature will affect the overall buckling capacity of the wall significantly.

The buckling load of the unit degrades with time during fire until it matches the value of the applied load. The degradation is due to the reduction in the mechanical properties of the elements exposed to fire beside the loose in section material because of charring.

When the critical buckling load meets with the actual applied load the failure in the wall happens. The duration between the fire event starting and the buckling failure represents the fire resistance of the wall.

The existent of the gypsum board has been considered here as a protection factor and thus the plywood temperature obtained from step 1 has been used to calculate the overall properties and loads.

The gypsum boards are not modeled since it does have structural capacity against the earthquake (Kato et al. 2006)

Figure 7-10 presents the degradation in buckling capacity of the F-19 unit during the fire. This curve is obtained in the current study by using the technique explained in section 6.2.

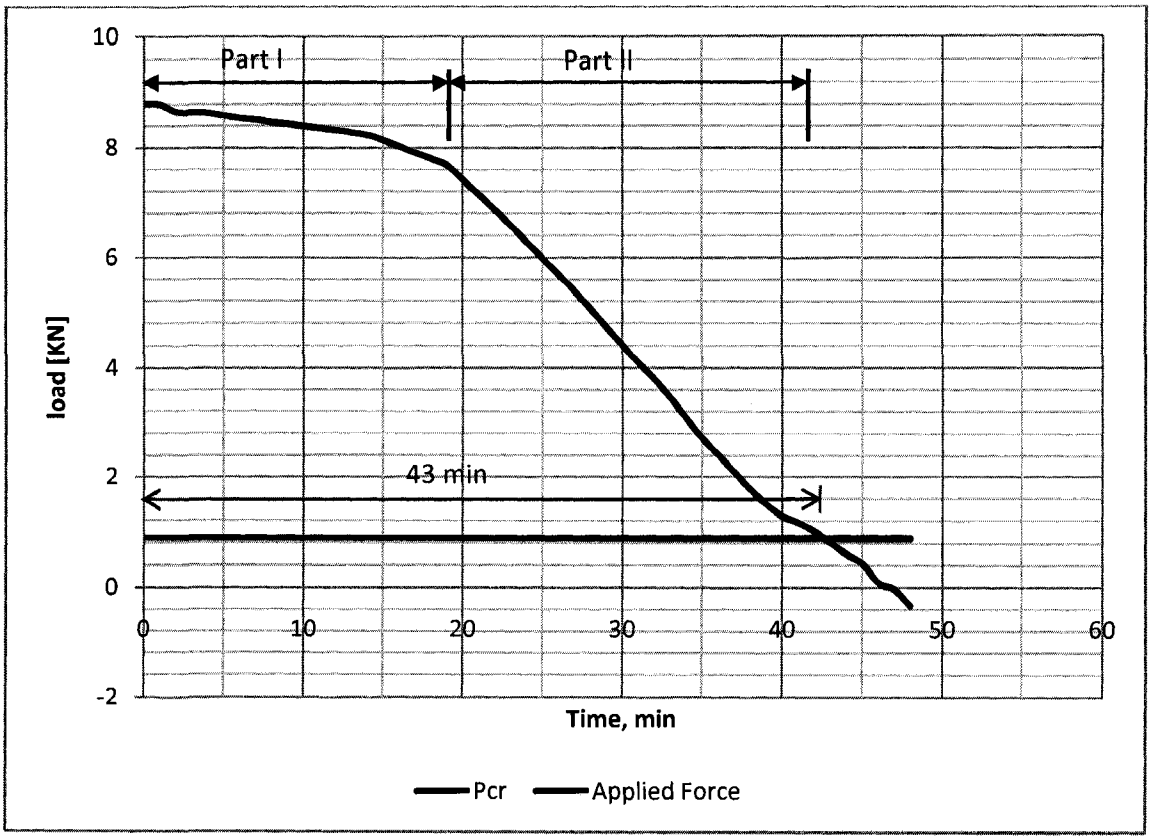

Figure 7-11 F-19 Buckling capacity degradation with time during fire

The fire resistant rate numerical model employed in the present study shows similar results to the NRC fire tests which reported a failure in the wall F-19 between 43 and 48 minutes.

From Figure 7-10 it can be observed that the degradation in buckling capacity can be divided into two parts. Part I represent the degradation in the capacity in the first stage of fire and before the charring start, this division lasts until the members' temperature reaches enough amount to start the charring. Part II represents the reduction in capacity because of the mass loss in the section beside the continuous degradation in the elements mechanical properties. It can be noticed that part I last between 0 and about 20 minutes and part II lasts between 20 and 43 minutes for the F-19 unit.

7.2.3.3 Step 3:

In this stage a fire resistance analysis due to PEF is performed the same model used in Step 2 and by modeling the damage because of the earthquake using the following assumptions:

a. The permanent lateral deflection in the wall is between 1.3% to 5% (Judd 2005). and in some cases 15% Dinehart et al. (1983) Figure 7-12 shows the wall deflection due to the earthquake.

b. The reduction in the fasteners stiffness and modulus of elasticity of wood and sheathing after the earthquake is between 30% and 50% (Judd 2005) and Dinehart et al. (1983)

c. The applied vertical load has two components in the stud local coordinate system. The axial component is approximately equal to the vertical load since the lateral deflection is relatively small and the drift angle is very small. The other component is neglected since it has very small value and it does not exceed the diaphragm action from the sheathing, hence there is no stud buckling in the plywood board plane.

d. The gypsum board has many cracks because of the earthquake and thus it assumed that it does not anymore protect the plywood from the fire. The temperature of the exposed plywood board is then calculated and plugged in to the equations to get the buckling capacity after earthquake.

By applying these factors to the buckling model which is explained in section 6-1 we get the PEF resistance for the wall after the earthquake.

The quickly repeated shaking of the wall because of the earthquake will reduce the stiffness of the wall. The reduction involves a reduction in the sheathing to framing stiffness which is defined in Equation 7-1.

$$\frac{1}{\beta} = K / S_p \quad \text{.....Equation 7-1}$$

Where K is the nails stiffness N/mm.

and S_p is the distant space between the nails mm.

It can be noticed from the previous equation that the reduction in sheathing to framing stiffness results directly from the reduction in nails stiffness K. In the present study; nails are modeled as linear springs.

Another effect from the earthquake load on the wood stud wall is the reduction in the wood and plywood structural elements capacity. This is implemented here by reducing the mechanical properties of those elements.

After the earthquake the wall will suffer a permanent lateral drift as presented in Figure 7-12. The wall at this stage has different situation from the initial one i.e. before earthquake. The damages in the wall presented by the permanent lateral deflection and the reduction in the stiffness and mechanical properties of members reduce the overall capacity of the structure.

In the present study a percent of reduction in the stiffness of nails K and mechanical properties of wood E_s and plywood E_p is assumed after the earthquake to calculate the buckling capacity of the wall during the fire.

For example a 30% earthquake damage ratio would reduce the fire resistant capacity of the F-19 wall to from 43 minutes to 23 minutes as presented in Figure 7-13.

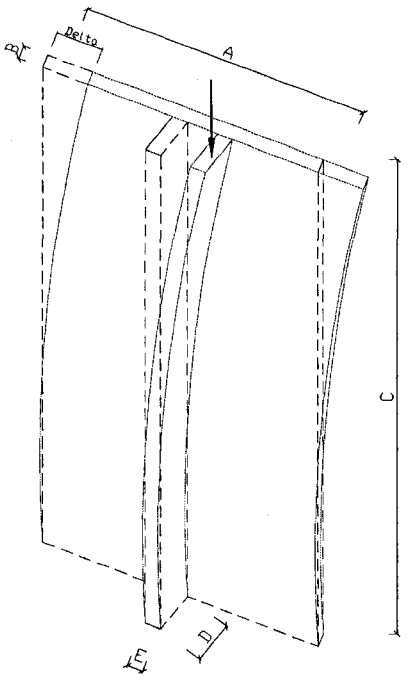

Figure 7-12 lateral deflection in the wall strip due to earthquake load.

Buckling load capacity curve in PEF is different from the same curve in normal fire. The pre-charring stage here is not clear as in the normal fire case. The curve shows a continuous degradation in the capacity until it meets the applied load line. This is can be clearly understood if we consider the new situation of the unit after earthquake. The wall suffers a lot of damages and cracks in its layers. The gypsum boards cracked a lot and it lost its protection tack and thus the members i.e. plywood, studs and cavity are exposed directly to fire and the temperature of those elements will rise very fast in a way that

cause charring in the first 10 or 15 minutes of fire instead of 20 to 25 minutes in normal fire.

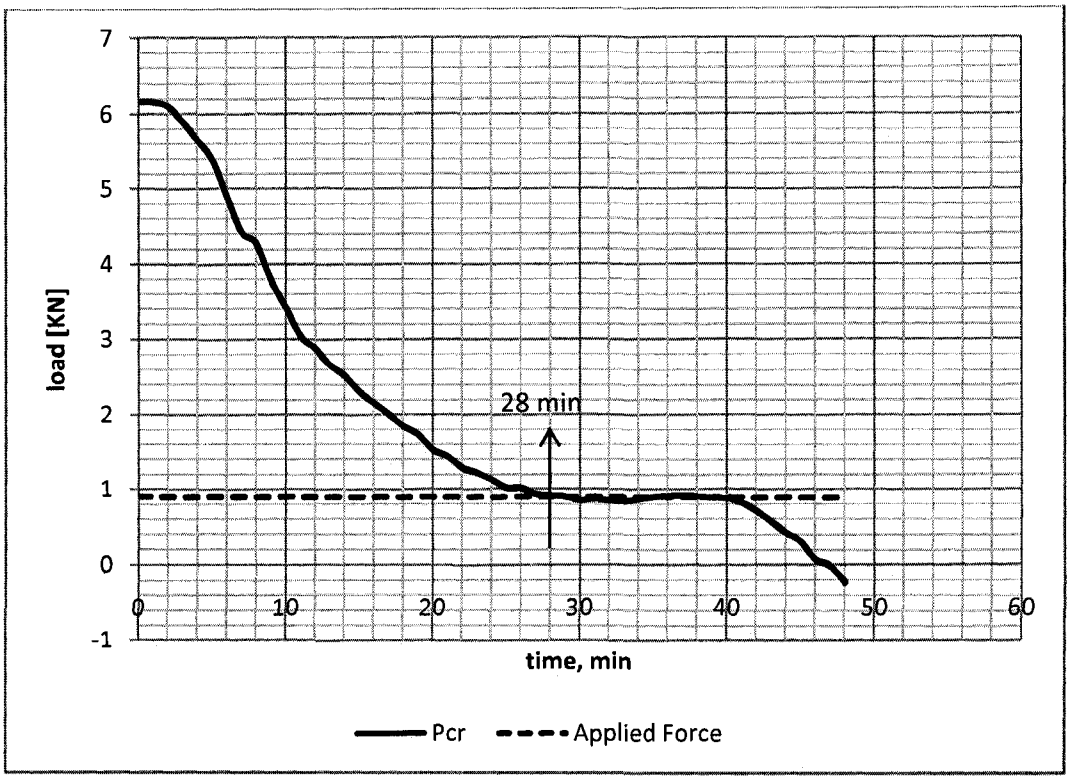

Figure 7-13 The wood stud wall buckling capacity during PEF and 30% earthquake damage ratio.

A comparison between the fire resistance rate of wall F-19 before and after earthquake is presented in Figure 7-14 The results show a reduction in the fire resistance of the wall to 28 minutes; which means that the wall has a 33% fire resistance less than its resistance before the earthquake.

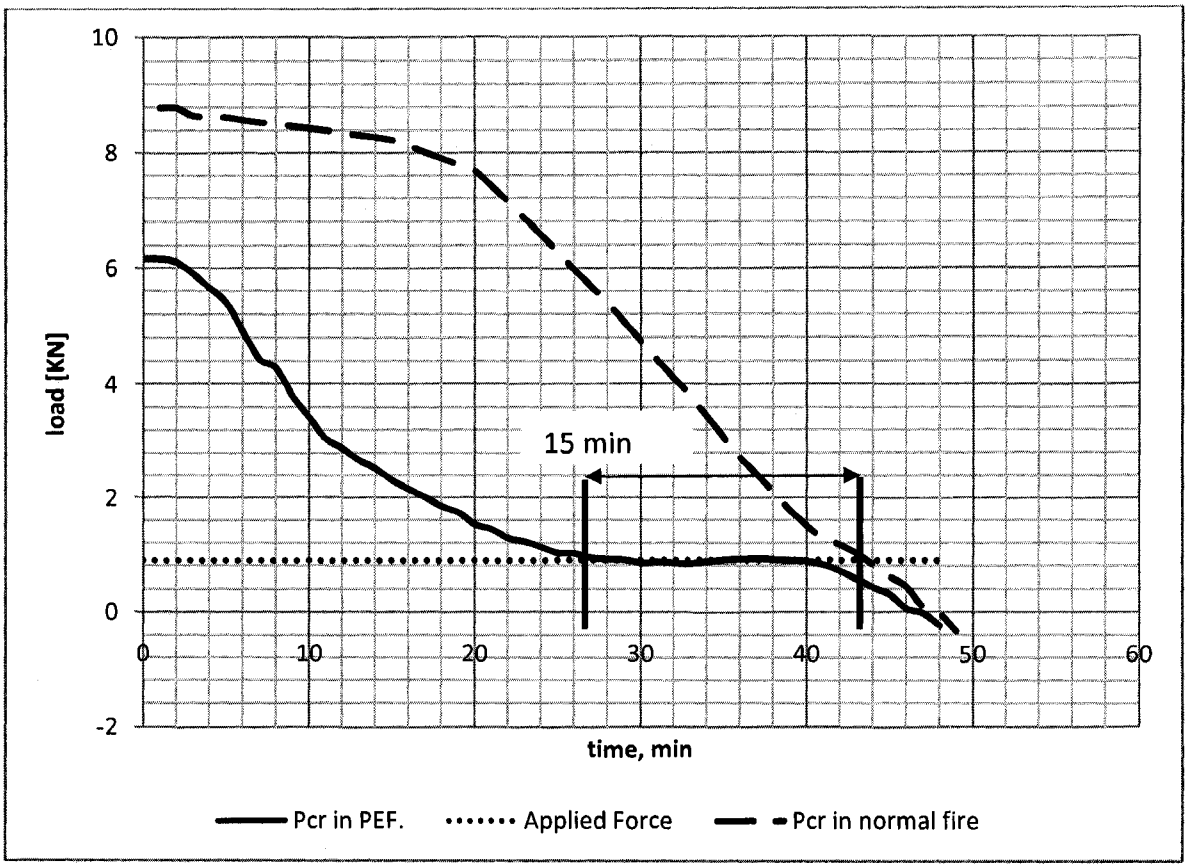

Figure 7-14 comparison between the wall buckling capacities in fire with and without earthquake (with 30% damage ratio)

Similarly, different earthquake damage ratios have been considered to calculate the reduction in the wall fire resistance rate. Damage ratios used are 10%, 20%, 30%, 40% and 50%. The correspondence critical buckling load has been calculated for each case at each instant during the fire. The obtained results are presented here in Figure 7-15. In this diagram it is clearly shown that the fire resistance rate for the F-19 wall is inversely proportional to the percentage of damage because of earthquake.

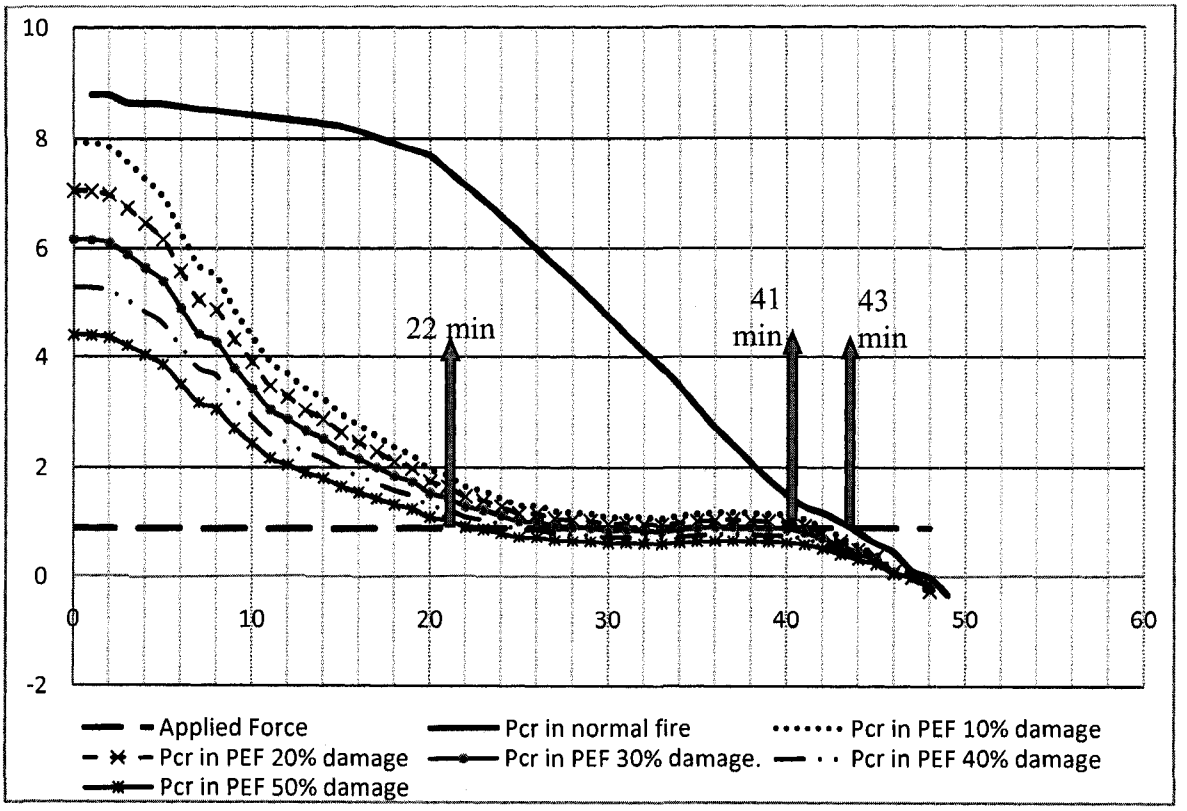

Figure 7-15 Reduction in the wall buckling capacity due to earthquake

A correlation between the fire resistant rates and earhtquake dmage ratios is presented in Figure 7-16. The reduction is mnormalized to the fire resistant rate in case of normal fire. Reduction factors for different damages ratios can be interpolated from this curve.

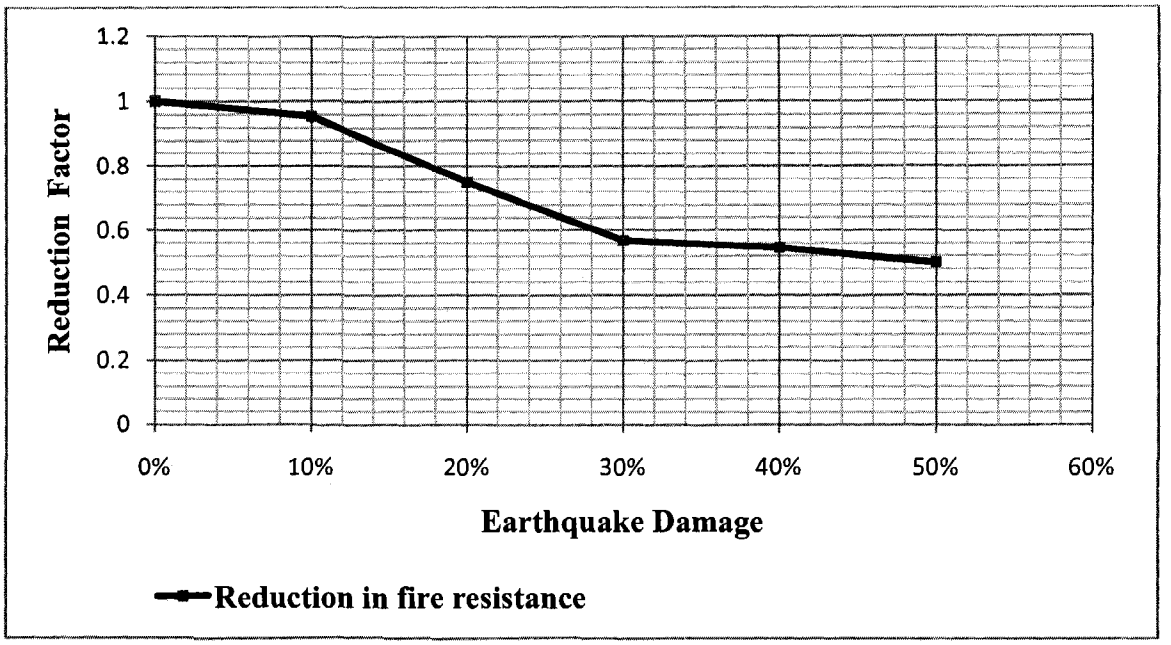

Figure 7-16 Reduction in fire resistance of the wood shear wall

It can be concluded here that there is a strong correlation between the fire resistant rate of the wood structure and the damage caused by earthquake. Wood stud walls in PEF are more vulnerable than before earthquake. This is due to the damage in gypsum boards after earthquake and the loss of fire protection members.

Chapter 8

PEF Analysis of Steel Structures

8.1 Introduction

Steel structures are vulnerable to fire exposure. Steel mechanical strength reduces drastically at high temperature. In a post-earthquake scenario, the construction frame and its fire protection arrangements may be considerably damaged and therefore its resistance to subsequent fire is reduced. Therefore , in addition to satisfying the structural design requirements for normal loads such as dead, , live loads including the seismic forces and normal fire hazards, structures should be designed to withstand the PEF events for certain minimum duration of time, which is critical for the safe evacuation of the buildings. This chapter presents the PEF vulnerability and the performance of steel-frame building structures under PEF conditions. An analytical study of two-dimensional steel frames under the effects of seismic lateral loads and subsequent fire has been presented.

The steel frames considered in the study are designed according to the NBCC 2005 code, the Limit States Design in Structural Steel (CSA-S16 2001) and the Handbook of Steel Construction. The loads are considered to be consistent with the NBCC 2005 specifications 4.1.4 for dead load, 4.1.5 for live load and 4.1.8.16(4) for earthquake load and its combinations. Two steel frames single-story and two-story high with simple

configuration has been studied. The reduction is steel mechanical properties due to earthquake and fire loads is considered during the analysis to represent the damage in the structure. Assessment of the structure condition after the seismic activity, which represents the initial condition for the subsequent fire action involve large uncertainty. The damage in the structure due to earthquake can be divided to two main categories:

1) Geometric damage, which is the change of initial structure geometry owing to the residual deformation produced by plastic excursions during the earthquake.
2) Mechanical damage, which is the degradation of mechanical properties of those structural components engaged in the plastic range of deformation during the earthquake.

8.2 Damage Modeling Methodology:

In this study two analytical approaches have been driven to model the DFAE (damage in the frame after earthquake).

1. In the first approach; the first category of damage has been considered to be enough for modeling DFAE, similar assumption has been made by Della Corte et al (2003) which is convenient to be used for parametric analysis. and thus for having this residual stains in the structure after earthquake it is assumed that a equivalent lateral load is applied on the structure in a way that cause enough lateral translation and hence enough internal stresses that would be taken into account later on when the structure is exposed to fire i.e. in the thermal stress analysis stage.

2. In the second method, the mechanical and geometrical damage has been considered and modeled; more accurate analysis has been conducted. The changes in the mechanical properties of the structural material because of the repeated cycles of load, induced by earthquake, plus the changes in properties due to high elevated temperature are considered through the analysis. In order to achieve a certain level of damage in the structure an excessive seismic excitation has been applied to the structure; the time history acceleration data is taken from a real earthquake event. A nonlinear modal and dynamic analysis is performed before the fire stage. The outcome from the dynamic analysis and the structure situation after the earthquake is considered as an initial condition for the thermal stress analysis step.

Choosing one of the two methods in modeling the earthquake damage depends on the different factors such as the level of accuracy needed for design, the level of impotence of the structure and the complexity in geometry of the structure. The price we have to consider here is the processing time. The nonlinear dynamic analysis methodology is more accurate than the lateral load mechanism, however the last one is much faster and simple to use.

8.3 SAFIR Model:

SAFIR analysis methodology is divided into two main steps: the thermal analysis step and structural analysis step. In the first step the program conduct finite elements 2D heat

transfer analyses for the given section of the structural member. The researcher can easily control the meshing procedure and fine the mesh wherever it is important for the results by using the WIZARD tool. This analysis produces a .tem file which has the time history temperature distribution within the section.

The ".tem" file will be then inputted to the structural analysis .in file. In the thermal stress analysis the software assumes that the given temperature distribution is uniformly distributed along the length of the structural element and then the member temperature is integrated from the gradient within the section for each time interval.

8.4 PEF Case Studies and Results

8.4.1 The first approach:

In this approach the damage due to earthquake is modeled by applying the methodology explained in section 8.2.1. In this study, a one story and two-storey one bay moment resisting steel building frames have been considered. Temperature dependent material properties for steel have been used. Canadian steel section W460X74 is used for column, and W360X51 steel section is used for beam. Vertical load on the beam is assumed to be 24 kN/m acting on the beams downward. Static loads are applied to cause lateral drift

before fire load is applied. For the fire load, standard fire curve similar to ASTM E119 fire curve as shown in Figure 8-1 is considered.

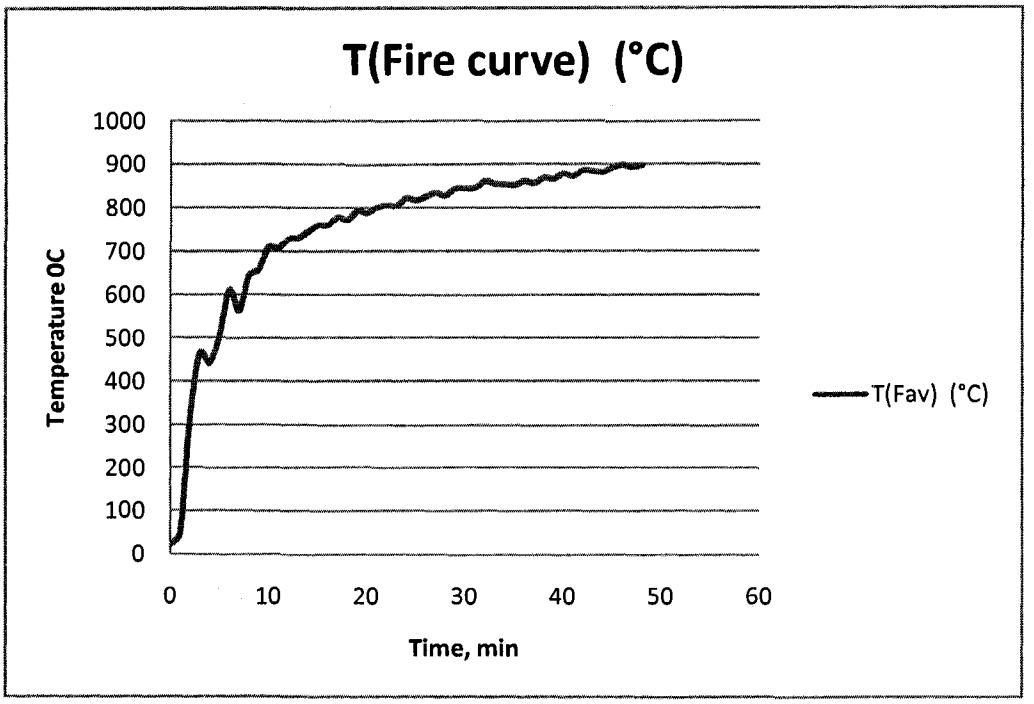

Figure 8-1 CAN/ULCS101 fire curve which is similar to ASTM E119 fire curve

The fire is assumed to happen at the center of the room i.e. the frame. The fire load is applied on three sides of section based on the assumed elements orientation.

8.4.1.1 Heat transfer analysis:

The time history of temperature distribution across the cross section has been obtained using SAFIR; specialized finite element software for fire-structure analysis (Franssen et al. 2000). Representative snapshots are shown in Figures 8-2 and 8-3.

The gradient in the beam section shows that at each instant during the fire the bottom flange temperature is higher than the top flange, however in the last stage temperature is almost uniform inside the section. Representative snapshots to the gradient in the beam section are shown in Figure 8-2. The results show that the bottom flange temperature rises up to 56 °C where the top flange temperature does not exceed 38 °C degrees. In the last stage of fire the bottom flange temperature is about 865 °C compared with 842 °C in the top flange.

In the column case, only one side of the section is exposed to fire. The inner flange in Figure 8-3 (a) refers to the flange exposed to fire inside the room. The snapshots presented in Figures 8-3 (a) (b) and (c) show the gradient inside the columns section at different instants during the fire. The inner flange temperature in the first moment of fire reaches 56 °C degrees where the outer does not exceed 35 °C degrees. In the late stage of fire when the whole column is heated, the section gradient becomes approximately uniform and no significant difference in temperature between the section's parts is observed as presented in Figure 8-3 (c).

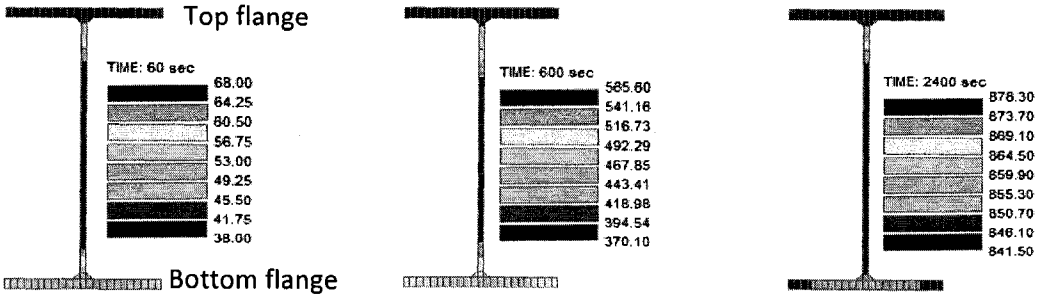

(a) (b) (c)

Figure 8-2 Snapshot of temperature distribution at different times in the beam Section W360X51

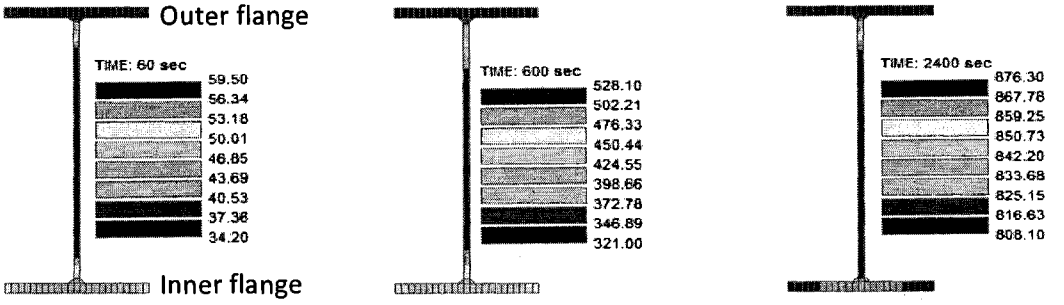

(a) (b) (c)

Figure 8-3 Snapshot of temperature distribution at different times in the column Section W460X74

8.4.1.2 Structural analysis:

The structure is analyzed using SAFIR for the vertical load and lateral load followed by fire load. The frame columns and beam modeled using 3-node beam elements with three degrees of freedom at each node. The frames mesh with elements numbers are shown in Figures 8-4 (a) and 8-6 (a). The results presented here in the following graphs are for the frames with fixed supports. The types of load applied on the frame are dead, live and lateral earthquake load followed by thermal load consists with the fire curve shown in Figure 8-1. Different levels of lateral load magnitude have been applied through the analyses to figure out the correlation between the level of geometrical damage and the rate of fire resistance t_f.

8.4.1.2.1 Case I Single Story Steel Frame:

In this case, a one story one bay frame with fixed supports has been analyzed as presented in Figure 8-4. The lateral load is applied in the negative direction of X axis

before and during fire period. Different levels of lateral load magnitude, starting from zero lateral load as presented in Figure 8-5 (f), have been considered during the analysis. The fire resistance t_f and maximum fire induced deformation have been determined at each level of lateral deformation. Results of the single storey frame have been shown in Figures 8-4 and 8-5.

Representative bending moment curves are shown for beams elements 1,4 and 5 in Figure 8-4 (b). The results shown in this diagram are for lateral load value zero. Beam 1 is the first element in the left side column, beam 4 is the first element in the bay and number 5 is the mid-span one. The graphs show that the bending moment in the column beside the fixed support increases negatively during fire time until it reaches 50 KN.m at minute 30, which is almost half of the total fire period, then it increases in the opposite direction towards zero moment at the end of fire. The bending moment changes in beams 4 and five are similar, however the moment values in the corner beam 4 is higher than beam 5. Beams 4 and 5's bending moment increases because of the thermal load due to fire until minute 20 then the curves go back down.

These changes can be understood easily if we understand how the frame acts when it exposed to fire. In the first stage of fire the frame members would expand outward the structure. The columns will expand vertically and rise the beam up; however, the beam will expand from both sides as can be seen from the displacements curves of corner nodes 7 and 13 in Figure 8-4 (c) and (d). So at the beginning it seems that the fire helps the structure members against the gravity loads. This explains the changes in the bending

moment values from positive to negative and vice versa. This continues until the bending moment values exceed the elements' capacity; at this point some elements start to yield. With the continuous increase in temperature the metal starts to melt at some points in the frame. This form plastic hinges in the weakened parts of the frame and decreases the bending moments significantly until it reaches zero.

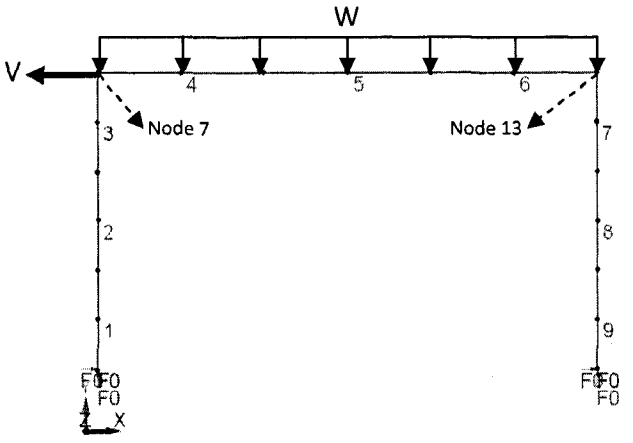

(a) Geometry of the single story frame with fixed supports.

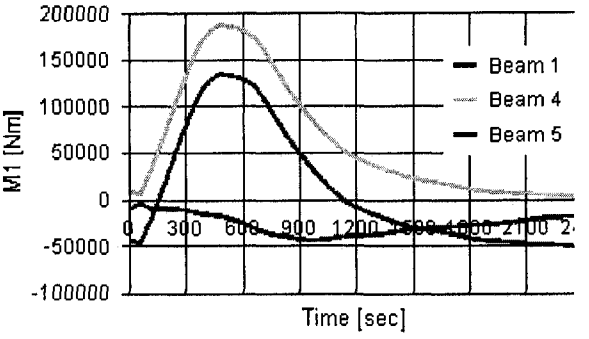

(b) BM history at no residual story drift

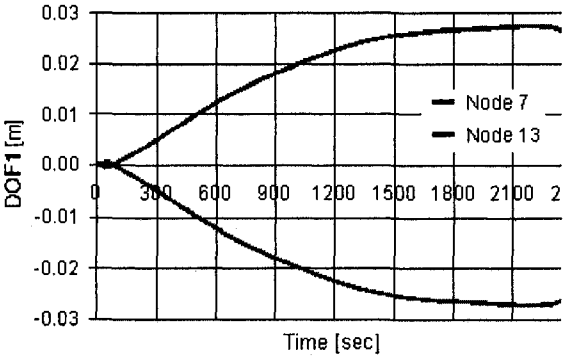

(c) Horiz disp at no residual story drift

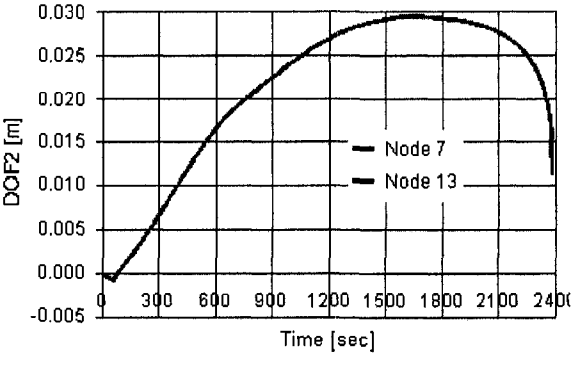

(d) Vert disp at no residual story drift

Figure 8-4 Structural model and summary of results for the single storey frame with no lateral load applied

In the case when the lateral load is applied on the top left corner of the frame, the structure shows different behavior during fire. When the lateral load applied, the structure drifts in the horizontal direction. The whole beam will drift according to the direction of the applied load. The amount of lateral displacement is proportional with the magnitude of the applied load. When the fire starts the structure starts to expand correspondingly. The columns expand upward and the beam expands from both ends. The pre-displaced structure, due to earthquake load, will deform because of thermal load applied from fire.

The type of analysis here involves applying a lateral load and reporting the outcome lateral drift as explained in the previous section. In other words the amount of the lateral displacement is unknown initially before the thermal analysis starts. The column drift ratio as a percentage to the column length is considered to represent the drift in the frame. Some representative results are shown if figure 8-5 (e) are chosen for a 0.43% lateral drift in the frame.

In our case the whole beam drifts in the negative X direction and all of its nodes has the same amount of displacement. The left corner node, node 7, which has already displaced in the negative direction of X axis, due to lateral load, will similarly displace in the negative direction of X because of the expansion in the beam end due to fire. This will increase the total negative displacement of node 7 until it exceed structure yield and fail as presented in Figure 8-5 (e). However, the thermal expansion in the beam will add displacement to the other corner node, node 13, in the positive direction. The total displacement in node 13 will decrees until it reaches zero. Then, the continuous applied

thermal load from fire will cause more thermal expansion in the beam and correspondingly node 13 continues displacing in the positive direction. This explains the slight increase in node 13's displacement above zero. Then the yielding in the frame starts and as a result, the whole structure will start to fail and collapse in the direction of the applied lateral load; this explicates the increased negative displacement in node 13 after the second 900 during the fire.

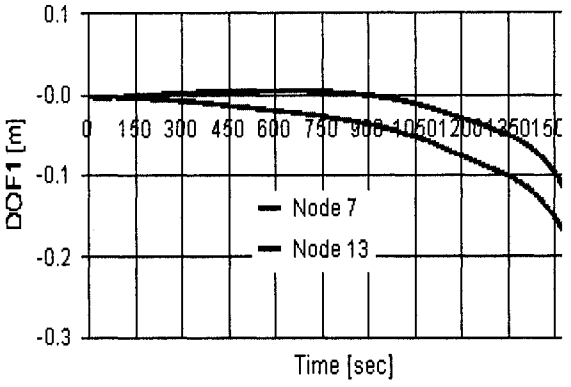

(e) Horiz. Disp. at story drift of 0.43%

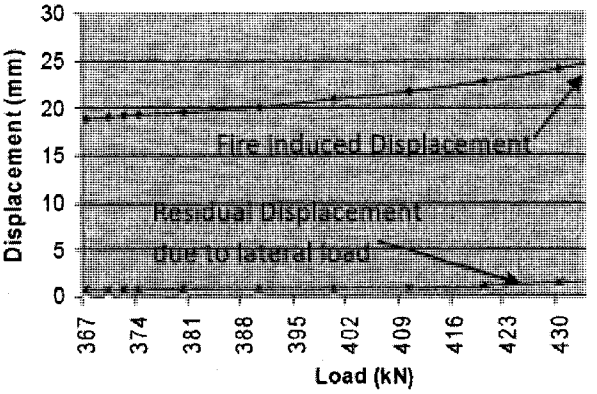

(f) Variation of lateral displacements with lateral load

Figure 8-5 Structural model and summary of results for the single storey frame with lateral load applied

8.4.1.2.2 Case II Two Storey Steel Frame:

In the second case study, a model of a two storey frame has been built as shown in Figure 8-6 (a). Results for the fixed support conditions case has been shown in the same Figure. In the deformed structure, due to the lateral load, the fire induced failure is asymmetric. In the absence of lateral deformation, the deformation pattern is symmetric until the fire

induced deformation becomes excessive. In that case, the frame undergoes sway as observed in Fig. 8-6 (c). In the single storey frame sway does not occur as the frame is much stiffer and the fire induced deformation is much higher compared to the deformation due to gravity and lateral loads. Figure 8-6 (d) shows the variation of normalized fire resistance (tf/tf0) with lateral story drift, where tf is the time of failure of the frame under fire with lateral deformation, and tf0 is that for no lateral drift.

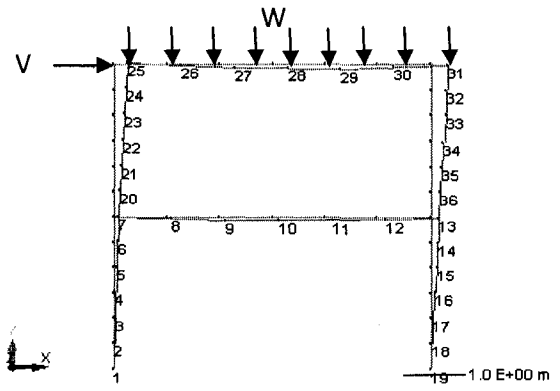

(a) Geometry

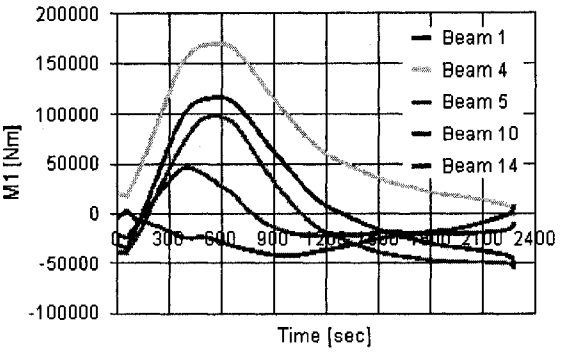

(b) BM at no residual story drift

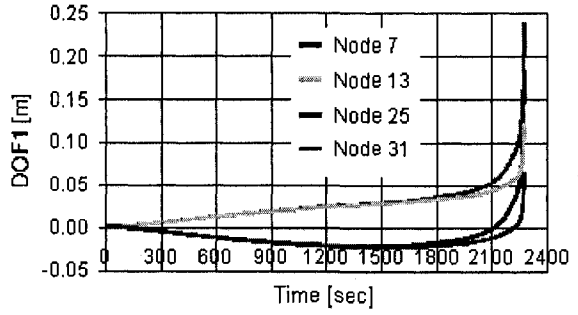

(c) Horiz disp at no residual story drift

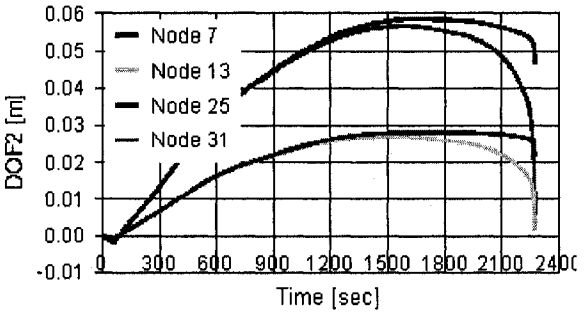

(d) Vert disp at no residual story drift

Figure 8-6 Structural model and summary of results for the two storey frame with no lateral drift

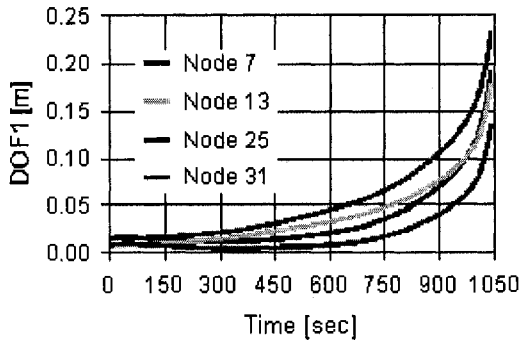

(a) Horiz disp at story drift of 0.27%

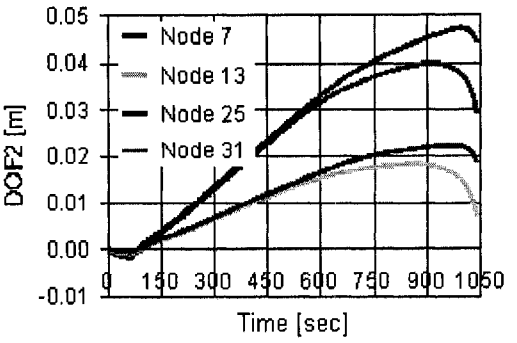

(b) Vert disp at story drift of 0.27%

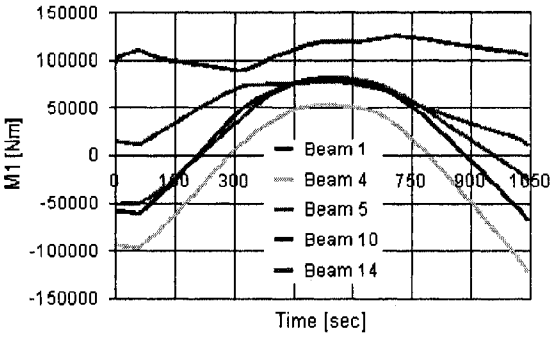

(c) BM at no residual story drift of 0.27%

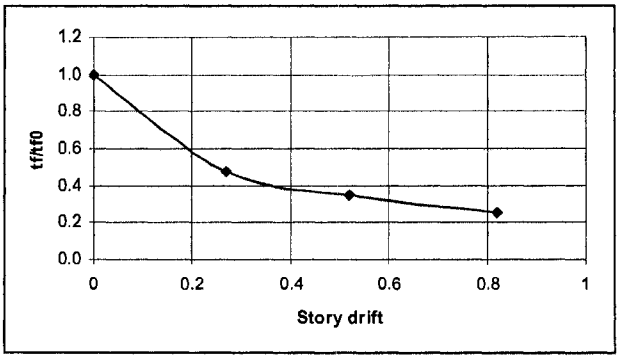

(d) the correlation between the story drift the fire resistance reduction of the frame

Figure 8-7 Summary of results for the two storey frame with lateral drift.

8.4.2 The second approach:

A one-story one-bay moment-resistant steel frame has been modeled in this method. The damage induced by earthquake is obtained as a resultant of the nonlinear dynamic analysis performed by using ANSYS. The heat transfer analysis is performed on the elements sections in 2D by using SAFIR. ANSYS is also used to perform the thermal stress analysis in the frame. The limited capability in performing nonlinear dynamic analysis in SAFIR makes it necessary to divide the analysis procedure steps between SAFIR and ANSYS.

8.4.2.1 Summary of analysis steps:

1) Designing the Frame: In this step the moment resistant steel frames under possible normal and earthquake loads is designed and appropriate sections and grades have been chosen consistently with the NBCC 2005. This could be done by using any commercial tool like SAP2000 or ETABS. For the current study we used a verified designed steel frame from the verification manual of ANSYS Version.11. The frame dimensions as well the used sections and the applied vertical load are given in Table 8-1. Figure 8-8 gives sketch draw to the analyzed frame.

   The frame is considered to be a mid span frame. The distance between the frames in the longitudinal direction is 6 m. vertical load applied on the frames comes from the reinforced concrete slab over the frame and the loads applied on it. The slab thickness is assumed to be 15 cm. the studied frame carries half of the slab from each side, which means that the area of the slab over the frame is 6L. The mass of the slab is obtained from its area times the volume weight of concrete which is assumed to be

2400 kg/m^3. The slab mass is lumped on the corner nodes B and C during the analysis and modeled by using mass element mass21.

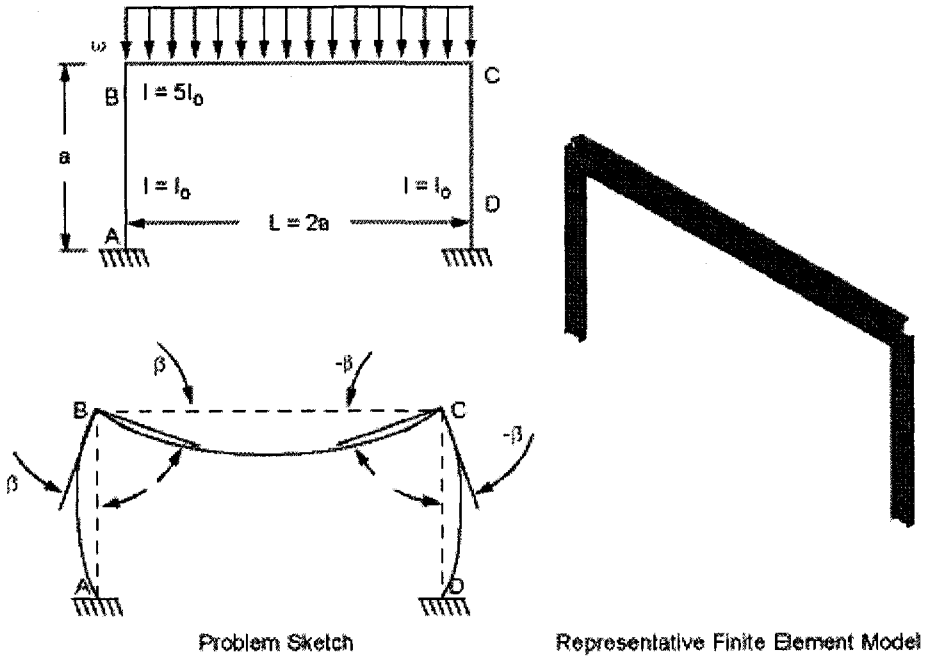

Figure 8-8 Moment resistant steel frame, ANSYS verification manual, VM217

Table 8-1 geometry and section properties of the frame, ANSYS manual 2008.

Loading ω = -500 lb/in **Geometric Properties** a = 400 in L = 800 in $I_{span} = 5\ I_{col}$ $I_{col} = 20300\ in^4$	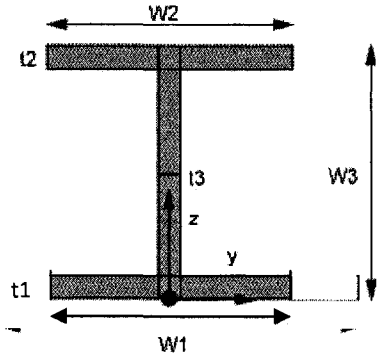	**I-Beam Section Data** W1 = W2 = 16.655 in W3 = 36.74 in t1 = t2 = 1.68 in t3 = 0.945 in

2) Heat Transfer Models: The selected sections are modeled in a modeling tool comes with SAFIR package called Wizard. The wizard generates a (.in) file which is the input for the thermal analysis process. In case of different sections are used in the structure a separate .in file should be written based on whether or whether not the section is exposed to fire. Another issue here should be considered during the modeling procedure, is the orientation of the section within the structural element which determines the exposed faces.

   In this analysis the columns and beam elements oriented in a way that one side of the structural members is exposed to fire. One flange faces the fire where the other one is exposed to ambient temperature.

   Figure 8-9 shows the 2D finite element model in ANSYS with the orientation of the sections in the global axis.

3) Heat Transfer Analysis: a 2D heat transfer analysis is performed using the generated .in file in step 2 by running the SAFIR solver. These results are summarized in a .tem file for each given section.

   The post processing results of SAFIR analysis can be presented using the DIMOND tool which comes with SAFIR. Some snapshots for the thermal gradient in the section are shown in Figure 8-10.the gradient in the columns and beam section is shown in Figures 8-10 (a), (b) and (c).

   The results show that the temperature in the exposed flange increases from 62 °C in the early stage of fire up to 673 °C at the end, However the unexposed flange remains cooler and in and its temperature does not exceed the ambient

temperature. This is due to the big size of the sections which delay the heating of the whole section.

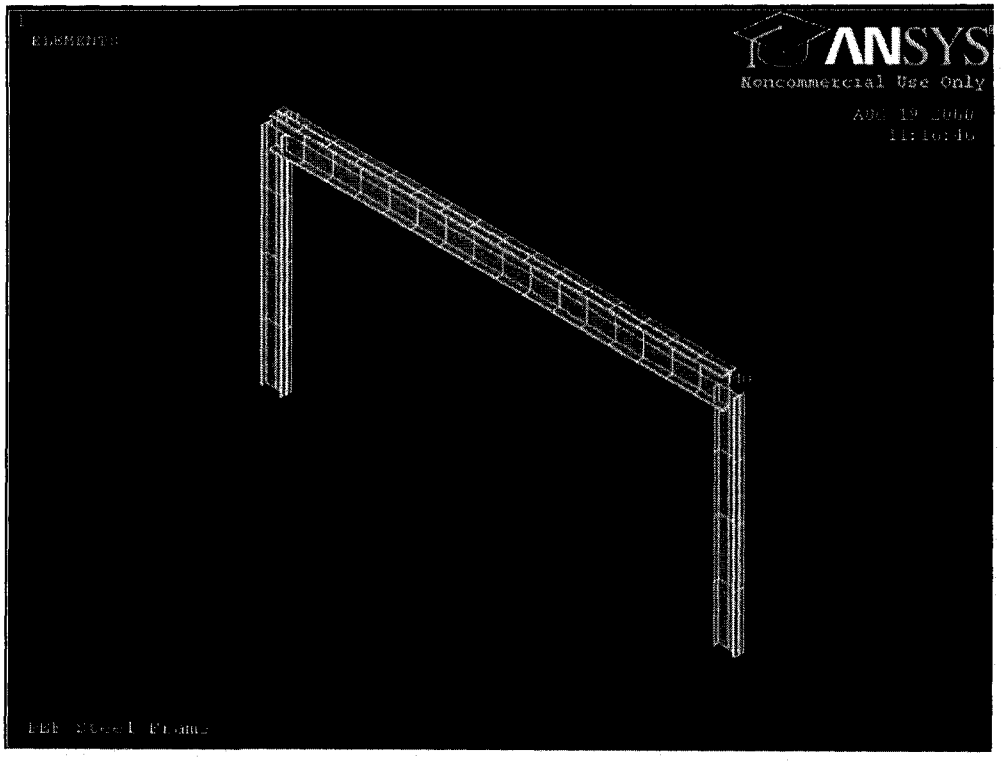

Figure 8-9 2D finite element model for the frame showing the beam-column orientation in 3D

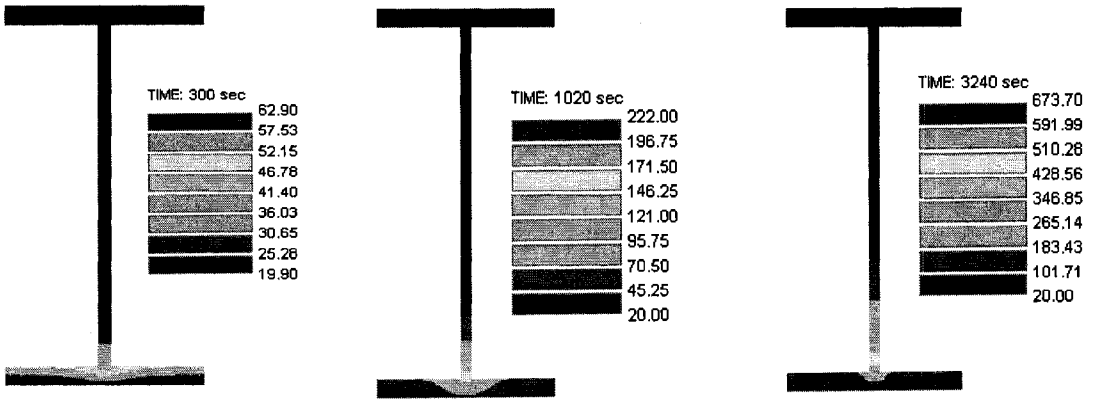

(a) (b) (c)

Figure 8-10 Snapshots for the thermal gradient in the beam section at different instances during the fire

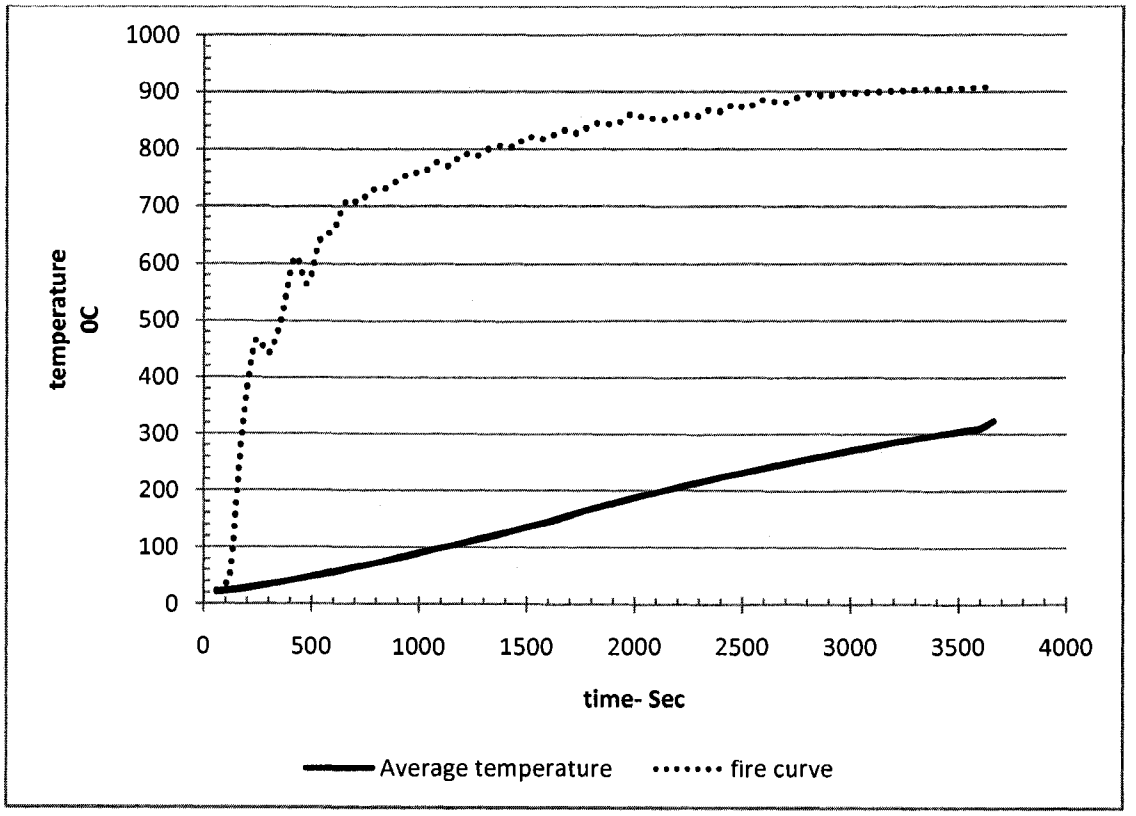

Figure 8-11 Average element temperature during fire

4) Thermal Load: The time history temperature gradient in the section is used then to calculate the average temperature of the element at each moment during the fire. The total average temperature of the section at each instant is applied in later stage as a thermal load on the frame model in ANSYS to calculate the thermal stress induced by fire.

5) Material Properties: The changes in steel properties have been considered in ANSYS model and are taken from SAFIR code. Figure 8-12 shows the changes in the modules of elasticity of steel in high temperatures. The reduction factor in modulus of elasticity of steel is presented in Figure 8-14. The thermal expansion coefficient for steel in high temperature is shown if Figures 8-13.

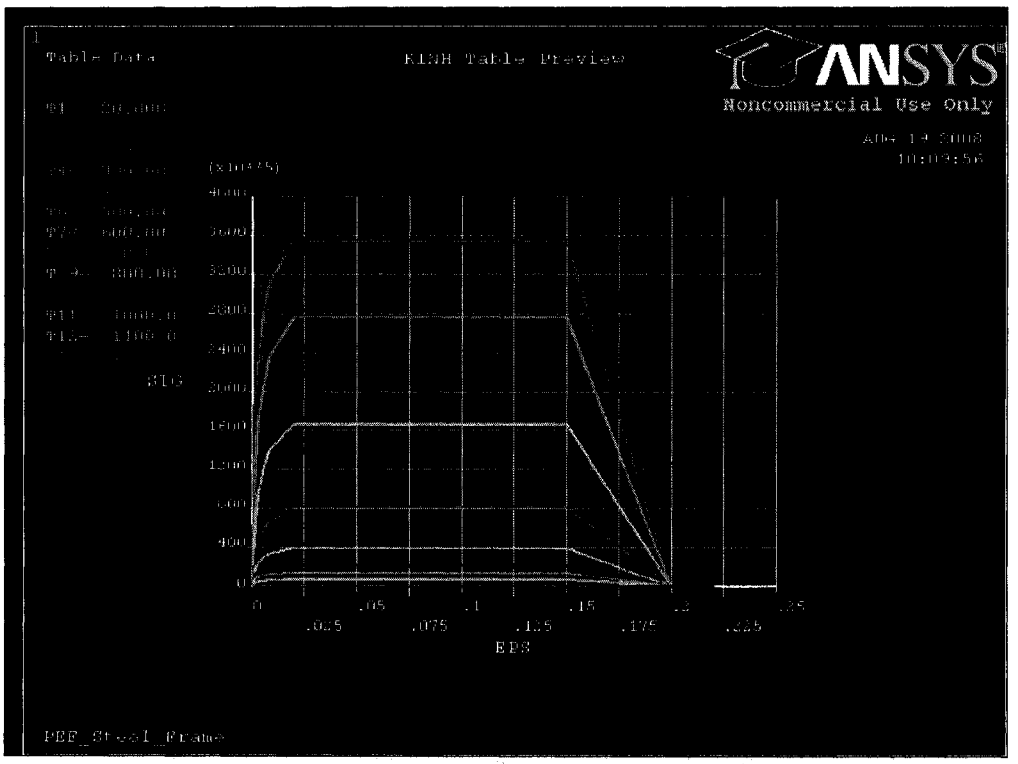

Figure 8-12 Stress strain relationship for steel

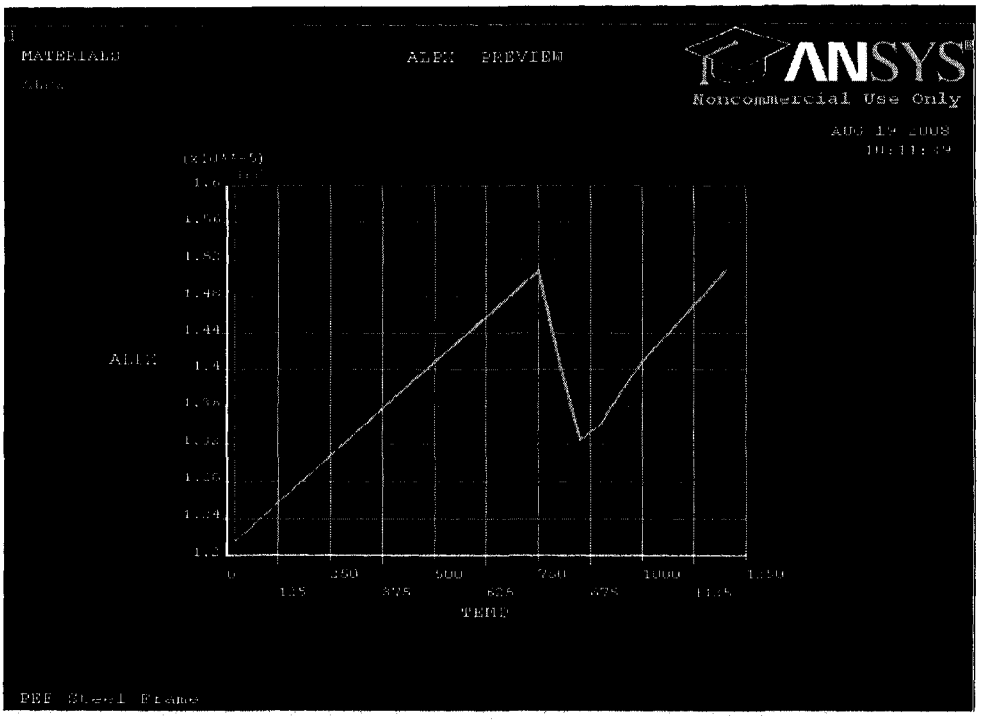

Figure 8-13 Thermal expansion coefficient for steel

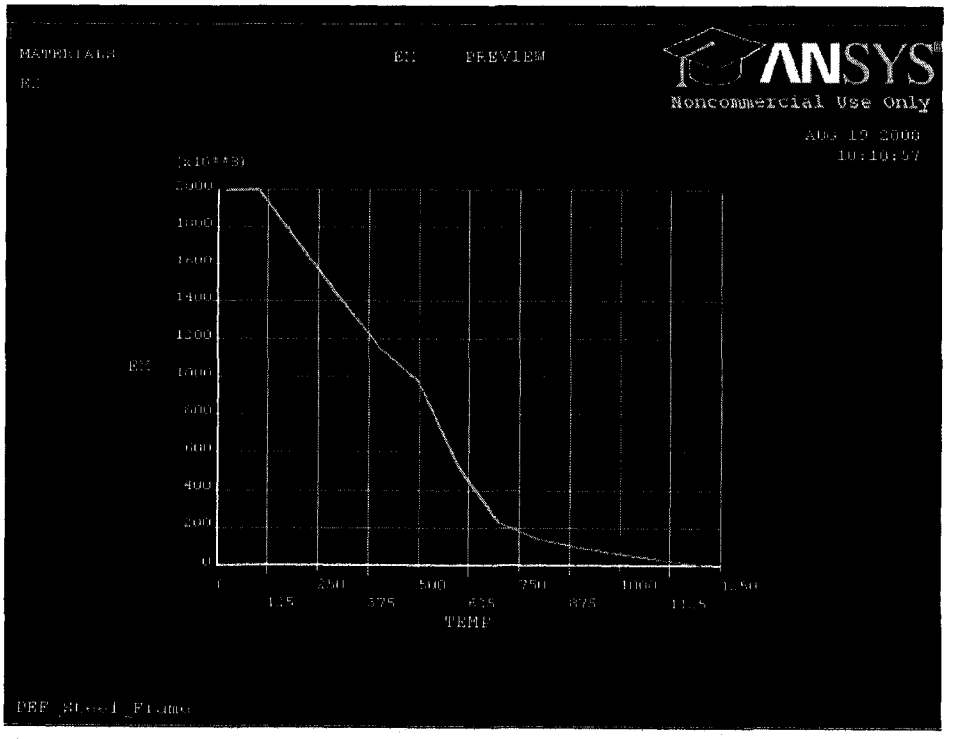

Figure 8-14 Reduction factor for steel modulus of elasticity due to high temperatures

6) Thermal Stress Analysis with the Absence of Earthquake Event: In this step the thermal stress analysis is performed to calculate the thermal stresses and deflections in the model nodes due to fire load only. ANSYS has been used to perform this stage. The deflection at node B of the frame is shown in Figure 8-16 and the mid-span deflection is shown in Figure 8-17.

7) Dynamic Analysis with no Fire Applied: For the nonlinear dynamic analysis requirements a modal analysis has been performed through ANSYS to get the fundamental frequency of the structure from the first mode.

The fundamental frequency of the frame is used then in the dynamic calculations of the frame. The modeling of the steel frame for the earthquake analysis has been done without any thermal load and by applying the north-south component time history acceleration data of the famous El Centro earthquake (the 1940 Imperial Valley earthquake) see Figure 8-15. .The acceleration has been applied in the X direction.

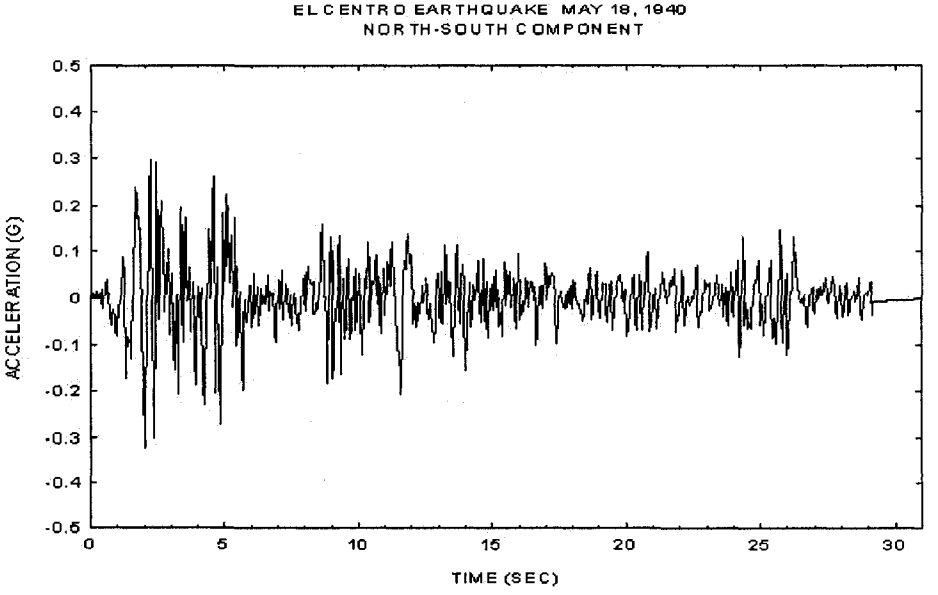

Figure 8-15 El Centro time history acceleration data (PEER)

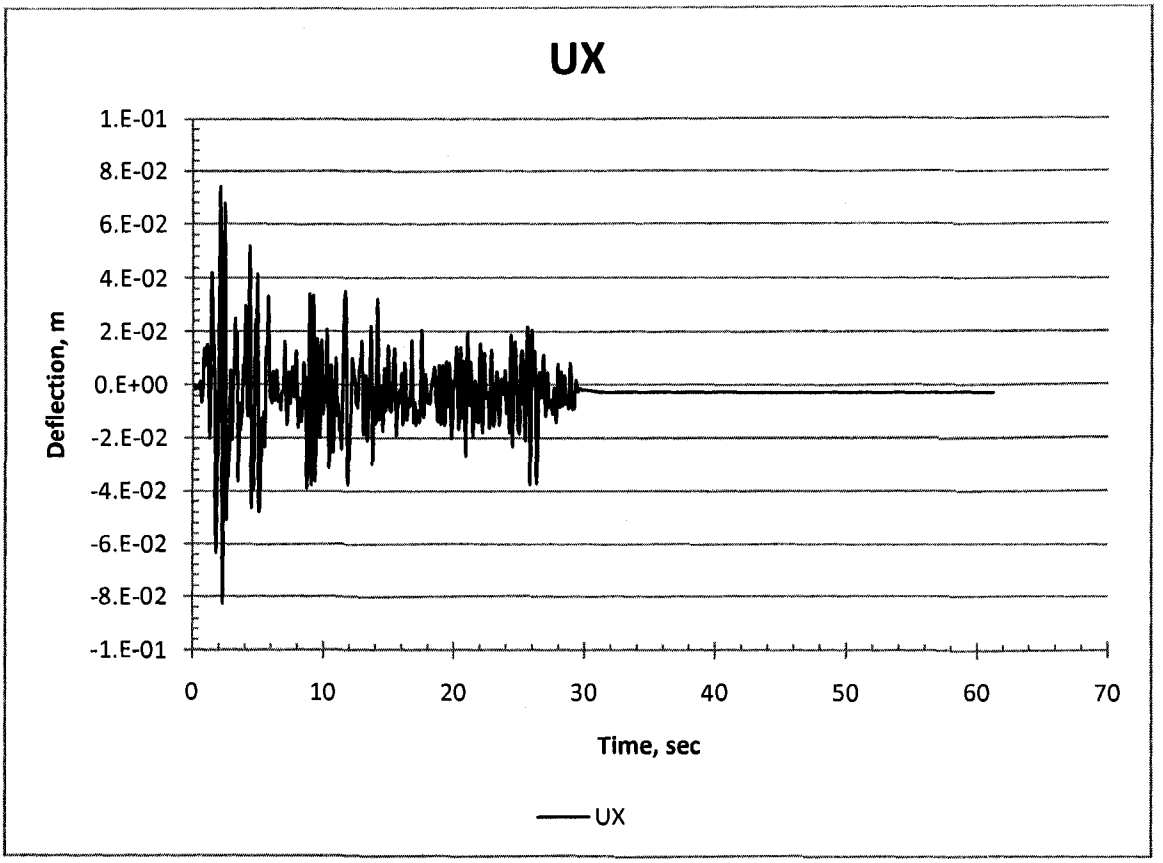

Figure 8-16 Residuals deformation after the end of earthquake

8) Dynamic Analysis Results: the results from dynamic analysis performed in step 7, show that after the earthquake event ends, the frame has some residuals strains and the structure suffers from some damages. The new geometry of the frame, due to the permanent deflections, and new initial stresses are then considered input for the following stage. The thermal load applied directly to the deformed frame after the end of earthquake and thermal stress analysis is conducted in ANSYS for the new structure (i.e. after damage).

9) PEF analysis or Dynamic Analysis with Fire Applied: the procedure explained in step 7 is repeated here and followed by a transient thermal stress analysis for the time dependent thermal load applied on frame from fire and obtained as explained

in step 4. The whole analysis, except of the heat transfer analysis, is performed in ANSYS.

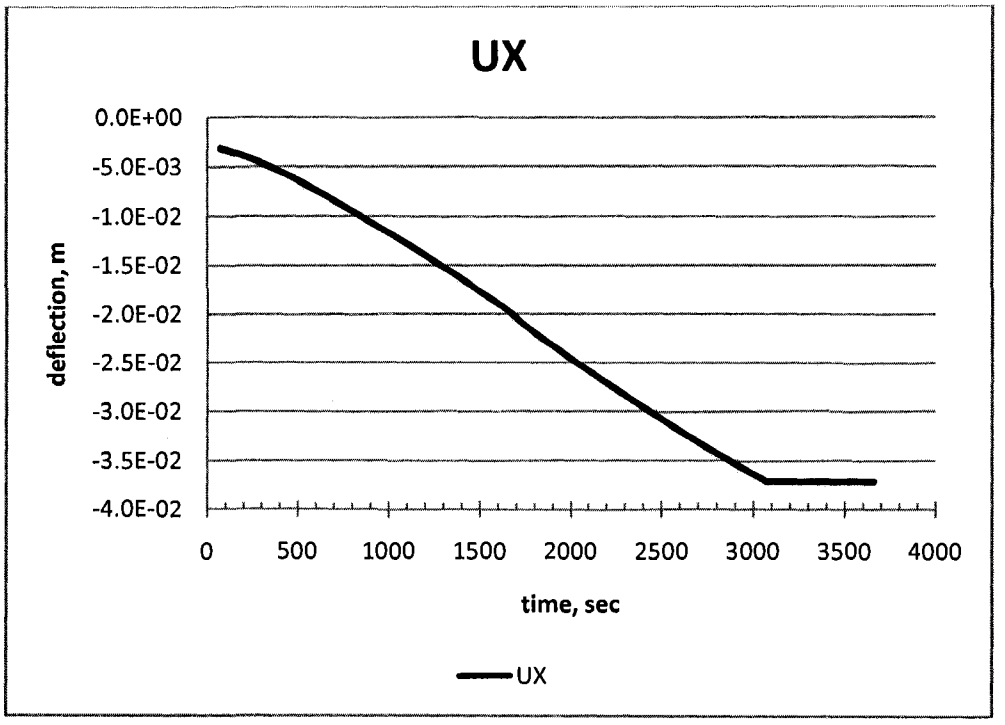

Figure 8-17 Horizontal deflection at the mid-span node in case of normal fire

10) Results Analysis: PEF analysis results are presented through Figures 8-14 to 8-17. The comparison between the lateral or vertical displacement in the frame nodes in normal and post-earthquake fire as presented in Figures 8-20 and 8-21, shows a shift in the deflection occurrence; which indicates an atelier failure in the structure in the case of PEF. The shift time duration between the two curves is 4 minutes for the applied magnitude.

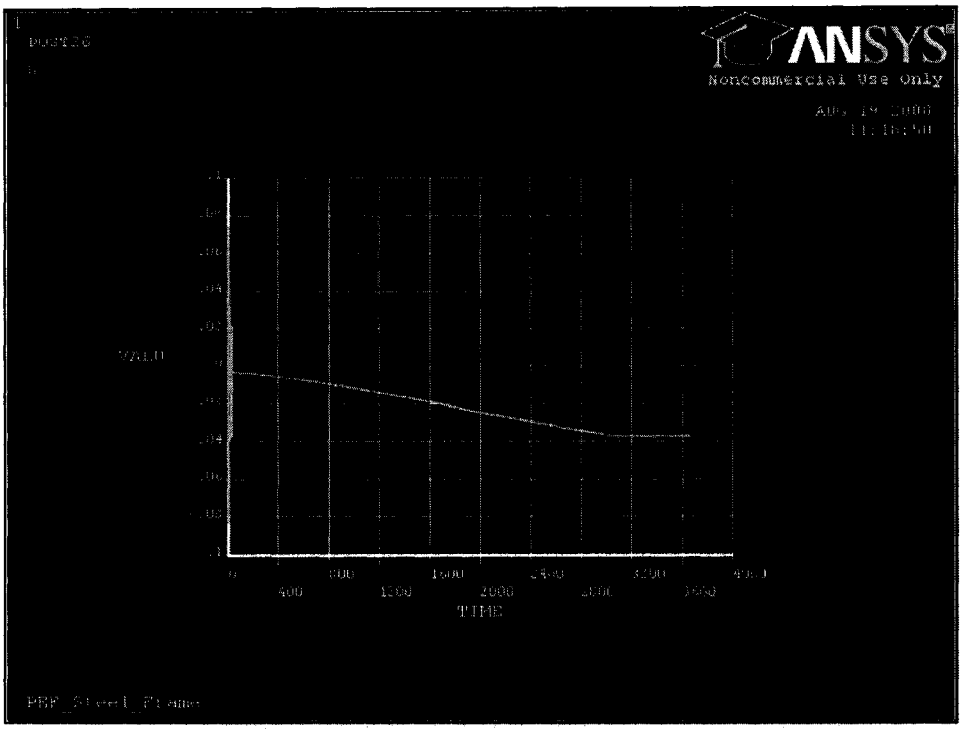

Figure 8-18 Horizontal deflection in the beam in case of PEE

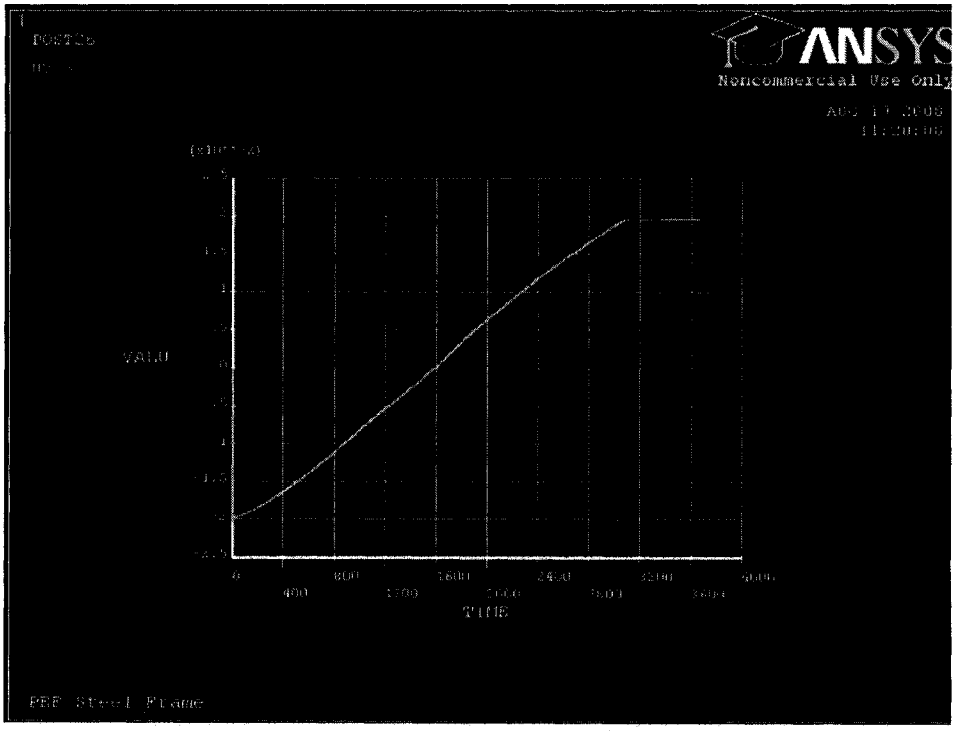

Figure 8-19 vertical deflection at the mid-span node in case of PEF

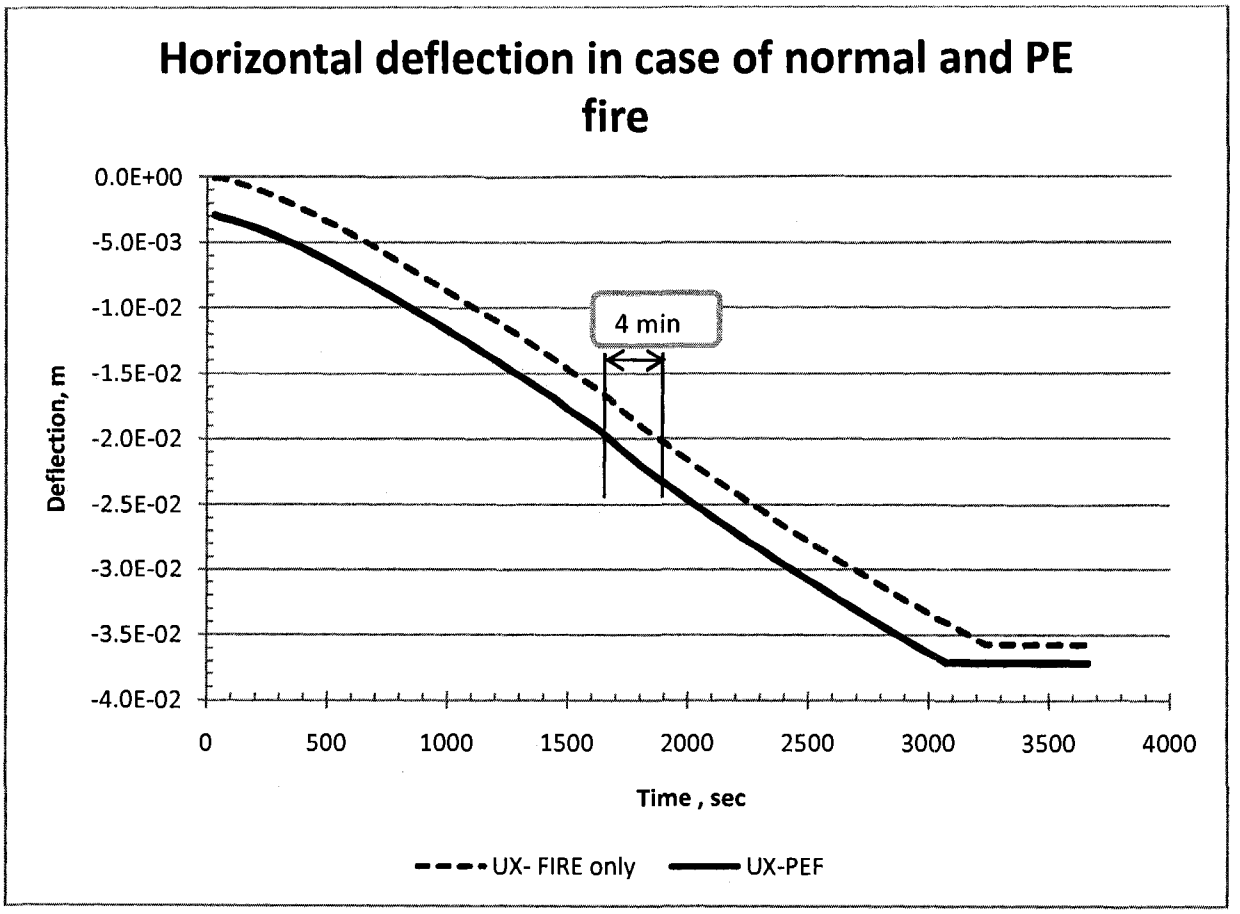

Figure 8-20 Horizontal deflection in case of normal and PE fire

11) Applying different Peak Ground Acceleration (PGA) Magnitude: The procedure explained in the previous steps is repeated by applying magnified acceleration data by several factors. For each degree of magnification the displacement in the frame nodes is calculated and the shift from the displacement curve for normal fore is measured. A correlation between the magnitude of earthquake and the reduction the fire rate resistance is then obtained. The curve is normalized to the frame fire resistant rate t_f in normal fire. The reduction factor in the fire resistant rate due to different levels of earthquake is presented in Figure 8-22.

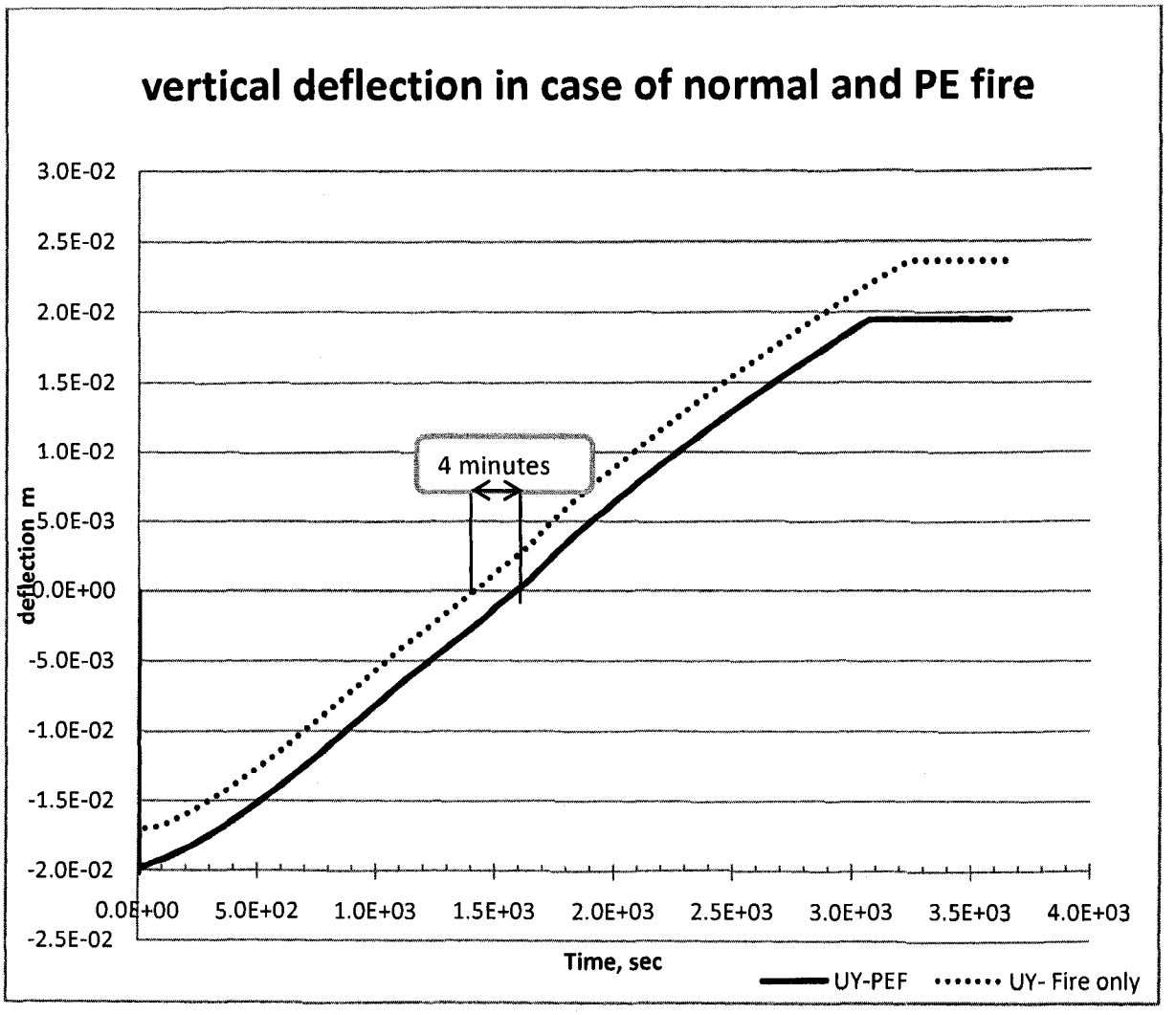

Figure 8-21 Vertical deflection in case of normal and PE fire

The magnified factor is multiplied by the PGA which is equal to 0.3g for El Centro earthquake. The increasing in the earthquake tens continued until the frame failed at level 4*0.3g. Figure 8-22 indicates that there is a strong relationship between the remaining fire resistant rate of steel frame after earthquake and the intense if the ground motion.

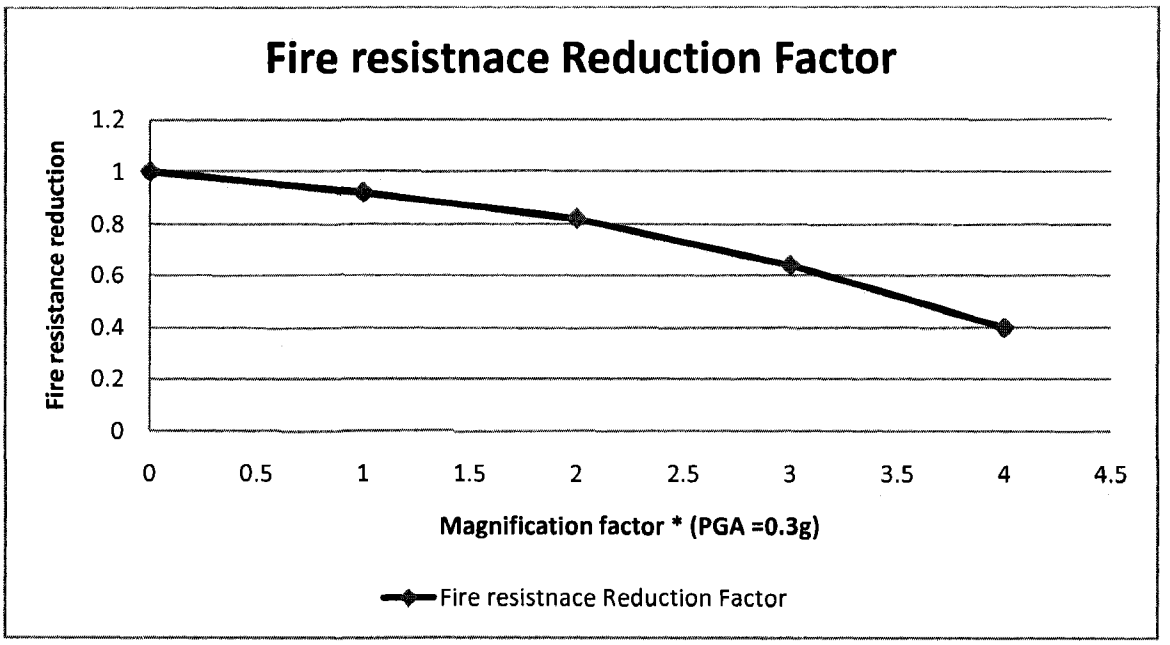

Figure 8-22 The correlation between the acceleration magnitude and the fire resistance.

It can be concluded from this analysis that the PEF analysis should be performed by combining between different types of simulators. The nature of metaphysics involved in the PEF event makes it so complex to perform the analysis in one environment. The analysis could be simplified by dividing the whole procedure into sup steps which can be performed separately and in sequence.

Chapter 9

Summary and Conclusion

9.1 Summary:

Although major earthquakes are followed by subsequent fires, the current design codes do not explicitly consider them as possible design scenarios, However, in a performance-based design paradigm, such scenario should also be considered in order to afford a desired level of performance, particularly of the important structures. Steel and wood structures are vulnerable to fire in normal conditions. For that reason, they are usually fire-proofed. Earthquake structure may cause damage to the fire protection system as well as the structure itself. Fire followed by such events finds steel structures particularly vulnerable.

The current study presented a review of literature on post-earthquake fire, and proposed analysis procedures to study wood-framed and steel-framed structure. The study shows a reduction in the fire resistance of the structure when it exposed to fire after the earthquake. A preliminary study of a limited set of steel frames and wood frame, which shows that lateral load induced deformation, can reduce the fire performance of such building frames is presented here. The reduction in the overall fire resistant of the structure can be estimated by applying different levels of ground excitations and compare

the deflections at the structure nodes for normal and post-earthquake scenarios. Further three dimensional (3D) analysis is strongly recommended to extend this thesis work.

9.2 Conclusions:

- PEF received very little attention. In performance based design all hazard must be considered in a systematic way.
- The present work provided a systematic analysis schemes for PEF post-evaluation which was not available in existing literature, preliminary set of study using proposed schemes have been presented.
- PEF can represent a serious hazard from the point of life safety, property damage and economic loss in seismically active regions. So there is a strong need to consider appropriate hazard mitigation technique to overcome PEF problem.
- At present there are very little information or design guidelines in codes and standards to address the problem of PEF in buildings and built infrastructure.
- The main factors affecting PEF hazard are earthquake intensity and aftershocks, fire scenarios, performance of active and passive fire protection systems, materials used in construction, and availability of emergency services following earthquake.
- Two schemes for analysis of steel frame structures under PEF events have been proposed here. Both schemes produce consistent results for PEF performance of these structures.
- Ensuring structural fire safety is a key consideration in developing strategies at individual building level. Other aspects include, developing relevant design scenarios,

proper selection of materials, detailed analysis for various design scenarios and evaluation of risk based on performance based design.

- The proposed buckling analysis model for use stud wall system exposed to fire following an earthquake or lateral load produce very close estimate of fire resistance of wood stud wall to that observed in the fire test of such system conducted at NRC.
- It can be concluded from the presented analysis that the fire resistant rate, which is important for fire safety, is affected significantly when the structure is exposed to earthquake load especially in wood structures.
- The reduction in the fire resistance t_f is function of the lateral deflection in the structure caused by the earthquake.
- Performance evaluation of building under fire or under earthquake separately is not sufficient for performance-based design. Building should be evaluated under the combined effect of fire following earthquake. The level of seismic performance of the structure should be correlated with the fire performance of the structure.

9.3 Scope for future work:

This presented study proposed a systematic way for analyzing structure in PEF scenario and developed appropriate schemes of analysis for PEF performance of wood stud wall systems and steel moment resisting frames, However, the study presented here is limited in nature which needs to be expanded to include more complex and realistic structural systems and various other seismic and fire exposure scenarios. The study included 2D analysis for two types of structures. The 3D modeling of such structures would be more

appropriate way to extend this study in order to understand the behavior of structures in PEF.

References:

ABAQUS, cited November 11, 2007, "ABAQUS FEA", http://www.simulia.com/products/abaqus_fea.html, Dassault Systèmes, USA.

Anchor R.D., Malhotra H.L., and Purkiss J.A., 1986,Design of structures against fire. In Proceedings of the international conference on Design of Structures against Fire, Aston University, Birmingham, UK

ANSYS,2008, Ansys Documentations. Version 11

ANSYS,2008, Ansys Verification Manual. Version 11

ANSYS, cited August 17, 2007,ANSYS-CFX: http://www.ansys.com/products/cfx.asp

ASCE Standard No. 7-05, 2005," Minimum Design Loads for Buildings and Other Structures", ASCE-SEI 7-05. American Society of Civil Engineers, Reston, VA, U.S.A.

Beer, Ferdinand P.; Dewolf, John T. 2005, Mechanics of Materials ,McGraw-Hill College

Bénichou, N.; Sultan, M.A.; MacCallum, C.; Hum, J. 2001, Thermal Properties of Wood, Gypsum and Insulation at Elevated Temperatures, IRC-710

Benichou, N; Morgan,D; April 2003,"Structural Response Model for Wood Stud Wall Assemblies"- Theory Manual, Irc-Rr-128.

Bernhart D., 2004, "The Effect of Support Conditions on the Fire Resistance of a Reinforced Concrete Beam" Research project report, University of Canterbury, Christchurch, New Zealand

Buchanan ,Andrew H; 2001, "Structural Design for Fire Safety" , John Wiley & Sons, Inc.

CAN/CSA-A82.27-M91, 1991 ,Gypsum Board-Building Materials and Products. Canadian Standards Association, Rexdale, Ontario.

CAN/CSA -A82.31-M91, 1991,Gypsum Board Application, Canadian Standards Association, Rexdale, Ontario.

CAN/ULC-S101-M89, 1989, Standard Methods of Fire Endurance Tests of Building

Construction and Materials, Underwriters' Laboratories of Canada, Scarborough, Ontario.

CANPLY, 2008, Plywood Design Fundamentals

Chang J., 2003, 2D Analysis of the Performance of Connections with Unprotected Steel Structural Members Exposed to Parametric Fire. Research project report, University of Canterbury, Christchurch, New Zealand

Chen S., Lee G.C., and Shinozuka M., 2004, " Hazard Mitigation for Earthquake and Subsequent fire", ANCER Annual Meeting: Networking of Young Earthquake Engineering Researchers and Professionals, July, Honolulu, Hawaii, U.S.A.

Chen S., Lee G.C.;Shinozuka M., 2004, " Hazard Mitigation for Earthquake and Subsequent Fire", Ancer Annual Meeting: Networking of Young Earthquake Engineering Researchers and Professionals, Honolulu, Hawaii, U.S.A.

Chopra. A.K. 1995, "Dynamics of Structures", Prentice Hall, New Jersey.

Chung R.M., Jason N.H., Mohraz B. Mowrer F.W. and Walton W.D., 1995, "Post-Earthquake Fire and Lifelines Workshop: Long Beach California, January 30-31, proceedings ".

Chung R.M., Jason N.H., Mohraz B., Mowrer F.W., and Walton W.D., 1995," Post-Earthquake Fire and Lifelines" Workshop: Long Beach, California. National Institute of Standards and Technology, Gaithersburg, MD.

Compliance Document for New Zealand Building Code , 2006– Fire Safety, Department of Building and Housing, September, Wellington, New Zealand.

CSA 0141; 1970, Softwood Lumber, Canadian Standards Association, Rexdale, Ontario.

Della Corte, G., Landolfo R., and Mazzolini, F.M., November 2003,"Post-earthquake fire resistance of moment resisting steel frames", Fire Safety Journal, Volume **38** Issue 7, P: 593-612.

Dinehart D. W. ; Shenton H. W. (1983);Model for dynamic analysis of wood frame shear walls,Journal of engineering mechanics,2000, vol. 126, n°9, pp. 899-908 (18 ref.),American Society of Civil Engineers, Reston, VA, ETATS-UNIS

EC1, 1994, Actions on Structures. Eurocode 1, European Committee on Standardization (CEN), Brussels, Belium.

Eidinger J.M., 2004, "Fire Following Earthquake- Flex Hose", 13th World Conference on Earthquake Engineering Vancouver, B.C., Canada August 1-6, ,

Paper No. 3268.

FEMA 349, 2001, Action Plan for Performance Based Seismic Design, Federal Emergency Management Agency , Earthquake Publications and Resources

FEMA, Federal Emergency Management Agency ,2006, Hazus, Http://Www.Nibs.Org/Hazusweb/Overview/Hazus.Php, , U.S.A.

FLUENT, 2006, Http://Www.Fluent.Com/Solutions/Examples/X3.Htm.

Fonseca, F.S. et J.P. Judd. 2004. Effect of overdriven-nail-depth combinations on wood shear wall strength. Proceedings of the 8th World Conference on Timber Engineering. Lahti, Finland.

Franssen J. M., Kodur V. K.R., and Mason J. 2000, User's Manual for Safir 2002 – "A Computer Program for Analysis of Structures Submitted To Fire", Department Structures Du Génie Civil, Service Ponts Et Charpentes, University of Liège, Belgium.

Grosshandler ,W., 2002, "Fire Resistance Determination and Performance Prediction Research Needs Workshop": Proceedings, Nistir 6890.

Harmathy S., 1978,"Design of Buildings for Fire Safety", ASTM Stp 685

Harmathy, T.Z., 1993, "Fire Safety Design and Concrete", Longman Scientific &Technical, Essex, UK, Pp. 412.

Incropera, 2007, Frank P Introduction To Heat Transfer 5th Ed, Publisher New York :Wiley.

International Building Code, 2003, International Code Committee, Washinton D.C.,U.S.A.

Judd,John P.; 2005, Analytical Modeling of Wood-Frame Shear Walls and Diaphragms.

Kamiya, F. 1987, "Buckling of Sheathed Walls: Linear Analysis", Journal of Structural Engineering, Vol. 113 Pp.2009-22.

Kodur, V.K.R. , Sultan, M.A. ,1998, "Structural Behaviour of High Strength Concrete Columns Exposed To Fire", International Symposium on High Performance and Reactive Powder Concrete, Sherbrooke, Qc, Pp. 217-232.

Kodur, V.K.R. 2000, "Spalling In High Strength Concrete Exposed To Fire – Concerns, Causes, Critical Parameters and Cures", Conference Proceeding Paper, Ascs, Section 48, Chapter 1, (Doi 10.1061/40492(2000)180)

Kodur, V.K.R., 2002," Fire resistance research needs for high performing materials. In Proceedings", Workshop: Making the Nation Safe from Fire: A Path Forward in Research. The New Academic Press, National Academy of Sciences, 237-243, Washington D.C., U.S.A.

Kodur, V.K.R; Sultan, M.A.; Denham, E.M.A.; 1996, IRC-IR-729 Temperature Measurements In Full-Scale Wood Stud Shear Walls.

Kodur, V.R., 2005,"Guidelines for fire resistance design of high strength concrete columns", Journal of Fire Protection Engineering, **15**(2): 93-106.

Kodur, V.R., and McGrath, R.C., 2003," Fire endurance of high strength concrete columns", Fire Technology – Special Issue, 39(1): 73-87.

Kodur, V.R., and Sultan, M.A., 2000," Performance of wood stud shear walls exposed to fire", Fire and Materials, 24, 9-16.

Kodur, V.R., Green, M.F., and Bisby, L.A., 2006," Fire Resistance of FRP-Strengthened Concrete Systems", Monograph –FRP- Strengthened Concrete, ISIS, Canada, in Press.

Kosaka S., 2004, "Estimation of Damage Due To Fires-Refuge Simulation Technique Considered Fire Break Out Probability on An Earthquake", 13th World Conference on Earthquake Engineering Vancouver, B.C., Canada August 1-6, 2004 Paper No. 1902.

Legrone P.D., 2004, "An Analysis of Fire Sprinkler System Failures During The Northridge Earthquake and Comparison with The Seismic Design Standard for These Systems", 13th World Conference on Earthquake Engineering Vancouver, B.C., Canada August 1-6, 2004 Paper No. 2136.

Lie, T.T. and Woollerton, J.L. 1988, "Fire Resistance of Reinforced Concrete Columns: Test Results", Institute for Research in Construction Internal Report No. 569, National Research Council of Canada, Ottawa, ON., 302 Pp.

Marrion C., 2005, "Design of Structures for Fire Loading and Understanding Fire/Life Safety System Interdependencies", Conference Proceeding Paper, ASCE .

Medearis, K., Nov 1978,"Blasting Vibration Damage Criteria for Low-Rise Structures," J. Sound Vib.

Moody, R.C., Nov 1986,"A Structural Analysis Model for Three-Dimensional Behavior of Wall Systems In Light-Frame Buildings," U.S. Dept. of Agriculture, Forest Serv., Forest Prod. Lab., Unpub. Res. Paper.

Moore A.E., Albano L.D., Fitzgerald R.W., and Meacham B.J., April 20-24, 2005,"

Defining Design Fires for Structural Performance", In Proceedings of ASCE Structures Congress and Forensic Engineering Symposium, Structural Engineering Institute of the American Society of Civil Engineers, New York, NY, (doi:10.1061/40753(171)55).

Mousavi,S.; Bagchi A.; Kodur V. K. R.; 2008, a review of post-earthquake fire hazard to building structures. Canadian Journal of Civil Engineering, Volume 35, Number 7, July 2008

Naik, T.R., Mar 1982,"Torsional Response of Low-Rise Timber Structures Subjected To Seismic Ground Motion", Univ. of Wisconsin, Miiwaukee and Forest Prod. Lab., Coop. Res. Rept.

NBCC, 2005,National Building and Fire Code of Canada, National Research Council, Ottawa, Canada.

NRC, 2006, National Research Council Canada, Http://Irc.Nrc-Cnrc.Gc.Ca/Fr/Frhb/Firecamnew_E.Html

Needs Workshop on Analysis, Design and Testing of Timber Structures Under Seismic Loads, Forest Products Laboratory, University of California, Richmond, California, 3–8.

NIST, 1995, "Post-Earthquake Fire and Life Lines Workshop Proceedings", Long Beach, California, January, Editors: Chung R.M., Jason N.H., Mowrer F.W. and Walton W.D., Nist Special Publication 889.

NIST, 2004, "NIST-SFPE Workshop for Development of a National R&D Roadmap for Structural Fire Safety Design and Retrofit of Structures: Proceedings ", Report No. NlSTlR 7133, National Institute of Standards and Technology, USA.

NIST, 2006, Fire Dynamics Simulator (Fds) and Smokevie, Http://Www.Fire.Nist.Gov/Fds/

Phan, L.T. ,1996, "Fire Performance of High-Strength Concrete: A Report of The State-of-The-Art", National Institute of Standards and Technology, Gaithersburg, Md, Pp. 105.

Rosowsky, D. V., Ellingwood, B. ,2002, "Performanced-Based Engineering of Wood Frame Housing." Journal of Structural Engineering, American Society of Civil Engineers,Vol. 128, No. 1, 32–38.

Scawthorn C., Eidinger J.M., and Schiff A.J., 2005, Fire Following Earthquake. Technical Council on Lifeline Earthquake Engineering, Monograph No. 26, American Society of Civil Engineers (Asce), Reston, Va.

Scawthorn C., Eidinger J.M., and Schiff A.J., 2005, "Fire Following Earthquake", Technical Council on Lifeline Earthquake Engineering, Monograph No. 26, American Society of Civil Engineers (ASCE), Reston, VA.

Seputro J., 2001, "Effect of Support Conditions on Steel Beams Exposed To Fire", Fire Engineering Research Report, Department of Civil Engineering, University of Canterbury, Christchurch, New Zealand.

SFPE, 2004,Fire Exposures to Structural Elements - Engineering Guide. Society of Fire Protection Engineers, Bethesda, MD, pp. 150.

Sharp G., 2003, "Earthquake Damage To Passive Fire Protection Systems In Tall Buildings and Its Impact on Fire Safety", Research Project Report, University of Canterbury, Christchurch, New Zealand

SUEL, 2006, cited August 17, 2007, Vulcan – A software for Structural Fire Engineering. Vulcan Solutions Ltd – a Company of Sheffield University Enterprises Limited, Sheffield, UK. Available from http://www.shef.ac.uk/suel/companies/vulcan.html.

Sugiyama, H., May 1984,"Japanese Experience and Research on Timber Buildings In Earthquakes," Proc. Pacific Timber Engrg. Conf., Auckland, New Zealand.

Sultan, M.A.; Kodur, V.R.; Light-Weight Fram Wall Assemblies: Parameters for Consideration In Fire Resistance Performanc-Based Design, Fire Technology, Vol. 36 No. 2,2000

Lee, Tae-Hyung; Kato, Mikiko; Matsumiya, Tormohiro; Keiichiro, Suita; and Nakashima, Masayoshi, 2006, "Seismic Performance Evaluation of Nonstructural Components:Drywall Partitions. Abstracts for Annuals". Disaster Prevention Research Institute, Kyoto University 49c,177-188

Tae-Hyung Lee, Mikiko Kato, Tormohiro Matsumiya, Keiichiro Suita, Masayoshi Nakashima2006, "Seismic Performance Evaluation of Nonstructural Components:Drywall Partitions. Abstracts for Annuals". Disaster Prevention Research Institute, Kyoto University 49c,177-188

Taylor J., 2003, "Post Earthquake Fire In Tall Buildings and The New Zealand Building Code", Research Project Report, University of Canterbury, Christchurch, New Zealand.

Todd, D. R., Carino, N. J., Chung, R. M., Lew, H. S., Taylor, A. W., Walton, W. D., Cooper, J. D., and Nimis, R., 1994, Northridge Earthquake: Performance of Structures, Lifelines and Fire Protection Systems, NIST Special Publication 862, National Institute of Standards and Technology, Gaithersburg, MD.

University of Liège , 2006, Department of Mechanics of Materials and Structures, Www.Ulg.Ac.Be/Matstruc/En/Download.

Wang Y.C. , 2002,"Steel and Composite Structures – Behavior and Design for Fire Safety", Spon Press.

Wang Y.C., 2002, "Steel and Composite Structures – Behavior and Design for Fire Safety", Spon Press.

Wang Y.C., and Kodur V.K.R., 2000,"Research towards unprotected Steel Structures", ASCE Journal of Structural Engineering, 126 (12): 1442-1450.

Wastney C., 2002, "Performance of Unprotected Steel and Composite Steel Frames Exposed To Fire", Research Project Report, University of Canterbury, Christchurch, New Zealand.

Wickstrom, U.; Duthinh, D.; Mcgrattan, K. B.; 2007, "Adiabatic Surface Temperature for Calculating Heat Transfer To Fire Exposed Structures".

Williamson R.B., 1999," Manual of Evaluation Procedures for Passive Fire Prevention Following Earthquake" Report - NIST GCR 99-768, National Institute of Standards and Technology (NIST), Gaithersburg, MD, U.S.A.

Y. Anderberg, Modelling Steel Behaviour. Fire Safety J 13 1 (1988), Pp. 17–26.

Zacher, E. G. ,1994, "Past Seismic Performance of Timber Buildings." Procedings, Research.

Zhao S.J., Xiong L.Y. and Ren A.Z., 2006, "A Spatial-Temporal Stochastic Simulation of Fire Outbreaks Following Earthquakes Based on GIS", Journal of Fire Sciences, 24: 313-339.

Appendix:

ANSYS Script:

```
FINI
/CLEAR
/FILNAME, Seismic_analysis,1
/TITLE, PEF_Steel_Frame
/UNITS,SI
/CWD,'C:\Documents and Settings\hany_yassin\My
Documents\ansys_work\seismic'
/input,read,txt,'',,,,,,,,,,,,,,,1
/PREP7
SAVE, Frame, db,, all
/GRA,POWER
/GST,ON
/TRIAD,OFF
/ESHAPE,1
/PREP7
TOFFST,273
TB,KINH,1,13,15,
TBTEMP,20
TBPT,,0,0
TBPT,,0.00125,2.5E+008
TBPT,,0.002,2.773E+008
TBPT,,0.00275,2.8935E+008
TBPT,,0.0035,2.9831E+008
TBPT,,0.00425,3.0561E+008
TBPT,,0.005,3.118E+008
TBPT,,0.00575,3.1719E+008
TBPT,,0.0065,3.2195E+008
TBPT,,0.00725,3.2618E+008
TBPT,,0.008,3.2998E+008
TBPT,,0.00875,3.334E+008
TBPT,,0.02,3.55E+008
TBPT,,0.15,3.55E+008
TBPT,,0.2,0
TBTEMP,100
TBPT,,0,0
TBPT,,0.00125,2.5E+008
TBPT,,0.002,2.773E+008
TBPT,,0.00275,2.8935E+008
TBPT,,0.0035,2.9831E+008
TBPT,,0.00425,3.0561E+008
TBPT,,0.005,3.118E+008
TBPT,,0.00575,3.1719E+008
TBPT,,0.0065,3.2195E+008
TBPT,,0.00725,3.2618E+008
TBPT,,0.008,3.2998E+008
TBPT,,0.00875,3.334E+008
TBPT,,0.02,3.55E+008
TBPT,,0.15,3.55E+008
TBPT,,0.2,0
```

```
TBTEMP,200
TBPT,,0,0
TBPT,,0.00125,2.144E+008
TBPT,,0.002,2.432E+008
TBPT,,0.00275,2.5989E+008
TBPT,,0.0035,2.726E+008
TBPT,,0.00425,2.8307E+008
TBPT,,0.005,2.9201E+008
TBPT,,0.00575,2.9982E+008
TBPT,,0.0065,3.0672E+008
TBPT,,0.00725,3.1289E+008
TBPT,,0.008,3.1842E+008
TBPT,,0.00875,3.234E+008
TBPT,,0.02,3.55E+008
TBPT,,0.15,3.55E+008
TBPT,,0.2,0
TBTEMP,300
TBPT,,0,0
TBPT,,0.00125,1.7867E+008
TBPT,,0.002,2.1018E+008
TBPT,,0.00275,2.3087E+008
TBPT,,0.0035,2.4707E+008
TBPT,,0.00425,2.6056E+008
TBPT,,0.005,2.7217E+008
TBPT,,0.00575,2.8235E+008
TBPT,,0.0065,2.9139E+008
TBPT,,0.00725,2.9947E+008
TBPT,,0.008,3.0674E+008
TBPT,,0.00875,3.1329E+008
TBPT,,0.02,3.55E+008
TBPT,,0.15,3.55E+008
TBPT,,0.2,0
TBTEMP,400
TBPT,,0,0
TBPT,,0.00125,1.4541E+008
TBPT,,0.002,1.7877E+008
TBPT,,0.00275,2.0273E+008
TBPT,,0.0035,2.2202E+008
TBPT,,0.00425,2.3832E+008
TBPT,,0.005,2.5246E+008
TBPT,,0.00575,2.6493E+008
TBPT,,0.0065,2.7604E+008
TBPT,,0.00725,2.8601E+008
TBPT,,0.008,2.9499E+008
TBPT,,0.00875,3.0311E+008
TBPT,,0.02,3.55E+008
TBPT,,0.15,3.55E+008
TBPT,,0.2,0
TBTEMP,500
TBPT,,0,0
TBPT,,0.00125,1.2158E+008
TBPT,,0.002,1.4654E+008
TBPT,,0.00275,1.6435E+008
TBPT,,0.0035,1.7865E+008
TBPT,,0.00425,1.9071E+008
TBPT,,0.005,2.0117E+008
TBPT,,0.00575,2.1039E+008
```

```
TBPT,,0.0065,2.186E+008
TBPT,,0.00725,2.2597E+008
TBPT,,0.008,2.326E+008
TBPT,,0.00875,2.3859E+008
TBPT,,0.02,2.769E+008
TBPT,,0.15,2.769E+008
TBPT,,0.2,0
TBTEMP,600
TBPT,,0,0
TBPT,,0.00125,6.4667E+007
TBPT,,0.002,8.0657E+007
TBPT,,0.00275,9.2284E+007
TBPT,,0.0035,1.0168E+008
TBPT,,0.00425,1.0965E+008
TBPT,,0.005,1.1656E+008
TBPT,,0.00575,1.2267E+008
TBPT,,0.0065,1.2811E+008
TBPT,,0.00725,1.3299E+008
TBPT,,0.008,1.374E+008
TBPT,,0.00875,1.4138E+008
TBPT,,0.02,1.6685E+008
TBPT,,0.15,1.6685E+008
TBPT,,0.2,0
TBTEMP,700
TBPT,,0,0
TBPT,,0.00125,2.8134E+007
TBPT,,0.002,3.6294E+007
TBPT,,0.00275,4.2334E+007
TBPT,,0.0035,4.7251E+007
TBPT,,0.00425,5.143E+007
TBPT,,0.005,5.5068E+007
TBPT,,0.00575,5.8285E+007
TBPT,,0.0065,6.1156E+007
TBPT,,0.00725,6.3736E+007
TBPT,,0.008,6.6062E+007
TBPT,,0.00875,6.8166E+007
TBPT,,0.02,8.165E+007
TBPT,,0.15,8.165E+007
TBPT,,0.2,0

TBTEMP,800
TBPT,,0,0
TBPT,,0.00125,1.7381E+007
TBPT,,0.002,2.0804E+007
TBPT,,0.00275,2.3277E+007
TBPT,,0.0035,2.5271E+007
TBPT,,0.00425,2.6958E+007
TBPT,,0.005,2.8422E+007
TBPT,,0.00575,2.9713E+007
TBPT,,0.0065,3.0864E+007
TBPT,,0.00725,3.1897E+007
TBPT,,0.008,3.2828E+007
TBPT,,0.00875,3.3669E+007
TBPT,,0.02,3.905E+007
TBPT,,0.15,3.905E+007
TBPT,,0.2,0
TBTEMP,900
```

```
TBPT,,0,0
TBPT,,0.00125,11814142.46
TBPT,,0.002,13336839.3
TBPT,,0.00275,14424106.51
TBPT,,0.0035,15297438.45
TBPT,,0.00425,16034454.71
TBPT,,0.005,16673404.71
TBPT,,0.00575,17236531.75
TBPT,,0.0065,17738137.49
TBPT,,0.00725,18188061.54
TBPT,,0.008,18593410.91
TBPT,,0.00875,18959508.97
TBPT,,0.02,21300000
TBPT,,0.15,21300000
TBPT,,0.2,0
TBTEMP,1000
TBPT,,0,0
TBPT,,0.00125,7876094.973
TBPT,,0.002,8891226.202
TBPT,,0.00275,9616071.007
TBPT,,0.0035,10198292.3
TBPT,,0.00425,10689636.48
TBPT,,0.005,11115603.14
TBPT,,0.00575,11491021.17
TBPT,,0.0065,11825425
TBPT,,0.00725,12125374.36
TBPT,,0.008,12395607.27
TBPT,,0.00875,12639672.65
TBPT,,0.02,14200000
TBPT,,0.15,14200000
TBPT,,0.2,0
TBTEMP,1100
TBPT,,0,0
TBPT,,0.00125,3938047.486
TBPT,,0.002,4445613.101
TBPT,,0.00275,4808035.503
TBPT,,0.0035,5099146.152
TBPT,,0.00425,5344818.238
TBPT,,0.005,5557801.57
TBPT,,0.00575,5745510.584
TBPT,,0.0065,5912712.498
TBPT,,0.00725,6062687.181
TBPT,,0.008,6197803.637
TBPT,,0.00875,6319836.325
TBPT,,0.02,7100000
TBPT,,0.15,7100000
TBPT,,0.2,0
TBTEMP,1200
TBPT,,0,0
TBPT,,0.00125,250
TBPT,,0.002,277.3
TBPT,,0.00275,289.35
TBPT,,0.0035,298.31
TBPT,,0.00425,305.61
TBPT,,0.005,311.8
TBPT,,0.00575,317.19
TBPT,,0.0065,321.95
```

```
TBPT,,0.00725,326.18
TBPT,,0.008,329.98
TBPT,,0.00875,333.4
TBPT,,0.02,355
TBPT,,0.15,355
TBPT,,0.2,0
MPTEMP,,,,,,,,
MPTEMP,1,20
MPTEMP,2,100
MPTEMP,3,200
MPTEMP,4,300
MPTEMP,5,400
MPTEMP,6,500
MPTEMP,7,600
MPTEMP,8,700
MPTEMP,9,800
MPTEMP,10,900
MPTEMP,11,1000
MPTEMP,12,1100
MPTEMP,13,1200
MPDATA,EX,1,1,2E+11
MPDATA,EX,1,2,2E+11
MPDATA,EX,1,3,1.7152E+11
MPDATA,EX,1,4,1.42936E+11
MPDATA,EX,1,5,1.16328E+11
MPDATA,EX,1,6,97264000000
MPDATA,EX,1,7,51733600000
MPDATA,EX,1,8,22507200000
MPDATA,EX,1,9,13904800000
MPDATA,EX,1,10,9451313968
MPDATA,EX,1,11,6300875978
MPDATA,EX,1,12,3150437989
MPDATA,EX,1,13,200000
MPDATA,PRXY,1,,0.3
MPDATA,PRXY,1,,0.3
MPDATA,PRXY,1,,0.3
MPDATA,PRXY,1,,0.3
MPDATA,PRXY,1,,0.3
MPDATA,PRXY,1,,0.3
MPDATA,PRXY,1,,0.3
MPDATA,PRXY,1,,0.3
MPDATA,PRXY,1,,0.3
MPDATA,PRXY,1,,0.3
MPDATA,PRXY,1,,0.3
MPDATA,PRXY,1,,0.3
MPTEMP,,,,,,,,
MPTEMP,1,20
MPTEMP,2,749.99
MPTEMP,3,750
MPTEMP,4,800
MPTEMP,5,820
MPTEMP,6,840
MPTEMP,7,850
MPTEMP,8,900
MPTEMP,9,950
MPTEMP,10,1000
```

```
MPTEMP,11,1200
MPDATA,ALPX,1,,1.216E-005
MPDATA,ALPX,1,,1.508E-005
MPDATA,ALPX,1,,1.5069E-005
MPDATA,ALPX,1,,1.4103E-005
MPDATA,ALPX,1,,1.375E-005
MPDATA,ALPX,1,,1.3415E-005
MPDATA,ALPX,1,,1.3253E-005
MPDATA,ALPX,1,,1.3409E-005
MPDATA,ALPX,1,,1.3763E-005
MPDATA,ALPX,1,,1.4082E-005
MPDATA,ALPX,1,,1.5085E-005
MPDATA,DAMP,1,,DAMPRATIO
MP,DENS,1,7800
Cin=0.0254 !converter factor from inches to meters
C1b=4.448222 !converter factor from Lb to newton
fo=C1b/Cin
ET,1,BEAM188
ET,2,BEAM189
SECTYPE,1,BEAM,I
SECDATA,16.655*Cin,16.655*Cin,36.74*Cin,1.68*Cin,1.68*Cin,.945*Cin
SECPLOT,1
C = 1.49535*Cin
SECTYPE,2,BEAM,I
SECDATA,C*16.655,C*16.655,C*36.74,C*1.68,C*1.68,C*.945
SECPLOT,2
A = 400*Cin
COLUMDIV = 4
SPANDIV = 16
K,1
K,2,,A
K,3,2*A
K,4,2*A,A
L,2,1
L,3,4
L,4,2
LSEL,,,,1
LATT,,,,,3
LSEL,,,,2
LATT,,,,,1
LSEL,,,,3
LATT,,,,,1
ALLSEL
LESIZE,1,,,COLUMDIV
LESIZE,2,,,COLUMDIV
LESIZE,3,,,SPANDIV
TYPE,1
SECNUM,1
REAL,1
LMESH,1,2
TYPE,2
SECNUM,2
REAL,2
LMESH,3
ALLSEL
ET,3,MASS21,,,4
R,3,21945.6,21945.6
```

```
TYPE,3
REAL,3
E,1
E,11
DK,1,ALL
DK,3,ALL
LSEL,,,,3
ESLL
SFBEAM,ALL,1,PRESS,-500*fo,-500*fo
ALLSEL
/VIEW,1,1,1,1
/ANG,1
EPLOT
FINISH
/SOLU
ANTYPE,0
CNVTOL,F,,0.00001,2,10.0
CNVTOL,U,,0.00001,2
NSUBST,10,20,1
OUTRES,ERASE
OUTRES,ALL,1
TIME,1e-6
SOLVE
FINISH
/SOLU
ANTYPE,2
MODOPT,SUBSP,8
MXPAND,8, , ,1
CNVTOL,F,,0.00001,2,10.0
CNVTOL,U,,0.00001,2
SOLVE
FINI
*GET,FREQ1,MODE,1,FREQ
/ESHAPE,1.0
/CONFIG,NRES,200000
/SOLU
ANTYPE,TRANS
TRNOPT,FULL
NLGEOM,1
OUTRES,ALL,1
ALPHAD,2*DAMPRATIO*FREQ1*2*3.1415926
BETAD,2*DAMPRATIO/(FREQ1*2*3.1415926)
CNVTOL,F,,0.00001,2,10.0
CNVTOL,U,,0.00001,2
*DO,I,1,NT
ACEL,AC(I)*9.81,0
TIME,I*0.02
OUTRES,ALL,ALL
SOLVE
*ENDDO
*DIM,fire,TABLE,61,1,1,Time,Temp, ,    0
*TREAD,fire,'Ansys_section_Average_temp_one_hour','txt',' ', ,
BFL,1,TEMP, %fire%
BFL,2,TEMP, %fire%
BFL,3,TEMP, %fire%
DELTIM,30,5,60
TIME,3660
```

```
TREF,20,
SOLVE
FINISH
EPLOT
/ESHAPE,1.0
```

SAFIR Script

```
   NPTTOT     14080
     NNODE    61
      NDIM     2
 NDIMMATER     1
   NDDLMAX     3
      FROM     1   TO    61 STEP     2 NDDL     3
      FROM     2   TO    60 STEP     2 NDDL     1
END_NDDL
    STATIC     PURE_NR
     NLOAD     1
   OBLIQUE     0
  COMEBACK         1.
 LARGEUR11       2000
 LARGEUR12        100
   NORENUM
      NMAT     3
  ELEMENTS
      BEAM    30     2
        NG     2
    NFIBER   242
END_ELEM
     NODES
      NODE     1    0.00000    0.00000
     GNODE    21    0.00000    3.00000     1
     GNODE    41    5.00000    3.00000     1
     GNODE    61    5.00000    0.00000     1
 FIXATIONS
     BLOCK     1               F0         F0         F0
     BLOCK    61               F0         F0         F0
END_FIX
 NODOFBEAM
c30x30.tem
 TRANSLATE     1     2
 TRANSLATE     2     3
END_TRANS
heb200.tem
 TRANSLATE     1     1
END_TRANS
ELEM      1     1     2     3     1
GELEM    10    19    20    21     1     2
ELEM     11    21    22    23     2
GELEM    20    39    40    41     2     2
ELEM     21    41    42    43     1
GELEM    30    59    60    61     1     2
 PRECISION      1.E-3
     LOADS
  FUNCTION         F1
```

```
  NODELOAD          21          0.    0.     0.
 DISTRBEAM          11          0.    -14000.
GDISTRBEAM          20          0.    -14000.     1
END_LOAD
 MATERIALS
  STEELEC3
    210.E9        0.3    355.0E6
SILCONCEC2
                  0.2     25.0E6      0.0E6     0.
  STEELEC2
    210.E9        0.3    500.0E6
      TIME
                   1.          2400.
END_TIME
LARGEDISPL
     EPSTH
IMPRESSION
 TIMEPRINT
                   1.     2400.
END_TIMEPR
   PRINTMN
PRINTREACT
```

FDS Script

```
&HEAD CHID='Wood_Stud_Wall'/
&MESH IJK=10,10,20, XB=2,3,0,1.0,0,2.0 /
&TIME TWFIN=1180. /
&DUMP DT_PROF=60. /
&MATL ID                  = 'GYPSUM'
      FYI                 = 'TYPE X '
      CONDUCTIVITY_RAMP   = 'K_GYPSUM'
      SPECIFIC_HEAT_RAMP  = 'C_GYPSUM'
      DENSITY             =  615 /
&RAMP ID='C_GYPSUM', T=42 ,F=0.8942 /
&RAMP ID='C_GYPSUM', T=44 ,F=0.9048 /
&RAMP ID='C_GYPSUM', T=46 ,F=0.9268 /
&RAMP ID='C_GYPSUM', T=48 ,F=0.9481 /
&RAMP ID='C_GYPSUM', T=50 ,F=0.9788 /
&RAMP ID='C_GYPSUM', T=52 ,F=0.9942 /
&RAMP ID='C_GYPSUM', T=54 ,F=0.2788 /
&RAMP ID='C_GYPSUM', T=56 ,F=1.0501 /
&RAMP ID='C_GYPSUM', T=58 ,F=1.304 /
&RAMP ID='C_GYPSUM', T=60 ,F=1.5484 /
&RAMP ID='C_GYPSUM', T=62 ,F=1.7049 /
&RAMP ID='C_GYPSUM', T=64 ,F=1.6418 /
&RAMP ID='C_GYPSUM', T=66 ,F=1.3821 /
&RAMP ID='C_GYPSUM', T=68 ,F=1.4865 /
&RAMP ID='C_GYPSUM', T=70 ,F=1.7367 /
&RAMP ID='C_GYPSUM', T=72 ,F=2.1346 /
&RAMP ID='C_GYPSUM', T=74 ,F=2.756 /
&RAMP ID='C_GYPSUM', T=76 ,F=3.5232 /
&RAMP ID='C_GYPSUM', T=78 ,F=4.4841 /
&RAMP ID='C_GYPSUM', T=80 ,F=5.6056 /
&RAMP ID='C_GYPSUM', T=82 ,F=6.8596 /
&RAMP ID='C_GYPSUM', T=84 ,F=8.3185 /
```

```
&RAMP ID='C_GYPSUM', T=86 ,F=9.7813 /
&RAMP ID='C_GYPSUM', T=88 ,F=11.39 /
&RAMP ID='C_GYPSUM', T=90 ,F=13.046 /
&RAMP ID='C_GYPSUM', T=92 ,F=14.652 /
&RAMP ID='C_GYPSUM', T=94 ,F=16.688 /
&RAMP ID='C_GYPSUM', T=96 ,F=19.275 /
&RAMP ID='C_GYPSUM', T=98 ,F=22.253 /
&RAMP ID='C_GYPSUM', T=100 ,F=24.323 /
&RAMP ID='C_GYPSUM', T=102 ,F=25.049 /
&RAMP ID='C_GYPSUM', T=104 ,F=23.274 /
&RAMP ID='C_GYPSUM', T=106 ,F=18.398 /
&RAMP ID='C_GYPSUM', T=108 ,F=8.9021 /
&RAMP ID='C_GYPSUM', T=110 ,F=2.7905 /
&RAMP ID='C_GYPSUM', T=112 ,F=1.4954 /
&RAMP ID='C_GYPSUM', T=114 ,F=1.12 /
&RAMP ID='C_GYPSUM', T=116 ,F=1.0024 /
&RAMP ID='C_GYPSUM', T=118 ,F=0.9588 /
&RAMP ID='C_GYPSUM', T=120 ,F=0.9326 /
&RAMP ID='C_GYPSUM', T=122 ,F=0.9153 /
&RAMP ID='C_GYPSUM', T=124 ,F=0.9012 /
&RAMP ID='C_GYPSUM', T=126 ,F=0.8933 /
&RAMP ID='C_GYPSUM', T=128 ,F=0.8887 /
&RAMP ID='C_GYPSUM', T=130 ,F=0.8868 /
&RAMP ID='C_GYPSUM', T=132 ,F=0.8757 /
&RAMP ID='C_GYPSUM', T=134 ,F=0.8779 /
&RAMP ID='C_GYPSUM', T=136 ,F=0.8747 /
&RAMP ID='C_GYPSUM', T=138 ,F=0.8718 /
&RAMP ID='C_GYPSUM', T=140 ,F=0.8689 /
&RAMP ID='C_GYPSUM', T=142 ,F=0.8735 /
&RAMP ID='C_GYPSUM', T=144 ,F=0.87 /
&RAMP ID='C_GYPSUM', T=146 ,F=0.8688 /
&RAMP ID='C_GYPSUM', T=148 ,F=0.8706 /
&RAMP ID='C_GYPSUM', T=150 ,F=0.8709 /
&RAMP ID='C_GYPSUM', T=152 ,F=0.8712 /
&RAMP ID='C_GYPSUM', T=154 ,F=0.8775 /
&RAMP ID='C_GYPSUM', T=156 ,F=0.8791 /
&RAMP ID='C_GYPSUM', T=158 ,F=0.8828 /
&RAMP ID='C_GYPSUM', T=160 ,F=0.8824 /
&RAMP ID='C_GYPSUM', T=162 ,F=0.8827 /
&RAMP ID='C_GYPSUM', T=164 ,F=0.8881 /
&RAMP ID='C_GYPSUM', T=166 ,F=0.8866 /
&RAMP ID='C_GYPSUM', T=168 ,F=0.8907 /
&RAMP ID='C_GYPSUM', T=170 ,F=0.8964 /
&RAMP ID='C_GYPSUM', T=172 ,F=0.8984 /
&RAMP ID='C_GYPSUM', T=174 ,F=0.9069 /
&RAMP ID='C_GYPSUM', T=176 ,F=0.9174 /
&RAMP ID='C_GYPSUM', T=178 ,F=0.9178 /
&RAMP ID='C_GYPSUM', T=180 ,F=0.932 /
&RAMP ID='C_GYPSUM', T=182 ,F=0.9403 /
&RAMP ID='C_GYPSUM', T=184 ,F=0.9451 /
&RAMP ID='C_GYPSUM', T=186 ,F=0.9573 /
&RAMP ID='C_GYPSUM', T=188 ,F=0.962 /
&RAMP ID='C_GYPSUM', T=190 ,F=0.9727 /
&RAMP ID='C_GYPSUM', T=192 ,F=0.9776 /
&RAMP ID='C_GYPSUM', T=194 ,F=0.9929 /
&RAMP ID='C_GYPSUM', T=196 ,F=1.0105 /
&RAMP ID='C_GYPSUM', T=198 ,F=1.0088 /
```

```
&RAMP ID='C_GYPSUM', T=200 ,F=1.0146 /
&RAMP ID='K_GYPSUM', T=22 ,F=0.23/
&RAMP ID='K_GYPSUM', T=23 ,F=0.232/
&RAMP ID='K_GYPSUM', T=25 ,F=0.227/
&RAMP ID='K_GYPSUM', T=71 ,F=0.205/
&RAMP ID='K_GYPSUM', T=73 ,F=0.209/
&RAMP ID='K_GYPSUM', T=119 ,F=0.155/
&RAMP ID='K_GYPSUM', T=121 ,F=0.148/
&RAMP ID='K_GYPSUM', T=125 ,F=0.152/
&RAMP ID='K_GYPSUM', T=197 ,F=0.118/
&RAMP ID='K_GYPSUM', T=298 ,F=0.122/
&RAMP ID='K_GYPSUM', T=299 ,F=0.122/
&RAMP ID='K_GYPSUM', T=301 ,F=0.115/
&RAMP ID='K_GYPSUM', T=302 ,F=0.119/
&RAMP ID='K_GYPSUM', T=390 ,F=0.11/
&RAMP ID='K_GYPSUM', T=393 ,F=0.121/
&RAMP ID='K_GYPSUM', T=394 ,F=0.121/
&RAMP ID='K_GYPSUM', T=495 ,F=0.122/
&RAMP ID='K_GYPSUM', T=596 ,F=0.125/
&RAMP ID='K_GYPSUM', T=601 ,F=0.125/
&RAMP ID='K_GYPSUM', T=602 ,F=0.14/
&RAMP ID='K_GYPSUM', T=696 ,F=0.137/
&RAMP ID='K_GYPSUM', T=707 ,F=0.147/
&RAMP ID='K_GYPSUM', T=710 ,F=0.147/
&RAMP ID='K_GYPSUM', T=808 ,F=0.141
&RAMP ID='K_GYPSUM', T=810 ,F=0.147/
&RAMP ID='K_GYPSUM', T=815 ,F=0.152/
&RAMP ID='K_GYPSUM', T=915 ,F=0.195/
&RAMP ID='K_GYPSUM', T=916 ,F=0.212/
&RAMP ID='K_GYPSUM', T=917 ,F=0.275/
&RAMP ID='K_GYPSUM', T=1012 ,F=0.825/
&RAMP ID='K_GYPSUM', T=1014 ,F=1.106/
&RAMP ID='K_GYPSUM', T=1015 ,F=0.942/
&MATL ID                 = 'INSULATION'
      FYI                = 'GLASS FIBER'
      CONDUCTIVITY_RAMP  = 'K_INSULATION'
      SPECIFIC_HEAT_RAMP = 'C_INSULATION'
      DENSITY            = 64/
&RAMP ID='K_INSULATION', T=24,F=0.022 /
&RAMP ID='K_INSULATION', T=100,F=0.029 /
&RAMP ID='K_INSULATION', T=198,F=0.051 /
&RAMP ID='K_INSULATION', T=299,F=0.082 /
&RAMP ID='K_INSULATION', T=407,F=0.131 /
&RAMP ID='K_INSULATION', T=515,F=0.204 /
&RAMP ID='K_INSULATION', T=632,F=1.587 /
&RAMP ID='C_INSULATION', T=40,F=0.758 /
&RAMP ID='C_INSULATION', T=50,F=0.7745 /
&RAMP ID='C_INSULATION', T=60,F=0.7895 /
&RAMP ID='C_INSULATION', T=70,F=0.8016 /
&RAMP ID='C_INSULATION', T=80,F=0.8087 /
&RAMP ID='C_INSULATION', T=90,F=0.8211 /
&RAMP ID='C_INSULATION', T=100,F=0.8318 /
&RAMP ID='C_INSULATION', T=110,F=0.8456 /
&RAMP ID='C_INSULATION', T=120,F=0.8388 /
&RAMP ID='C_INSULATION', T=130,F=0.8451 /
&RAMP ID='C_INSULATION', T=140,F=0.8499 /
&RAMP ID='C_INSULATION', T=150,F=0.8513 /
```

```
&RAMP ID='C_INSULATION', T=160,F=0.8578 /
&RAMP ID='C_INSULATION', T=170,F=0.8618 /
&RAMP ID='C_INSULATION', T=180,F=0.8647 /
&RAMP ID='C_INSULATION', T=190,F=0.8735 /
&RAMP ID='C_INSULATION', T=200,F=0.8798 /
&RAMP ID='C_INSULATION', T=210,F=0.8816 /
&RAMP ID='C_INSULATION', T=220,F=0.8817 /
&RAMP ID='C_INSULATION', T=230,F=0.8868 /
&RAMP ID='C_INSULATION', T=240,F=0.8922 /
&RAMP ID='C_INSULATION', T=250,F=0.8949 /
&RAMP ID='C_INSULATION', T=260,F=0.8971 /
&RAMP ID='C_INSULATION', T=270,F=0.8918 /
&RAMP ID='C_INSULATION', T=280,F=0.8912 /
&RAMP ID='C_INSULATION', T=290,F=0.8876 /
&RAMP ID='C_INSULATION', T=300,F=0.8884 /
&RAMP ID='C_INSULATION', T=310,F=0.8872 /
&RAMP ID='C_INSULATION', T=320,F=0.8887 /
&RAMP ID='C_INSULATION', T=330,F=0.8939 /
&RAMP ID='C_INSULATION', T=340,F=0.8839 /
&RAMP ID='C_INSULATION', T=350,F=0.8764 /
&MATL ID                  = 'WOOD'
      FYI                 = 'SPF'
      SPECIFIC_HEAT = 1.4
      CONDUCTIVITY_RAMP   = 'K_WOOD'
      DENSITY             = 420. /
&RAMP ID='K_WOOD', T= 20. , F=0.078  /
&RAMP ID='K_WOOD', T= 75. , F=0.081  /
&RAMP ID='K_WOOD', T= 100., F=0.085  /
&RAMP ID='K_WOOD', T= 120., F=0.094  /
&RAMP ID='K_WOOD', T= 147., F=0.099  /
&RAMP ID='K_WOOD', T= 174., F=0.101  /
&RAMP ID='K_WOOD', T= 200., F=0.0101 /
&RAMP ID='K_WOOD', T= 231., F=0.091  /
&RAMP ID='K_WOOD', T= 263., F=0.058  /
&RAMP ID='K_WOOD', T= 323., F=0.122  /
&MATL ID                  = 'PLYWOOD'
      FYI                 = 'PLYWOOD '
      CONDUCTIVITY_RAMP   = 'K_PLYWOOD'
      SPECIFIC_HEAT       = 1.4
      DENSITY             = 544 /
&RAMP ID='K_PLYWOOD', T=24,F=0.106 /
&RAMP ID='K_PLYWOOD', T=60,F=0.116 /
&RAMP ID='K_PLYWOOD', T=103,F=0.116 /
&RAMP ID='K_PLYWOOD', T=146,F=0.115 /
&RAMP ID='K_PLYWOOD', T=205,F=0.135 /
&RAMP ID='K_PLYWOOD', T=309,F=0.202 /
&RAMP ID='K_PLYWOOD', T=522,F=0.173 /
&SURF ID='HOT', TMP_FRONT=897.2,RAMP_T='Fire_curve',  COLOR='GRAY' /
&RAMP ID='Fire_curve', T=0 ,F=0 /
&RAMP ID='Fire_curve', T=1380 ,F=1 /
&RAMP ID='Fire_curve', T=2880 ,F=1 /
&SURF ID                  = 'STUDS'
      COLOR               = 'CHOCOLATE'
      BACKING             = 'EXPOSED'
      MATL_ID             = 'WOOD'
      THICKNESS           = 0.038 /
&SURF ID                  = 'INSULATION'
```

```
      COLOR                = 'BLACK'
      BACKING              = 'EXPOSED'
      MATL_ID              = 'INSULATION'
      THICKNESS            =  0.181/
&SURF ID                   = 'PLYWOOD'
      COLOR                = 'CHOCOLATE'
      BACKING              = 'EXPOSED'
      MATL_ID              = 'PLYWOOD'
      THICKNESS            =  0.0127/
&SURF ID                   = 'GYPSUM'
      COLOR                = 'WHITE'
      BACKING              = 'EXPOSED'
      MATL_ID              = 'GYPSUM'
      THICKNESS            =  0.0127/
&OBST XB= 2.8271, 2.9271, 0.5, 0.7, 0.6, 0.8, SURF_ID='HOT' /
&OBST XB= 2.6, 2.6127, 0.4, 0.8, 0.0, 2.0, SURF_ID='GYPSUM' / GYPSUM
BOARD
&OBST XB= 2.6127, 2.7017, 0.4, 0.581, 0.0, 2.0, SURF_ID='INSULATION' /
INSULATION 1
&OBST XB= 2.6127, 2.7017, 0.581, 0.619, 0.0, 2.0, SURF_ID='STUDS' /
STUD
&OBST XB= 2.6127, 2.7017, 0.619, 0.8, 0.0, 2.0, SURF_ID='INSULATION' /
INSULATION 2
&OBST XB= 2.7017, 2.7144, 0.4, 0.8, 0.0, 2.0, SURF_ID='PLYWOOD' /
PLYWOOD
&OBST XB= 2.7144, 2.7271, 0.4, 0.8, 0.0, 2.0, SURF_ID='GYPSUM' /EXPOSED
GYPSUM
&VENT MB='XMIN', SURF_ID='OPEN' /
&VENT MB='XMAX', SURF_ID='OPEN' /
&VENT MB='YMIN', SURF_ID='OPEN' /
&VENT MB='YMAX', SURF_ID='OPEN' /
&VENT MB='ZMIN', SURF_ID='OPEN' /
&VENT MB='ZMAX', SURF_ID='OPEN' /
&SLCF PBZ=1.0,QUANTITY='TEMPERATURE',VECTOR=.TRUE. /
&BNDF QUANTITY='GAUGE_HEAT_FLUX' /
&BNDF QUANTITY='WALL_TEMPERATURE' /
&BNDF QUANTITY='ADIABATIC_SURFACE_TEMPERATURE' /
&DEVC XYZ=2.7271,0.6,0.77,QUANTITY='WALL_TEMPERATURE',
ID='TEMP_EXT_IOR=+1', IOR= 1 /
&DEVC XYZ=2.7271,0.6,0.77,QUANTITY='INSIDE_WALL_TEMPERATURE',
ID='TEMP_INS_IOR=+1', IOR=1,DEPTH=0.0127 /
&DEVC XYZ=2.7271,0.6,0.77,QUANTITY='INSIDE_WALL_TEMPERATURE',
ID='TEMP_INS_IOR=+1', IOR=1,DEPTH=0.0254 /
&DEVC XYZ=2.7271,0.6,0.77,QUANTITY='INSIDE_WALL_TEMPERATURE',
ID='TEMP_INS_IOR=+1', IOR=1,DEPTH=0.0699 /
&DEVC XYZ=2.7271,0.6,0.77,QUANTITY='INSIDE_WALL_TEMPERATURE',
ID='TEMP_INS_IOR=+1', IOR=1,DEPTH=0.1144 /
&DEVC XYZ=2.7271,0.6,0.77,QUANTITY='INSIDE_WALL_TEMPERATURE',
ID='TEMP_INS_IOR=+1', IOR=1,DEPTH=0.1271 /
&DEVC XYZ=2.7271,0.6,0.77,QUANTITY='BACK_WALL_TEMPERATURE',
ID='TEMP_INT_IOR=+1', IOR= 1 /
&DEVC XYZ=2.6,0.6,0.77,QUANTITY='BACK_WALL_TEMPERATURE',
ID='TEMP_EXT_IOR=-1', IOR=-1 /
&DEVC XYZ=2.6,0.6,0.77,QUANTITY='INSIDE_WALL_TEMPERATURE',
ID='TEMP_INS_IOR=-1', IOR=-1,
DEPTH=0.0127 /
```

```
&DEVC XYZ=2.6,0.6,0.77,QUANTITY='WALL_TEMPERATURE',
ID='TEMP_INT_IOR=-1', IOR=-1 /
&TAIL /
```